NTNU – Trondheim
Norwegian University of
Science and Technology

Modeling the heating of the Green Energy Lab in Shanghai by the geothermal heat pump combined with the solar thermal energy and ground energy storage

Candice Yau May Yu

Master of Energy and Environmental Engineering
Submission date: August 2012
Supervisor: Trygve Magne Eikevik, EPT
Co-supervisor: Yong Li, Shanghai Jiao Tong University
Arne M. Bredesen, EPT

Norwegian University of Science and Technology
Department of Energy and Process Engineering

NTNU

Norwegian University
of Science and Technology

Department of Energy
and Process Engineering

EPT-M-2012-96

MASTER THESIS

for

student Candice Yu

Spring 2012

Modeling the heating of the Green Energy Lab by the geothermal heat pump combined with the solar thermal energy and ground energy storage in Shanghai

Modellering av oppvarmingsystem for "Green Energy Lab" ved bruk av geotermisk varmepumpe i kombinasjon med termisk energi fra sol og grunnvarmelager i Shanghai

Background and objective

Solar energy is abundant while the demand of heating/hot water is small in Summer. To make full use of solar energy, a system has been proposed to store the solar thermal energy in the ground soil, using U-tube heat exchanger in the seasons solar thermal energy is not used. The heat can be used by just circulating the water if the ground temperature reached certain value. The heat can also be used by geothermal heat pump when the ground temperature is not so high. The objective of this research is to develop a model using TRNSYS based on design parameters of Green Energy Lab (GEL) in Shanghai Jiao Tong University and the weather conditions of Shanghai. The performance of such system will be studied. Suggestions on improve such system will be provided.

The following tasks are to be considered:

1. Literature review on solar energy seasonal storage in the ground, geothermal heat pump and solar heating technologies and related researches. Study related models developed before.
2. Develop a ground storage model using TRNSYS based on design parameters of Green Energy Lab (GEL) in Shanghai Jiao Tong University. Develop the system model.
3. Develop heat storage scheme and heating scheme of GEL. Simulate the heat storage performance and heating performance based on the equipments available in the GEL.
4. Study the influence of important design parameters on the system performance.
5. Make a draft paper of the results from the project
6. Make proposal for further work

-- " --

Within 14 days of receiving the written text on the master thesis, the candidate shall submit a research plan for his project to the department.

When the thesis is evaluated, emphasis is put on processing of the results, and that they are presented in tabular and/or graphic form in a clear manner, and that they are analyzed carefully.

The thesis should be formulated as a research report with summary both in English and Norwegian, conclusion, literature references, table of contents etc. During the preparation of the text, the candidate should make an effort to produce a well-structured and easily readable report. In order to ease the evaluation of the thesis, it is important that the cross-references are correct. In the making of the report, strong emphasis should be placed on both a thorough discussion of the results and an orderly presentation.

The candidate is requested to initiate and keep close contact with his/her academic supervisor(s) throughout the working period. The candidate must follow the rules and regulations of NTNU as well as passive directions given by the Department of Energy and Process Engineering.

Risk assessment of the candidate's work shall be carried out according to the department's procedures. The risk assessment must be documented and included as part of the final report. Events related to the candidate's work adversely affecting the health, safety or security, must be documented and included as part of the final report.

Pursuant to "Regulations concerning the supplementary provisions to the technology study program/Master of Science" at NTNU §20, the Department reserves the permission to utilize all the results and data for teaching and research purposes as well as in future publications.

The final report is to be submitted digitally in DAIM (http://daim.idi.ntnu.no/). An executive summary of the thesis including title, student's name, supervisor's name, year, department name, and NTNU's logo and name, shall be submitted to the department as a separate pdf file. The final report, with summery and all other material and documents have to be given to the supervisor in digital format on a CD.

Department of Energy and Process Engineering, 16. February 2012

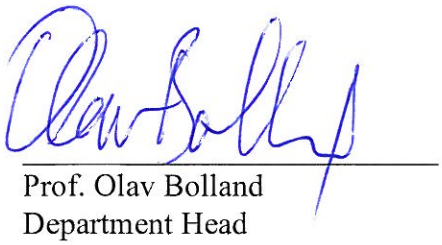

Prof. Olav Bolland
Department Head

Prof. Trygve M. Eikevik
Academic Supervisor
e-mail: trygve.m.eikevik@ntnu.no

Co-supervicers:
Prof. Yong Li, Shanghai Jioa Tong University, e-mail: liyo@sjtu.edu.cn
Prof. Arne M. Bredesen, NTNU, e-mail: arne.m.bredesen@ntnu.no

Preface

This report is the written work of my Master thesis at the Norwegian University of Science and Technology (NTNU), Department of Energy and Process Engineering. The subject of the thesis was decided in cooperation with Shanghai Jiao Tong University (SJTU) and Norwegian University of Science and Technology (NTNU) and was performed and written at SJTU in the spring of 2012. The thesis accounts for 30 credits of the master degree in the study program "Energy and Environmental Engineering". The title of the master thesis is "Modeling the heating of the Green Energy Lab in Shanghai by the geothermal heat pump combined with the solar thermal energy and ground energy storage".

I faced for the first time the challenges involved with big simulation models, as the learning of the simulations software TRNSYS and the understanding of the proposed heating system. This has made me gain knowledge about this field and how to solve challenges that come on the way. I gained insight into the complexity of combined systems with solar collectors, geothermal heat pump and ground storage. I have also gained insight in the use of transient simulations.

I would firstly thank my supervisor at SJTU, Professor Yong Li, for the excellent guidance and constructive feedback throughout the project. I also want to extend my gratitude to my supervisors at NTNU, Professor Trygve M. Eikeveik and Professor Arne Bredesen, for giving good advices and feedbacks about my project. I want to thank all of them for giving me this exciting opportunity of going to Shanghai to write my thesis and to gain cultural experiences.

Moreover, I also want to thank all the students working at the Green Energy Laboratory (GEL) for giving me good tips and raising interesting discussions about TRNSYS and also for providing me with information about the equipment at the GEL. We learned from each other in terms of knowledge, experience and cultural diversity.

Last, but not least, I would like to thank my family, especially my mum, who are always supporting me and for raising me.

Shanghai, August 2012

Candice Yu

Abstract

This work involves the study of heating systems that combine solar collectors, geothermal heat pumps and thermal energy storage in the ground. Solar collectors can reduce the electricity use in these systems by reducing the operation time of the geothermal heat pump and by increasing the ground source temperature. These systems can be designed in many ways, consequently the complexity is high. The purpose of this study has been to develop simulation models to study the behavior of these systems, with emphasis on the thermal energy storage in the ground.

A simulation tool with several models has been developed in the simulation software TRNSYS based on the proposed heating system at the GEL under the metrological conditions of Shanghai. The program was used for an intensive simulation study, in which the interaction with the borehole heat exchanger, the geothermal heat pump, the evacuated tube collector and the load requirements could be analyzed. A base case was developed to make it possible to vary and compare the design parameters of interest, such as the ground storage volume, the flow rate of the solar collector and the solar collector area. The base case was based on the design parameters of the GEL. The GEL was used as reference building and was simulated in TRNBuild with the thermal characteristics of the building material. From the simulations the heating demand of the building could be obtained and the building model could later on be used as a heat load for the other simulation models. The results showed that the there were heating demand from November to March.

The four operation modes of the proposed heating system at the GEL were presented. All of the operation modes were simulated in TRNSYS. The four operation modes were solar thermal ground storage, solar direct heating, direct heat exchange with the ground storage and geothermal heat pump. The operation modes worked in two different seasons, storage season and heating season. The ground storage mode was studied thoroughly by varying the parameters of interest. To test the significance of the borehole configuration, the storage volume was kept constant and the number of boreholes and the borehole spacing were varied. It was found that a compact pattern with a high number of boreholes and small borehole spacing is favorable for borehole thermal energy storages. The performance of a ground storage is directly linked to the storage size. The solar collector efficiency is highly dependent on the return temperature of the storage. It was decided to continue to work with a compact pattern of the storage, rather than the base case of the GEL. This is because this kind of storage showed the most promising storage efficiency and also reached a high ground temperature during storage season.

Simulations of the heating modes showed that the solar direct heating mode, the direct heat exchange with ground storage mode and the geothermal heat pump mode can each cover 37%, 25% and 38% of the heating demand respectively. For the simulations of the geothermal heat pump it was shown that the borehole depth is a very important factor for the system performance. Too short borehole depth will cause unstable and too low temperatures at the inlet of the evaporator. To compare the electricity use of a geothermal heat pump system with and without solar collectors there were also performed simulations for a traditional geothermal heat pump system. Results showed that 26.1% of the electricity consumption could be saved. The savings was mostly due to the reduced operation time of the heat pump, since other heating modes could be used. The studies showed that due to the complexity of such systems it is very important to perform simulations to optimize the performance. There are many factors that play an important role since there are so many components involved. The simulations showed that sizing of the system is critical for the system performance.

Sammendrag

I denne rapporten har det blitt sett på varmesystemer som kombinerer solfangere, geotermiske varmepumper og termisk energilagring i grunnen. Solfangere kan redusere elektrisitetsforbruket i disse systemene ved å redusere driftstiden til varmepumpen og ved å øke grunntemperaturen. Disse systemene kan utformes på mange måter og derfor er kompleksiteten høy. Hensikten med dette arbeidet har vært å utvikle simulasjonsmodeller for å studere egenskapene til disse systemene med vektlegging på energilagring i grunnen.

Et simuleringsverktøy med flere modeller har blitt utviklet i simuleringsprogrammet TRNSYS med data som er basert på det foreslåtte varmesystemet i GEL og værforholdene i Shanghai. Simuleringsprogrammet ble brukt til en intensiv simuleringsstudie, hvor samspillet mellom borehullsvarmevekslerne, varmepumpen, solfangeren og energibehovet kan analyseres. Et referansesystem ble utviklet for å gjøre det mulig å sammenligne de forskjellige parametrene av interesse. Referansesystemet var basert på designparametrene til GEL. Referansebygget ble simulert i TRNBuild med de termiske egenskapene til bygningsmaterialet. Fra simuleringene kunne varmebehovet til bygget bli innhentet og bygningsmodellen kunne senere bli brukt som varmelast i de andre simulasjonsmodellene. Resultatene viste at det var varmebehov fra november til mars.

Det foreslåtte systemet i GEL har fire operasjonsmoduser som blir presentert. Alle operasjonsmodusene ble simulert i TRNSYS. De fire modusene var lagring av solenergi i grunnen, solenergi brukt direkte til oppvarming, varmeveksling med grunnen til oppvarming og geotermisk varmepumpe. Operasjonsmodusene var i drift i to forskjellige sesonger, lagringssesong og oppvarmingssesong. Det ble utført grundige studier av lagring av solenergi i grunnen ved å variere forskjellige parametre. For å teste betydningen av konfigurasjonen av borehullene, så ble lagringsvolumet holdt konstant mens antall borehull og avstanden mellom borehullene ble variert. Det ble funnet at en kompakt konfigurasjon med stort antall borehull og liten avstand mellom borehullene er gunstig for lagring av termisk energi i grunnen. Systemytelsen til et termisk undergrunnslager er direkte knyttet til størrelsen på lageret. Effektiviteten til solfangeren er svært avhengig av returtemperaturen til undergrunnslageret. Det ble besluttet å fortsette å jobbe videre med et kompakt mønster av undergrunnslageret, istedenfor med referansesystemet til GEL. Dette skyldtes et kompakt mønster viste mest lovende lagringseffektivitet og oppnådde en høy temperatur i grunnen under lagringssesongen.

Simuleringene av oppvarmingsmodusene viste at solenergi brukt direkte til oppvarming, varmeveksling med grunnen og geotermisk varmepumpe kan henholdsvis dekke 37 %, 25 % og 38 % av varmebehovet. Simuleringene av den geotermiske varmepumpen viste at borehullsdybden er en svært viktig faktor for systemytelsen. For korte borehull vil føre til ustabile og for lave temperaturer ved innløpet til fordamperen. For å sammenligne elektrisitetsbruken til et geotermisk varmepumpesystem som er med og uten solfangere, ble det også utført simuleringer for et tradisjonelt geotermisk varmepumpesystem. Sammenligningen viste at elektrisitetsforbruket kunne innspares med 26.1 %. Størstedelen av besparelsene skyldtes redusert driftstid for varmepumpen, siden andre oppvarmingsmuligheter kunne bli brukt. Studiene viste at på grunn av kompleksiteten til slike systemer er det svært viktig å utføre simuleringer for å optimalisere systemytelsen. Siden det er så mange komponenter involvert er det mange faktorer som spiller en viktig rolle. Simuleringene viste at riktig dimensjonering av systemet er kritisk for systemytelsen.

Table of Contents

Nomenclature

Abbreviations

ATES	Aquifer Thermal Energy Storage
BTES	Borehole Thermal Energy Storage
COP	Coefficient of Performance
GEL	Green Energy Laboratory
GHE	Ground Heat Exchanger
GSHP(S)	Ground Source Heat Pump (System)
m	Meter
SAGSHP(S)	Solar Assisted Ground Source Heat Pump (System)
STES	Seasonal Thermal Energy Storage
UTES	Underground Thermal Energy Storage

Symbol list

$\dot{m}$	Mass flow rate	[kg/hr]
ρ	Density	[kg/m^3]
Q	Energy rate	[kJ/hr]
E	Total amount of energy	[kJ]
η	Efficiency	
T	Temperature	[°C]
c	Specific heat	[kJ/kgK]
V	Volume	[m^3]
A	Area	[m^2]
U	Loss coefficient	[kJ/hrm^{2}K]

Subscripts

u	Useful solar energy gain
sl	Storage losses
tl	Tank losses
inj	Injection
StU	Stored energy to useful solar energy gain
StL	Stored energy to injected energy
LU	Storage losses to useful solar energy gain
LL	Storage losses to injected energy
f	Fluid
amb	Ambient
in	Inlet
out	Outlet

1 Introduction

1.1 Background

In China the buildings are expected to account for more than 35% of the national energy use by the year 2020, where heating, ventilation and air-conditioning systems will account for more than 65% of the energy use in buildings (Xi et al, 2011). Most space heating plants are still predominantly fueled by coal and domestic hot water is widely provided by electric resistance heaters in China (Xi, Lin, & Hongxing, 2011). Coal accounted for 69.5% of the national energy consumption in 2007 (Yang et al, 2009). Considering that the coal emits more CO_2 and other pollutants than other energy resources, it can be concluded that it is very important to promote use of renewable energy sources and energy conservation in China. Ever since China's participation in the Kyoto Protocol, reducing CO_2-emission as well as energy saving have been propelling researchers to explore substitutes of traditional space heating and water heating systems in China. The Renewable Energy Law (RE Law) took into effect in 2006 in China; by 2020, 15% of all energy should come from renewable energy, including wind energy, solar energy, water energy, geothermal energy, etc (Gao et al, 2008). Therefore, renewable resources have a great potential for application in environmental friendly buildings.

Solar energy is an important alternative energy source for heating applications. Shanghai is in the hot summer and cold winter climatic zone; there is abundant solar energy during summer months. It is not the amount of solar heat that is a barrier for its use but the fact that the availability and demand are often out of phase (Kroll & Ziegler, 2011). In order to make use of abundant renewable energy resources, such as solar energy, it is necessary to combine the heating systems with thermal energy storages. Seasonal thermal energy storages enable greater and more efficient use of fluctuating energy resources by matching the energy demand with the supply. Solar energy can be captured when available and stored for use when there is a lower supply or a higher demand. The stored heat can either be extracted directly or extracted by a geothermal heat pump.

Geothermal heat pump with vertical/horizontal ground heat exchangers, known as ground source heat pump system, is considered relatively efficient for heating, air-conditioning or hot water supply. Because the underground soil temperature is kept higher than the ambient air in winter, the ground source heat pump system has made the operation of heat pump systems more reliable and practical under cold weather conditions. Heat pumps also reduce the amount of bought energy.

Recent years there have been a growing interest in solar assisted ground source heat pump systems (SAGSHPS). The solar thermal energy is stored in the ground and extracted by geothermal heat pump, because a high initial temperature in the ground is beneficial for the heat pump during heating. Without the heat injection the ground temperature would tend to be decreasing annually. There are many different ways to couple the solar collector and the heat pump. If efficient seasonal use of solar energy can be combined with the underground thermal energy storage for the use of GSHPS then it could be a great substitute of traditional space heating and water heating systems in China.

In the proposed system at the Green Energy Laboratory we want to make use of both direct heat extraction and heat extraction by heat pump from the ground storage in combination with solar collectors. The proposed system is an experimental suggestion. It is very important to study and

simulate borehole storage systems before they are built. These storages have a lot of parameters that have a big impact on the system performance, for example the borehole depth, number of boreholes, borehole spacing which are parameters that have big influence on the storage size. Once the storage has been built it is very difficult and expensive to change the size. In realized systems is not possible to change parameters of major interest, such as the borehole depth. The depth cannot be easily changed. The investment cost for the drilling of boreholes is very expensive. So it is very important the system is not oversized with too many boreholes. Therefore it is very essential with experimental research before the system is build.

1.2 Objectives

The objective with this study was to test the performance of a proposed experimental set-up of a heating system for heating of the Green Energy Laboratory (GEL) in Shanghai. One approach was to study the behavior of the borehole thermal energy storage during storage season by varying parameters with influence on the system. It was interesting to test the different borehole configurations for use of storage or heat extraction. Other approaches were to study the interaction of the ground storage with the solar collector, the geothermal heat pump and the heating load.

1.3 Outline

Chapter 2 – Combination of solar collector, heat pump and ground storage

In this chapter the status of combination of solar collectors, geothermal heat pumps and ground storage is presented. Previous related simulations models are introduced.

Chapter 3 – Description of the proposed system and operation principles

The working principles and the different operation modes of the proposed heating system at the GEL are presented.

Chapter 4 – Seasonal thermal energy storages

The ground storage is described. The different types of UTES are presented with emphasis on the BTES. Further, equations and characteristics of the BTES are presented and explained.

Chapter 5 – Geothermal heat pump

The geothermal heat pump and its use are presented.

Chapter 6 – Solar thermal collectors

The principles of solar thermal collectors and evacuated tube collectors are explained. The thermal efficiency equation of the solar collectors is derived.

Chapter 7 – Stratified water storage tank

The theory of a stratified water storage tank is explained.

Chapter 8 – TRNSYS

The simulations software TRNSYS is described and the used mathematical models for the different components are described. The parameters used in the simulation models are also presented.

Chapter 9 – Simulations and results
The simulation evaluation includes analyses of the performance of the different operation modes, by evaluating the temperature change in the storage, the energy flows and the demand of electricity. Because of the complexity of the simulation models, the simulations were divided in several parts.

In the first part the simulations of the base case of the ground storage model of the GEL is presented. Thereafter, the parameters of interest of the ground storage are varied to see the influence on the system efficiencies. Finally, summarization of the obtained results will be presented.

In the second part the operation conditions of the ground storage were simulated. The focus was to find the most suitable operation period of the storage season based on end temperature of the ground and storage efficiency.

In the third part the simulation results of the reference building is presented. Heating demand and power demand were simulated in TRNBuild based on the thermal characteristics and volume of the first floor of the GEL.

In the fourth part the simulations of heating operation modes are presented. The heating performance is presented and discussed. The chapter ends with calculations of the electricity consumption. The savings of electricity of the combined system compared to a traditional system is discussed.

Chapter 10 – Conclusion
Finally, the conclusion for all the obtained results and information are presented.

1.4 Delimitations
The cooling load is very big in Shanghai, cooling could also be provided by the proposed system, but in this work the focus is on the heating system. The solar collector system could also be utilized to heat the domestic hot water. Since the reference building is a working place, it will have a negligible hot water load. The hot water demand is not as significant as that in residential buildings. Therefore the heating system is a space-heat-only system.

The focus is directed towards fluid-based system, for the solar collectors, heat pump and heating system. It is therefore not considered air solar collectors or other components that are not compatible with water borne heating systems.

Although the thesis describes different kinds of ground storages the borehole thermal energy storage is the main focus. It is mainly related to the climatic conditions of Shanghai.

2 Combination of solar collectors, heat pump and ground storage

2.1 The use of combined systems

Combining solar collectors, geothermal heat pump and ground storage provides opportunities for different system solutions that can be adapted to different conditions and applications. The system is usually called combined systems. The benefits of a combined system are several and varied, depending on the type of solar collector, the system and how the system regulation is regulated (Kjellsson, 2009). The combination can lead to optimized use of renewable resources and minimized energy costs. The main principle is to combine the advantages of both systems in order to create new operational conditions for both systems.

One advantage is that the solar collectors can produce all heat for the domestic hot water during the summer; otherwise the heat pump needs to work during many but short periods of operation. This could increase the life span of the heat pump.

Through an efficient control strategy for the system, the solar heat can be used in other ways when the solar collector is not high enough to be utilized for domestic hot water. The solar heat can be used directly for the heating system in the building. When there is not heating demand during the summer the solar collectors can be used to recharge the ground storage. The solar collectors can collect energy and then store it in the storage. Continuous operation of the geothermal heat pump could bring down the soil temperature near the ground heat exchangers greatly and consequently bring down the system efficiency. The solar collector could improve the stability and efficiency of the heat pump by recharging the ground.

The solar heat in a combined system will decrease the use of electricity in the heat pump, as the operating time for the heat pump is reduced. The heat extraction from the ground will also decrease and the natural recharging of the soil temperature will increase.

2.2 Status

The Solar Assisted Ground Source Heat Pump (SAGSHP) was first introduced by Penrod in 1956 (Xi et al, 2011). However, the interest in combining solar collectors with heat pumps started to increase in the end of 1970s due to the oil crisis (Trillat-Berdal, Souyri, & Fraisse, 2006). At that time the focus was on the positive effect of the increased temperature in the ground, but there was not made any economic evaluations on these systems (Kjellsson, 2009). During the 1980s, the International Energy Agency (IEA) established three research programs; “Solar Heating and Cooling Programme”, “Energy Storage Programme” and “Advanced Heat Pump Programme”. Some of the research focus was on the design and economics. The interest was great in this period, but it started to decline when it became apparent that many of the SAGSHP systems were marked by technical and economical problems (Rönnelid & Tepe, 2004).

Towards the end of the 1990s there were more than 100 000 Ground Source Heat Pumps (GSHPs) in Europe, half of them in Sweden and the rest mainly in Germany, Austria and Switzerland (Kjellsson, 2009). Several combined systems were realized in this period. In Germany, a system of 28 U-tube boreholes and a 175 kW heat pump were combined with 161 m^2 of flat plate collectors. The heat pump delivered 75% and the solar collector 15% of the total yearly heat demand of 550 MWh. The SFP of the heat pump was 3.8. A research project in Switzerland identified the benefits of combining

geothermal heat pump and solar collectors, where the solar collectors are linked to the domestic hot water system. The results from Switzerland highlighted the complexity of optimization and the need of further studies (Kjellsson, 2009).

Five Swedish manufacturers presented three commercial system solutions in the 2000s. In these systems the solar heat either was just used to charge the borehole or to heat the domestic hot water with the possibility to charge the borehole in case of surplus solar heat. The last systems solution was using the solar energy for heating the building and to increase the temperature of the evaporator. Germany commenced their research project "SolarThermie-2000", which includes nine research and demonstration plants for solar assisted district heating with seasonal thermal energy storage. Research projects dealt with technology development for long term storage, solar system and related systems with a view to achieve integration in the market.

Research and practices on GSHPs in China started relatively much later than in developed countries. Three universities started to begin test and experiments on the performance of the GSHPs in the end of 1980s. Qingdao Technological University, Tianjin University and Tianjin University of Commerce conducted relevant research on GSHP technology. National Natural Science Foundation of China supported several theoretical and practical studies in all aspects of GSHPs in the end of 1990s (Yang et al, 2009). In recent years there has been a big interest in the GSHPS and the Ministry of Finance and Ministry of Construction have set up a special financial support for the GSHP pilot projects nationwide. According to Gao et al (2008) there are no soil/rock UTES in practical use in China. In China, the research of soil/rock UTES started in the last decade and there have been small developments (Gao et al, 2008).

2.3 Related simulation models developed before

Up to now, most researchers have been focusing on the simulative and theoretical studies on the SAGSHP systems (Xi, Lin, & Hongxing, 2011). There are simulation models that have been developed to test the performance of SAGSHP. There are many systems with different kinds of combinations. In this section it will be presented three SAGSHP-models with different kinds of combinations, operation and weather conditions.

Chapuis and Bernier (2009) proposed a house heating system, in Alberta, Canada, which consists of seasonal borehole thermal energy storage, with two independent networks of U-tube. One U-tube is dedicated to a solar charging network and the other to the house heating system through a discharging unit. The proposed BTES was used to provide space heating to 52 single family houses. Simulations were performed for two cases, case A and case B. In case A the BTES was kept at a high enough temperature in order to supply the entire house heating and minimize the use of an auxiliary boiler. This required a relatively large solar collector area of 2293 m^2 and a relatively small BTES volume of 22100 m^3. Case B used a different approach; the solar charging network was used to keep the BTES at a low temperature level suitable for use with heat pumps. This required a relatively small solar collector area of 573 m^2 and a relatively large BTES volume of 88000 m^3. Results of the simulations showed that it was possible to have a solar fraction of 0.98 for case A, but the storage temperature had to be kept high, which lead to large storage losses and small solar collector efficiency of 23%. For case B, the solar fraction was 0.78. Because of the lower temperature level, the storage losses were smaller and the solar collector efficiency was higher, 58%.

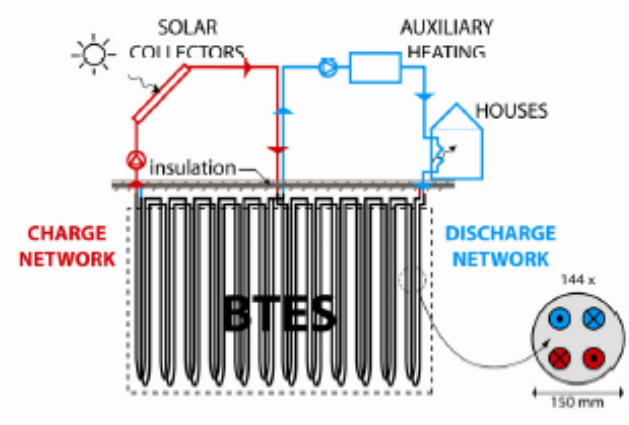

Figure 1: Proposed heating system in Alberta, Canada (Chapuis & Bernier, 2009).

Chen, Li and Hongxing (2011) proposed a heating system, in Beijing, China, which combines a solar collector with a GSHP system though a water storage tank and plate heat exchangers. The solar collector has an area of 45 m^2 and the total borehole length is 270 m. The system provides space heating and domestic hot water. The study suggests six different operation modes. For comparisons, simulations were also performed for a GSHP without solar collectors and with the same borehole length and load conditions. The results showed that the SAGSHP system can have an average COP of 3.89 for space heating, improved by 26.3% compared to a traditional GSHP and electricity consumption reduction of 5.6 GJ for space heating per year could be achieved. The solar fraction was found to be 0.4 for space heating and 0.75 for domestic hot water.

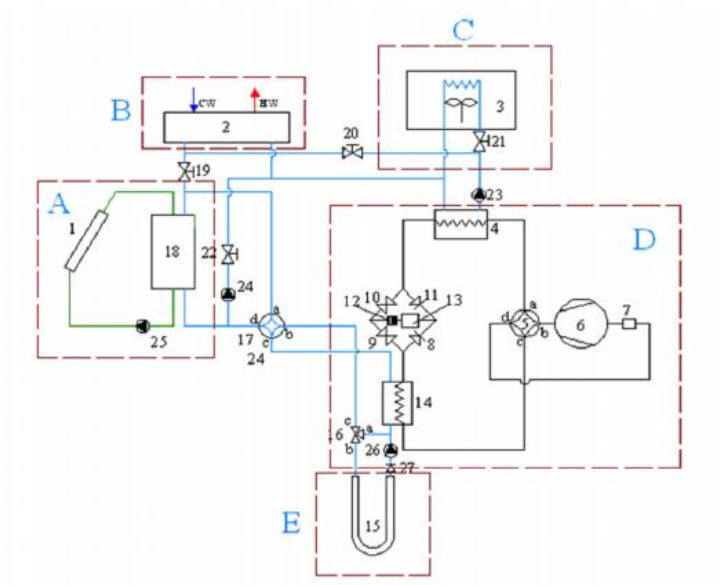

1. Solar collector 2.DHW tank 3.Indoor heating unit 4. load side heat exchanger 5.Four way valve (for refrigerant) 6.Compressor 7.Separator 8&11.Check valves 9&10.Throttle valves 12.Filter-drier 13.Accumulator 14.Source side heat exchanger 15.VGHE (vertical ground heat exchanger) 16.Three way valve 17.Four-way valve (for anti-freezing fluid) 18.Storage water tank 19-22. Control valve 23-26. Liquid pump 27.Check valve (for water and anti-freezing fluid) CW: cold water HW: hot water

Figure 2: Proposed heating system in Beijing (Xi et al, 2011).

Wang et al. (2011) proposed a novel hybrid solar GSHPS composed of a GSHPS and a SAGSHPS used in an office building, in Tianjin, China, used for cooling and heating. The GSHP was used to supply the entire building's cooling load and part of the heat load. The SAGSHP was coupled with a solar seasonal thermal energy storage to supply the remaining heating load requirement. A ground heat exchanger (GHE) and a borehole thermal energy storage (BTES) were designed corresponding to the two heat pump units. The BHE in the GSHPS was very different from the BTES in the SAGSHPS. The GHE was formed by 66 vertical boreholes with individual depth of 120 m and spacing of 4 m apart. The BTES was formed by 25 vertical boreholes with individual depth of 50 m and spacing of 2.5 m apart. The BTES consisted of boreholes with small spacing and shallow depth for the purpose of solar seasonal storage. Simulations were performed for a period of 15 years. The results showed that the temperature of the BTES increased annually because of the solar seasonal storage, the increase of the temperature in storage season was larger than the reduction in heating season every year. It also showed that the first operation time the evaporator outlet temperature of the SAGSHP drops below 0°C. This is because there was no solar heat stored in the BTES yet and the small spacing does not provide enough energy storage between boreholes, so the natural ground temperature drops quickly. The temperature of the GHE reduced very slightly over the years, because there was a little bit more heat extraction than heat injection into the GHE. The variation of the temperature of the GHE in an annual period was small too, due to the large spacing. The COP of the SAGSHP increased from 4.8 to 5.4 over the simulation period of 15 years, due to the annually temperature increase. The COP of the GSHP was around 4.6 and hardly changed from year to year, due to the small temperature change.

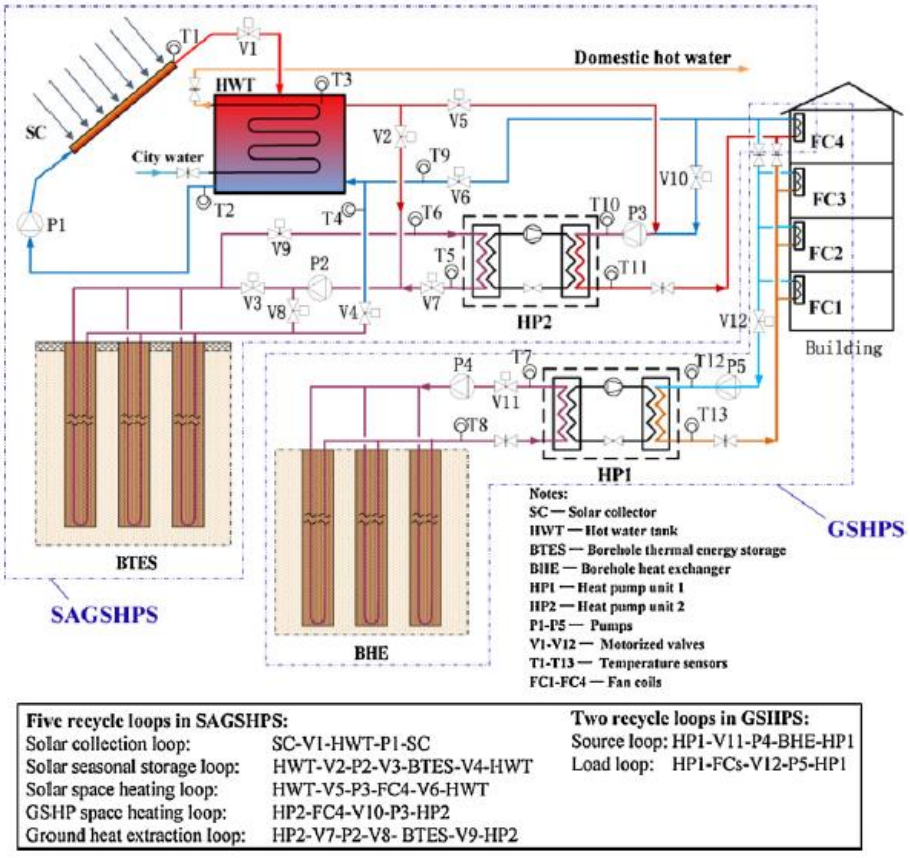

Figure 3: Proposed heating system in Tianjin, China (Wang et al, 2011).

In general, the results from the literature studies indicate that the systems are so complex and diverse, that it is difficult to draw any general conclusions about general design. The design will vary from place to place, due to weather, local conditions and energy performance. The prospects of the simulation projects have been so different and the possibility of combinations so many, that general applicable results are still not available. None of the reviewed earlier models make use of direct heating from the ground and geothermal heat pump at the same time. In our model we want to explore the use of direct heating with the ground further.

3 Description of the proposed system and working principles

3.1 Introduction of the GEL

The Green Energy Laboratory (GEL) is a study and test platform for analysis and experiments on building based energy systems, energy saving devices, indoor terminals and thermal environment. The building is under the climate of the middle and lower reached areas of Yangtze River. The building is located in Minhang campus of Shanghai Jiao Tong University. GEL integrates nearly 20 advanced technologies in terms of renewable energy, air conditioning, building automatic control and green buildings. Different types of solar collectors with corresponding solar air conditioning systems operate inside of the GEL. Cooling and heating power of GEL are provided by different heat pump technologies in terms of ground-, river-, air source heat pumps. The building is composed of three floors. It has a ground surface of 1600 m^2 and a height of 15.1 m (Favero & Milan Engineering, 2008). The first two floors host laboratories, a meeting room, a control room, student rooms and a exhibition hall. The third floor is designed like a residential space, and it is divided into apartments.

3.2 Overview of the proposed heating system at the GEL

The proposed heating system at the GEL combines a solar collecting system with borehole thermal energy storage and a ground-coupled heat pump. The solar collector and the ground storage are connected through a water tank. The simulated system also includes the indoor air-conditioning system. Valves are used to switch between the two heat sources; solar thermal energy and ground storage thermal energy. The working fluid throughout the whole system is water, because then the working fluid can flow though the solar collector, the fan coils, the borehole thermal energy storage, the hot water tank and the heat distribution system. The whole system can be divided into four different operation modes. One of the operation modes is used in the storage season. The remaining three operation modes are used in the heating season. The hot water production is not included in this system. Working places and offices often have a negligible hot water demand.

The four operation modes:

- Operation mode 1: Solar thermal ground storage → Storage season
- Operation mode 2: Solar direct heating
- Operation mode 3: Direct heat exchange with the ground storage } Heating season
- Operation mode 4: Geothermal heat pump

The operation modes in the heating season are presented in a prioritized order. Solar direct heating is the first choice, direct heat exchange with the ground is the second choice and the geothermal heat pump is the third choice. Direct heating with the solar collector and the ground is preferred to the heat pump, because these modes only use circulation pumps and thereby use less electricity. However, these two modes cannot cover the whole load, so a heat pump is needed. The heating is provided by the fan coils with the hot water coming from the solar storage water tank if the water is hot enough. If the tank water is not hot enough then the hot water is provided directly from the ground storage. If the water circulating through the ground storage is not hot enough for direct heating, then the hot water heated by the heat pump is used. The heat pump uses the remaining stored solar energy in the ground.

The solar collector subsystem includes evacuated tube collectors with an area of 216 m^2. The tank is connected to the ground storage and the space heating distribution system with the help of flow diverters, mixers and controllers. The switching between the different heating modes is based on tank temperature, storage temperature and solar radiation. The tank has a volume of 20 m^3. The ground storage volume consists of 9 boreholes. Each borehole has a length of 10 meters and a spacing of 5 meters. The geothermal heat pump is a water-to-water heat pump. Later on, some of the parameters presented in this section will be varied. The solar collector has several purposes. One purpose is to raise the ground temperature during storage season, so the ground can be used for direct heat exchange and also the source temperature at the evaporator side of the heat pump is raised, this will improve the annual performance factor and save electric energy. Second purpose is to cover some of the heat demand during heating season. The collector temperature is affected by the tank water temperature and the solar radiation. The tank temperature is also affected by the ground storage temperature and space-heating set point temperature.

3.3 Working principles of the main operation modes

In the following section each of the operation modes will be presented separately. The working principles of each mode will be presented. The sketches shown are only used as an illustration and do not show the exact setup with all components in the system. The valves and the controllers that connect and control the whole system are omitted from the drawings to give an easier view of the operation modes. The sizes of the components are not exact relative to each other.

3.3.1 Operation mode 1: Solar ground thermal storage

Solar thermal energy collected by the solar collectors is transferred to the water tank. Then the fluid on the source side in the tank exchanges heat to the fluid on the load side. The fluid on the load side circulates through the boreholes. The thermal energy is injected to the ground through the interaction between the boreholes and the ground. The whole ground temperature keeps an increasing tendency. This mode takes effect through the whole storage season. The solar collector is controlled by an ON/OFF differential controller.

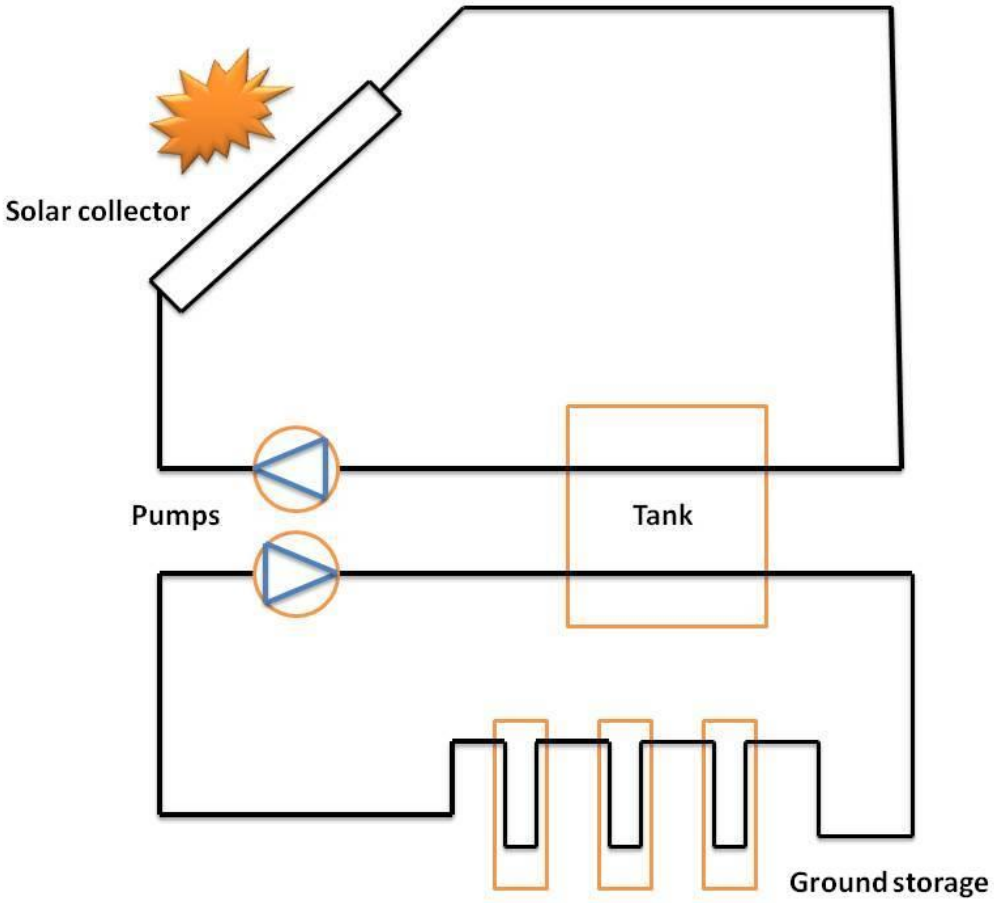

Figure 4: Sketch of operation mode 1: Solar ground thermal storage.

3.3.2 Operation mode 2: Solar direct heating

Solar collector is used to produce heat for the heating system during the heating season. When the water temperature in the tank is high enough for space heating (around 30-35°C for a fan coil heating terminal), the system can deliver hot water directly to the fan coil heating terminal. The hot water circulates through the tank. The hot water from the tank then exchanges heat with the air passing though the fan coil unit.

Generally, a lower temperature that is needed in the heating system will make it possible to utilize a bigger part of the available solar energy. This means that low-temperature heating systems such as floor heating, modern radiators and fan coils are beneficial when the solar collectors will be used to provide heat for space heating.

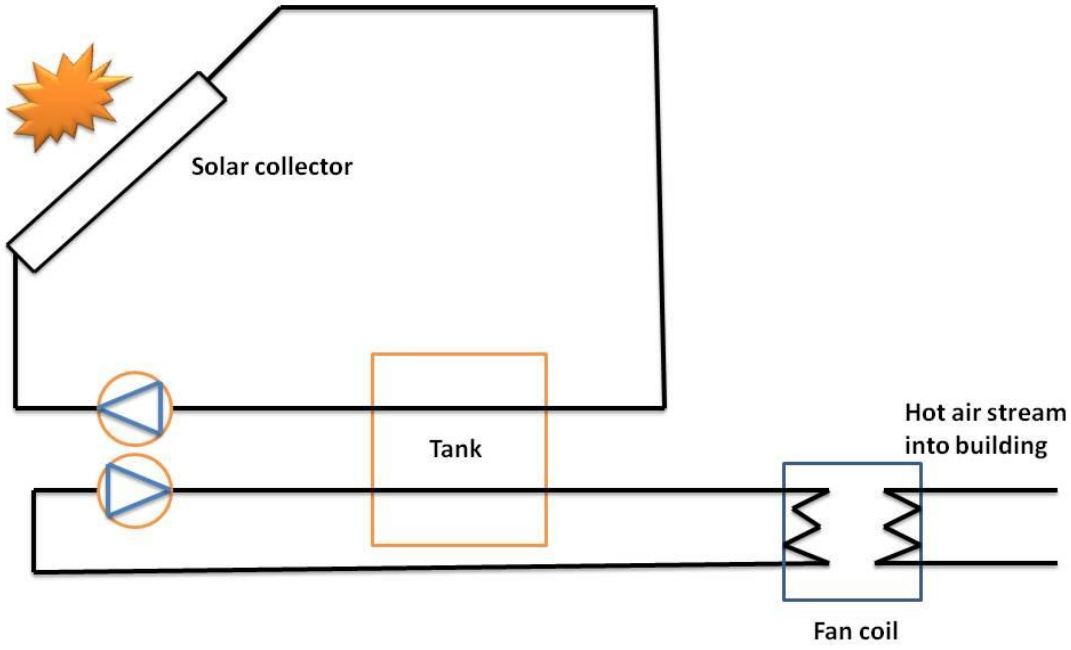

Figure 5: Sketch of operation mode 2: Solar direct heating.

3.3.3 Operation mode 3: Direct heat exchange with the boreholes

This mode takes effect when the solar collectors cannot produce sufficiently high enough temperatures to be used for the heating system. The boreholes are utilized to provide heating by direct heat exchange. After the storage season the ground has reached a certain temperature. The heat injected in the storage season is extracted from the ground by the ground heat exchangers to satisfy the space heating requirements.

The fluid on the source side is circulated though the boreholes and the exchanges heat with the air on the load side. The ground temperature should be higher than 30°C to operate in this mode. The whole ground temperature keeps a decreasing tendency. Since high temperatures are not desired at the inlet of the evaporator of the heat pump, it is favorable to use this mode first, so the ground temperature will be decreased. This mode will also decrease the operation time of the heat pump. The proposed heating system combines both use of direct heating and heat pump.

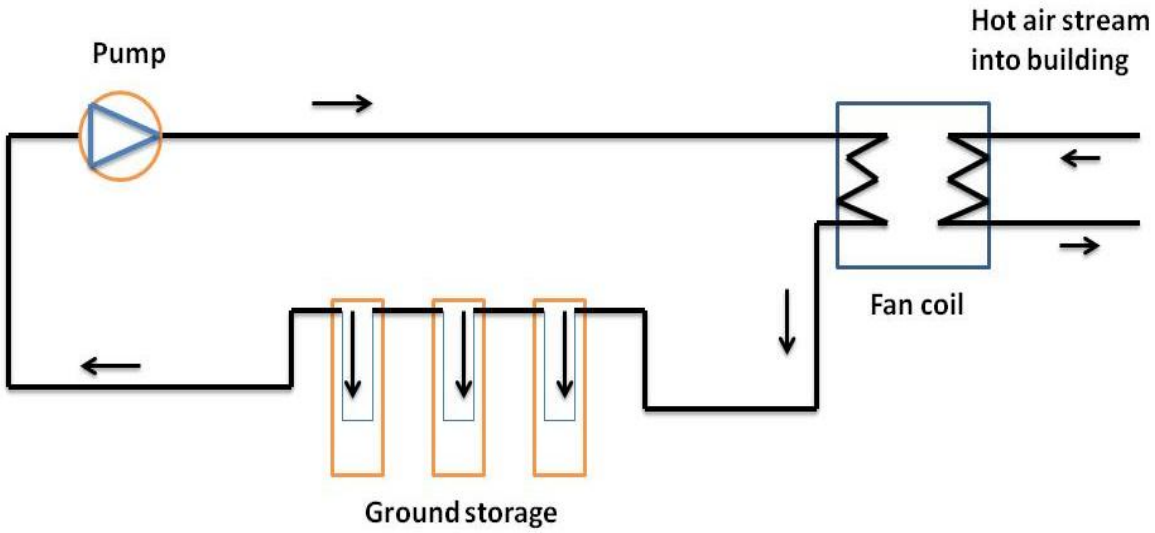

Figure 6: Sketch of operation mode 3: Direct heat exchange with the ground storage.

3.3.4 Operation mode 4: Geothermal heat pump

This mode takes effect when the ground temperature has dropped to a certain level and the ground temperature is not high enough to be utilized in direct heat exchange. The remaining heat in the ground storage is extracted by a heat pump. The ground storage acts as a heat source for the heat pump. The whole ground temperature keeps a decreasing tendency. The ground temperature has been heated to a higher level, so the COP of this heat pump will be higher than a normal geothermal heat pump with unheated ground. The compressor needs less work input. For a system without solar collector the source temperature may be only 15-18 °C in Shanghai, but for a system with solar collector, the source temperature may be around 20-30 °C.

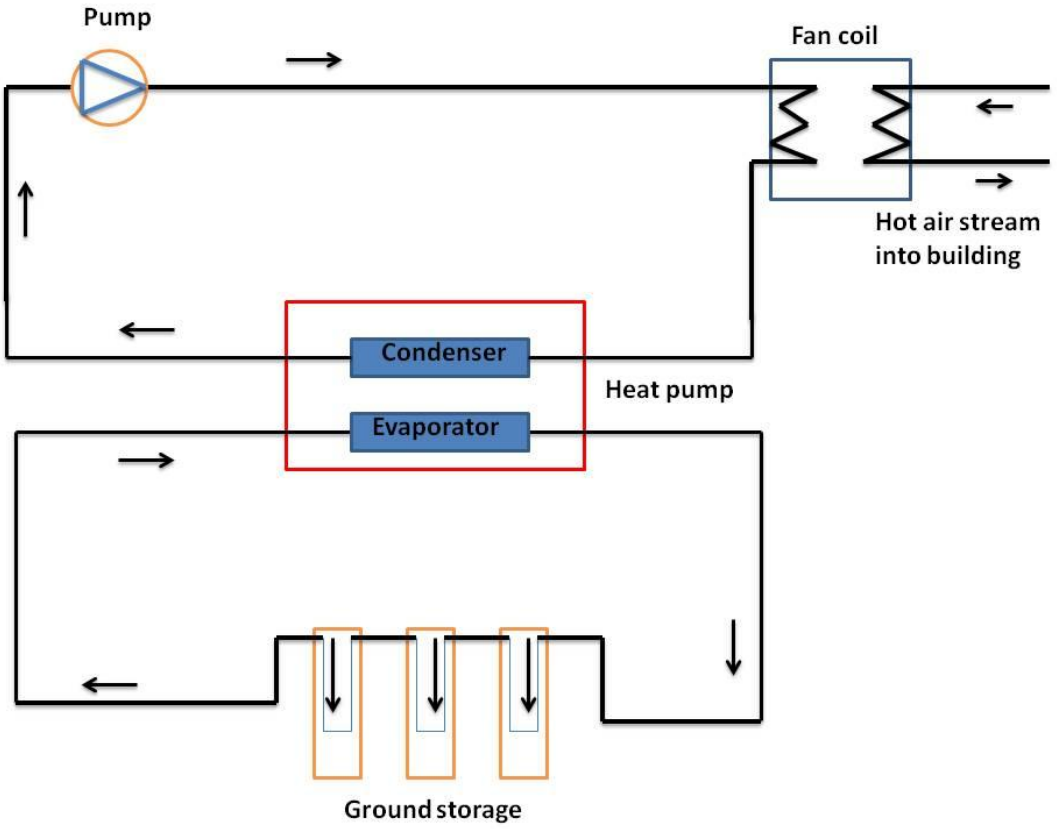

Figure 7: Sketch of the operation mode 4: Geothermal heat pump.

4 Seasonal thermal energy storage

4.1 Overview of Seasonal thermal energy storages

Demands for heating in a building vary on daily, weekly and seasonal basis. Solar energy is a renewable energy source that can cover some of these demands, but one of the main factors that limit its application is that it is a cyclic, time-dependent energy source. Most of the time, the supply of solar energy does not vary in accordance with the energy demands of the buildings. In the winter when the heat demand is at its highest, the sun is often absent. A storage that can keep large amounts of energy and have small losses, make it possible to utilize the solar energy in the winter. The solar energy can be stored during the summer and the stored energy can be used for heating during the winter. This kind of storage is called seasonal storage. Since seasonal storage requires large inexpensive storage volumes, the most promising technologies are mostly found underground. Such systems are called Underground Thermal Energy Storage (UTES) (Pavlov & Olesen, 2009). These kinds of systems can make use of soil, rock and groundwater as storage mediums. Basically, UTES systems can be used as energy source and sink when supply and demand for energy does not coincide. Among the UTES systems developed since 1970's, four different types of storages turned out most promising, illustrated in Figure 8 (Pavlov & Olesen, 2009):

- Aquifer Thermal Energy Storage (ATES)
- Water Tank Storage
- Water-Gravel Pit Storage
- Borehole Thermal Energy Storage (BTES)

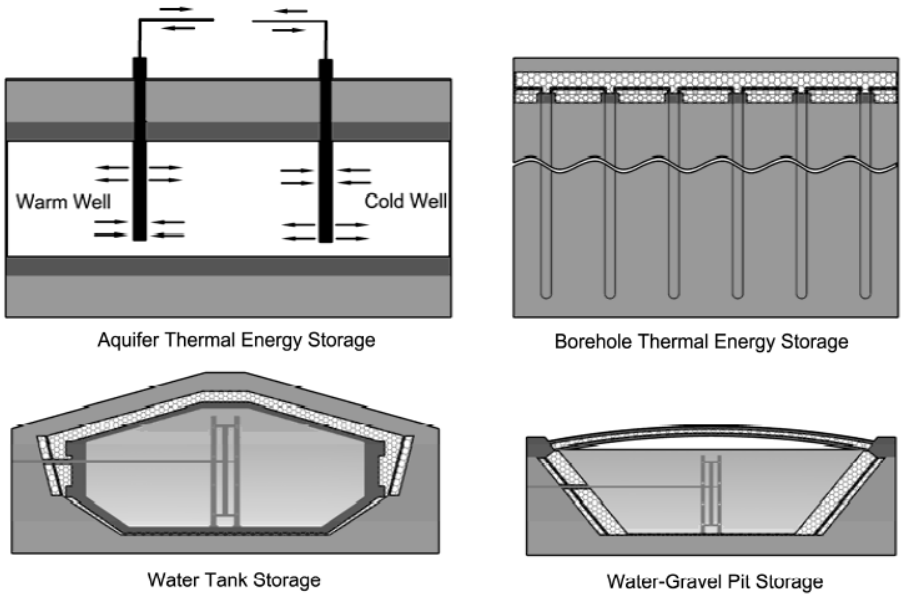

Figure 8: Types of seasonal thermal energy storages (Pavlov & Olesen, 2009).

The selection of storage type depends on the hydro geological and geological situation in the ground at the respective construction site (Bauer, 2009). It is important to perform a preliminary geological examination of the site. The proposed heating system at the GEL uses BTES, so the emphasis will be on this kind of system. The other systems will be briefly presented.

4.1.1 Aquifer Thermal Energy Storage

Heat transport in this kind of storage is both convective and conductive. Aquifers are below-ground widely distributed sand, gravel, sandstone or limestone layers with high hydraulic conductivity and are filled with groundwater. If there are no impervious layers above and below and only low natural groundwater flow; the below-ground layers can serve as a storage medium for the storage of heat or cold. Two wells are drilled into the aquifer and groundwater is pumped from or to the wells for either extraction or injection of thermal energy. During charging periods for the storage, cold groundwater is extracted from the cold well, heated up by the solar system and injected into the hot well (Schmidt, Mangold, & Müller-Steinhagen, 2003). In discharging periods the flow is reversed, the stored energy in the hot well is then utilized and the groundwater is injected into the cold well. Due to different flow directions, the system is equipped with pumps, injection and extraction pipes. To minimize thermal mixing within the aquifer, the hot and the cold wells have to be spaced at an appropriate distance apart.

4.1.2 Water Tank Storage

Water tank storage is usually built as a steel or reinforced pre-stressed concrete tank. The tank can be fully or partially buried in the ground. This type of storage can be built almost independently from geological conditions. Advantages with this storage are that water has a high specific heat capacity and high capacity rates for discharging and charging.

4.1.3 Water-Gravel Pit Storage

The store consists of a pit with a watertight plastic liner. The ground storage material, which is a gravel-water mixture, is filled into the pit. The side walls and the top of the store are heat insulated. Heat is charged out and discharged into the store by direct water heat exchange or by plastic pipes installed in different layers inside the store. This kind of store does not require load-bearing structure, because forces are taken down to the side walls and to the bottom by the gravel.

4.2 Borehole Thermal Energy Storage

In borehole thermal energy storage, the heat is stored directly in the ground. Heat exchange between the heat carrier fluid and the storage takes place in a channel system, a borehole or a duct. The heat carrier fluid is circulated through the ducts or the channel systems. The boreholes are usually 10-200 meters below ground (Pavlov & Olesen, 2009). Each borehole, duct or channel that is used for heat exchange in the ground is called ground heat exchanger. Common suitable geological formations are unsaturated soil, clay, peat or rock (Reuss, Beck, & Müller, 1997). Borehole thermal energy storages have horizontal temperature stratification from the centre to the borders. This is because the heat transfer from the duct system to the surrounding ground is driven by heat conduction and not convection (Schmidt & Miedaner, 2012). Because of the heat losses to the surroundings there will be a temperature decrease at the boundaries of the storage unit. To support the horizontal stratification in the ground, the supply pipes are connected in the centre of the storage and the return pipes are connected at the boundaries of the storage. During heat injection to the storage, the flow direction is from the centre to the boundaries of the storage to obtain high temperatures in the centre and lower ones at the boundary of the storage. During heat extraction from the heat storage the flow direction is reversed. The specific arrangement of the ground heat exchangers depend strongly on the geological medium.

There are typically a large number of boreholes in systems made of rock. The storage holes are uniformly placed in the storage region. Solid rock systems can either be open or closed. In open systems; a single plastic tube is inserted into the channels which the heat carrier fluid is carried down to the bottom. The region between the plastic tube and the borehole wall constitutes the channel for upward flow. Extraction of the heat carrier fluid takes place at the top of the storage and the fluid is taken further to the main distribution system. Since the heat carrier fluid is in direct contact with the storage walls it will be a very good heat transfer between these two media. Unfortunately, open systems are not suitable for all sites. The geo-hydrological and the geochemical conditions at a site are often unfavorable for an open system (Hellström, 1989). A closed system can be used instead, by inserting one or more U-tubes into the borehole. The U-tubes have a 180° smooth bend at the bottom. The heat transfer between the heat carrier fluid and the storage walls happens though the plastic material of the tubes. Thus the thermal contact between the media is not good as in the open system.

For soft media (e.g. clay, soil) the duct system can be obtained by driving down vertical U-tubes.
While water or some other fluid is running in the U-tubes, heat can either be charged or discharged into the ground. The energy is transferred to the ground, which serves as thermal storage, and the ground is heated up to required temperatures. Good thermal contact between the ground and the tubes is required to allow a good heat transfer rate per unit area of the tubes. U-tube-materials depend on the temperature required temperatures of the system. The boreholes have to be refilled from the bottom to the top with a special material providing good thermal contact between the tubes and the ground. These materials can be enhanced grouting, cement betonite mixture or sand. The borehole spacing in soft media systems is normally smaller than the spacing used in the rock systems, this is because of the lower heat conductivity of soil. That is, the thermal influence of neighboring boreholes is smaller in soil systems. For the studied system at the GEL, the boreholes are placed in soil, because this is the most available and suitable geological formation at the GEL.

Depending on the temperature levels in the storage there are different ways to extract energy from the storage. If there are low temperatures (e.g. 0°C-30°C); energy is extracted by a heat pump to raise the temperatures. If there are high temperatures (e.g. 30°C -80°C); energy is extracted directly from the boreholes.

The boreholes are hydraulically connected in series to a row and certain rows are connected in parallel. One advantage of this type of storage is the possibility of modular design. Additional boreholes can easily be connected and the size of the storage can grow with the size of the heat load.

4.3 Heat transfer analysis in borehole thermal energy storages

The model described here is the well known Duct Ground Heat Storage (DST) model. The DST Model will be used in this report for simulating such as the amount heat transferred from the fluid circulating in a borehole and the temperature in the ground. In the DST model in TRNSYS the heat transfer problem is solved by splitting the problem into simpler problems.

The thermal process in the storage region with its borehole system is quite complicated. The main model complexity is caused by the spatially distributed thermal process in the ground. This can be described by the governing equation for heat conduction, which is also known as Fourier's equation:

$$\frac{1}{a}\frac{\partial T}{\partial t} = \nabla^2 \mathrm{T}$$

Equation 1: Fourier's equation

T Ground temperature [°C]

a Thermal diffusivity [m^2/s]

The method of finite differences is a famous tool that can calculate the temperature field at several grid points. However, the number of temperature variables introduced can be very high. To keep the model simple as possible, the total thermal processes in the ground are divided into two sub-processes: a small-scale local thermal process around each duct and a large-scale global thermal process between the overall store and the surrounding ground. Each sub-process is treated separately. The total thermal process is given by superposition of the sub-process. The global thermal process is governed by the amounts of injected and the extracted heat and the thermal properties of the ground. The local thermal process depends largely on the specific arrangements of the flow channels in the ground heat exchanger. There are conductive and convective thermal processes in the ducts and the store, respectively.

After a short time of operation of the boreholes, maybe after some days, it can be seen that the shape of the local temperature field will become steady (Franke, 1998). Neglecting the time variation, the dynamic model for the local thermal process can be replaced by an analytical description of the local temperature field under steady-flux conditions. Accordingly, the heat transfer is assumed here to occur via time-invariant thermal resistances between the duct and the ground storage volume. The resistances are given by a logarithmic function of the duct spacing. The large-scale global thermal process in the ground is modeled by a rectangular mesh of a few hundred ground cells.

Superposition is used on three solutions; the local, global and the steady-flux solutions. These are the solutions to the three heat transfer problems: the global heat transfer between the storage volume as a whole and the far-field, the local heat transfer occurring around the boreholes at a short time-scale and a local steady-flux heat transfer around the nearest pipe (Spitler et al, 2009). The local and the global solutions are linked by sub-regions. Heat transfer between the circulating fluid and the ground is given by an analytical solution applied over borehole segments which is then used as a boundary condition in the local problem. At the end, a steady-flux analytical solution is used to redistribute the energy into the BTES volume.

The boreholes are assumed to be uniformly placed in the BTES volume, which has a cylindrical shape. The ground in the storage volume is assumed to have homogenous thermal properties. Outside the storage volume the ground may consist of different layers and thermal insulations can be placed on top of the storage (Holmberg, 2009).

4.4 Equations for describing the borehole thermal energy storage

There will be heat transfer between the heat carrier fluid and the ground when there is a temperature difference between these two parts. The fluid will lose or gain energy and its temperature will vary along its flow path through the storage volume. The heat balance for the heat carrier fluid is given by Equation 2.

$$c_f q_{fp} \frac{\partial T}{\partial s} + \alpha_p (T_f - T_a)$$

Equation 2: Heat balance for the heat carrier fluid (Hellström, 1989)

c_f Specific heat of the fluid [kJ/kgK]

q_{fp} Fluid flow rate per unit length of pipe [kg/hrm]

α_p Heat transfer coefficient [W/m^{2}K]

T_f Fluid temperature [°C]

T_{amb} Temperature of surrounding ground [°C]

s Length coordinates along the flow path [m]

The rate of injection of energy to the storage volume is given by Equation 3.

$$Q_{inj} = c_f Q_f (T_{fin} - T_{fout})$$

Equation 3: Rate of injection of energy to the storage volume (Hellström, 1989)

Q_{inj} Rate of injection of energy to the storage volume [kJ/hr]

$\dot{m}_f$ Mass flow of the fluid [kg/hr]

T_{fin} Inlet temperature of the fluid [°C]

T_{fout} Outlet temperature of the fluid [°C]

Storage capacity is the maximum amount of thermal energy that can be stored in the ground storage. The storage capacity C is given by the minimum and maximum average storage temperature during a season. It also clearly depends on the integration of the storage in the system, the system type and operation. In particular, the maximum storage temperature is conditioned by the temperature level of the heat source, the volume of the storage and the storage heat capacity.

$$C = \rho c_f V (T_{max} - T_{min})$$

Equation 4: Heat capacity for the storage volume (Pahud, 2002)

C Storage capacity [kJ]

ρc_f Storage heating capacity of the soil [kJ/m^{3}K]

V Ground storage volume [m^3]

T_{max} Maximum average storage temperature during one season [°C]

T_{min} Minimum average storage temperature during one season [°C]

The storage heat loss depends mainly on the mean annual storage temperature, the mean ambient temperature, the equivalent heat loss factor and the surface area of the storage border. The heat loss factor is conditioned by the store design (insulation of upper parts of storage border, geometry, etc.) and the ground properties. The factor is time-dependent. A transient thermal process usually lasts a few years until a steady-state thermal process is established. Forced and free convection in the ground will increase the heat losses. The storage heat losses can be reduced by storage insulation at the top of the storage, suitable storage shape and low temperature heat distribution. In the case of dominant conductive thermal processes, the storage heat losses can be found by Equation 5 for steady-state conditions. The heat transfer is only by conduction in ground storages with negligible ground water flow (Chapuis & Bernier, 2009).

$$E_{loss} = UA(T_{soil} - T_{amb})t_{year}$$

Equation 5: Storage heat loss (Pahud, 2002)

E_{loss} Annual storage heat losses [kJ]

U Equivalent mean storage heat loss factor [kJ/hrm^{2}K]

T_{soil} Mean annual storage temperature [°C]

T_{amb} Mean annual ambient temperature [°C]

t_{year} Duration of one year [s]

4.5 Borehole configuration

There are two types of use of the boreholes. One use can be long-term seasonal storage, which means storing injected solar heat during summer. One other use is to be a heat source for a heat pump and heat is extracted by the heat pump without. The latter use does not normally include solar collectors and the ground is naturally recharged in the summer. Typically, this kind of use only consists of one or two boreholes, while seasonal storages consist of several boreholes. There is a fundamental difference between a borehole configuration for storage of thermal energy and heat extraction. When storing energy the interaction between boreholes is favorable and therefore the boreholes should be placed in a compact pattern with smaller spacing. While for a system where either heat extraction or injection is the main purpose, interaction is undesirable and therefore prevented by a spread pattern with long distance between the boreholes (Holmberg, 2009).

Heat extraction from boreholes cools down the surrounding ground and the cooled area increases with time. When several ground heat exchangers are situated in vicinity of each other, the cooling of the ground will lead to a mutual influence. This may occur in areas with single family dwellings and can lead to undersized existing ground heat exchangers, if new ground heat exchangers are situated too close (Kjellsson, 2009). The reason heat extracting boreholes need a defined distance separating them is to compensate for thermal convection and conductivity between boreholes and ensure there is sufficient area for the natural regeneration of the ground temperature surrounding the borehole. If the ground cannot recharge naturally from the surroundings then the ground temperature will gradually drop (Värmebaronen, 2011).

As energy is being extracted or injected into the borehole, the surrounding ground layers will heat up or cool down over time. Energy is extracted from the ground when a fluid that is colder than the median temperature of the earth is circulated through the boreholes. Then the surrounding ground layers will try to replace the energy that is removed from the ground by heating up the area within the thermal envelope. This can happen when the heat pump is operating in the heating mode. If the boreholes are too close together then energy transfer between the boreholes and the ground will be at a rate higher than the earth can accommodate and the ground temperature will be equalizing close to the temperature of the thermal fluid. The thermal communication would be between the boreholes instead of between the source and sink. This will result in reduced thermal efficiency of the boreholes in the field, which in turn will lead to equipment stress or system inefficiency (Hoffman, 2012). The ground temperature can be charged with solar heat from solar collectors during the summer. If there are shortage of available space in the ground the solar heat makes it possible to space the boreholes more closely than the usual. Depending on the load and available space the boreholes can be placed in different patterns. Because of the thermal interaction will give different thermal response. A closed pattern would have better performance as energy storage and also be more sensitive for unbalanced loads than an open pattern.

4.6 Temperature characteristic of the ground

The natural ground temperature is dependent on the earth's surface temperature, i.e. solar radiation (Yuehong, 2004). The ground transports heat slowly and has a high heat storage capacity, the ground temperature changes slowly. Depending on the depth of measurement, the time of the temperature change can be in order of months or years. At depths of less than 2 meters the ground temperature will show marked seasonal variation above and below the annual average air temperature (Rawlings

et al, 2004). As the depth increases the seasonal swing in temperature is reduced and the maximum and minimum temperatures in the soil begin to lag the temperatures at the surface. The deeper the borehole depth the more stable the ground temperatures and the higher the collection efficiency, but the installation costs will increase accordingly.

Figure 9 shows the seasonal variations of the ground temperature distributions in Shanghai. In the winter the ground temperature close to the surface is lower than compared to deeper regions. This means that the heat is transferred up to the surface. At the end of March, the situation reverses and the heat are transferred down from the surface. The changes that occur in the deeper region lag farther behind those of the shallower ground due to the slow heat transport in the ground. As a consequence of the low thermal conductivity, the soil can transfer some heat from summer to winter. The ground temperature profile will shift later in the year so that it more closely matches the demand for heating and cooling. At the depth of 8 meters the ground temperature tends to be constant throughout the year and approximately equal to the annual air temperature, 18 °C.

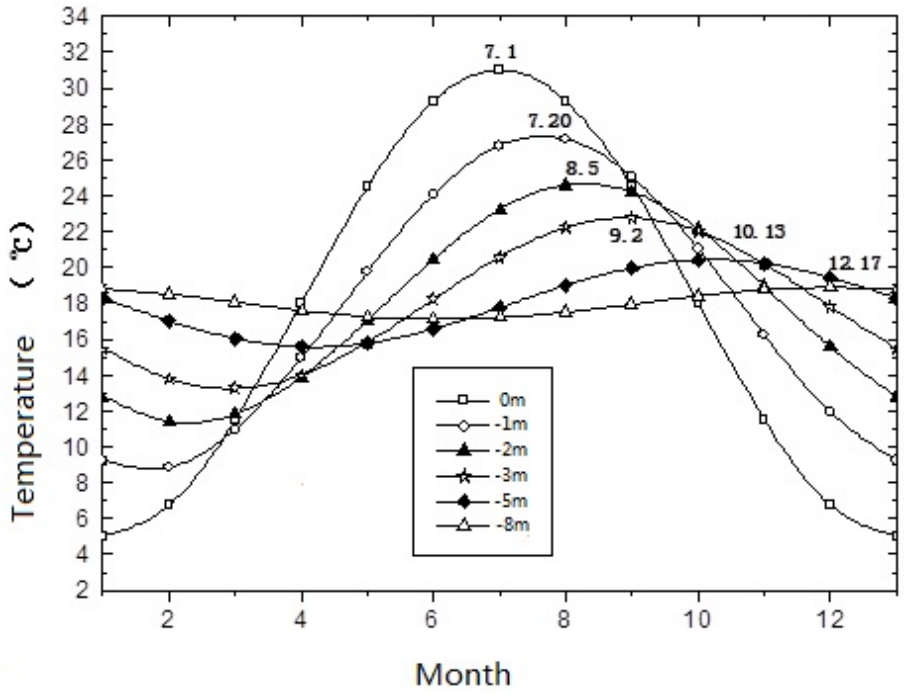

Figure 9: Seasonal variations of the ground temperature distribution in Shanghai.

4.7 Balance of thermal loads of the borehole thermal energy storage

The stable temperature of the ground provides good performance as long as the balance between the extracted and injected heat is kept. If the heat extracted during the winter can be compensated during the summer the temperature surrounding the boreholes will change little and thereby also the performance of the system. However, if the injected heat is less than the extracted the temperature will subsequently sink in the ground and the performance of the system will be weakened (Holmberg, 2009). The temperature of the earth cannot satisfy the energy demand for a long time. Long term operation could bring an irreversible temperature drop of the soil so that the COP of the heat pump could be reduced significantly (Xi et al, 2011). Although there is a ground temperature recovery in transient seasons, the imbalance cannot be ignored. This effect can be

moderated by increasing the ground storage size, but increasing the ground storage size can be very expensive (Gentry et al, 2006). Another alternative can be to add an additional heat source, such as solar collectors. Charging the boreholes with solar heat during the summer can be beneficial. The solar collectors can also improve the heat pump's operating condition during the winter. Solar heat can be a valuable supplement when the borehole is too short.

The ground temperature can be kept unchanged on an annual basis by estimating the amount of heat that is extracted from and injected into the ground through the borehole thermal energy storage. However, it is difficult to design the heating or cooling system with an exact balance because of many uncertainties. The uncertainties could be that the heat pump cannot operate under the rated condition resulting in varying COP of the heat pump; building's heating or cooling load cannot be determined exactly, the air conditioning unit can be turned on/off by occupants in different rooms; and extreme weather conditions will affect the building's heating and cooling load.

5 Geothermal heat pump

Geothermal heat pumps are heat pumps that exchange heat with the ground. A geothermal heat pump can use high, medium and low temperature heat sources. High and medium temperature heat sources are usually the product of the thermal flows produced by the molten core of the earth. While low temperature heat sources are near ambient temperature and are mostly attributable to the solar energy incident on the ground and ambient air. In this study we will focus on the geothermal heat pumps that use low temperature heat coming from the sun and absorbed in the ground. Heat pumps extract the low temperature thermal energy and raise the temperature to the required temperature for practical use. Geothermal heat pumps can provide an environmentally friendly and economically advantageous option for space heating.

The heat can be extracted from the ground through closed or open loop systems. The most common configuration is closed loops systems, where the heat transfer fluid is enclosed in a circulating loop and has no direct contact with the ground (Self, 2012). Heat transfer with the ground occurs through the piping material in the borehole thermal energy storage. These closed loops systems can collect heat from the ground either by vertical or horizontal piping in the ground. Open loop systems circulate well or surface water.

5.1 Vertical and horizontal closed loop system

A vertical closed loop system consists of a group of vertically oriented heat exchange pipes. As described before in chapter 4.2, a hole is bored into the ground and pairs of pipes, connected at the bottom by an U-shaped connector, are fed into the hole. One of the advantages with vertical loop configuration is reduced installation area; this configuration requires least amount of surface ground area. Vertical loops are generally considered when land surface is limited. Another advantage with this configuration is that the temperature below a certain depth remains constant over the year. This will allow a consistent heat pump performance and reduces overall loop length. Also, vertical loops has low landscape disturbance, since drilling has a reduced impact compared to trenching. The main disadvantage is the cost of drilling. The drillings costs are much higher than horizontal drenching costs. Consequently, vertical loops systems are normally more economic for larger applications.

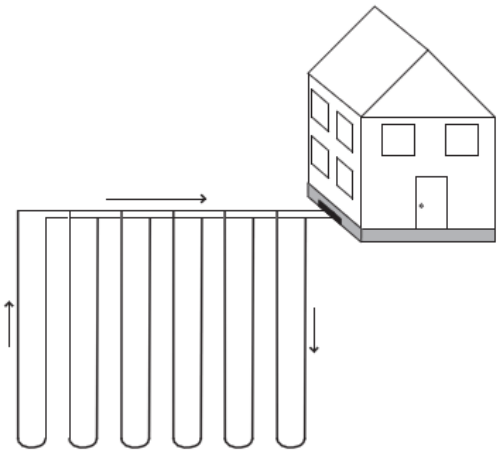

Figure 10: Vertical closed loop heat exchange system for a geothermal heat pump (Self, 2012).

Horizontal closed loop systems are more common where ample area is available. The ground loop is laid out horizontally slightly below earth's surface in backfilled trenches. The trenches that house the piping usually do not exceed more than a couple meters below the surface, but in areas of frost they are located below the frost line. Since the depths are shallower than the vertical loop configuration there is increased interaction between the soil and the ambient environment. This will lead to daily and annual variation of ground temperatures, which affects the heat transfer and system performance. The thermal properties of soil will fluctuate with rain, snow, vegetation growth and shade. Because of these factors, longer pipe lengths are required than for vertical arrangements. Horizontal arrangements require a water/antifreeze mix to protect against freezing during winter in cold climates. The viscosity of the antifreeze mix will increase the pumping energy, which will decrease the heat transfer rate and thus reduce overall system efficiency.

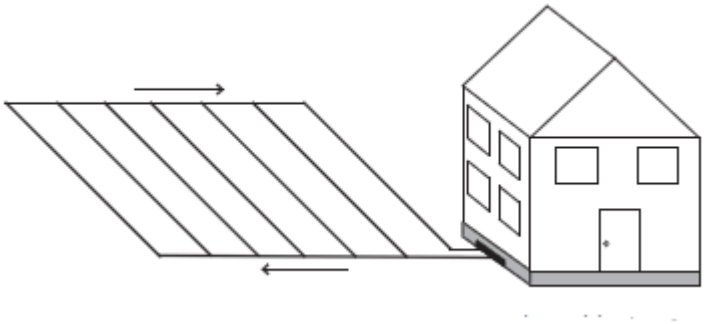

Figure 11: Horizontal closed loop system for a geothermal heat pump (Self, 2012).

5.2 Principles of geothermal heat pumps

A geothermal heat pump moves thermal energy between the earth and the heated space by controlling pressure and temperature by means of compression and expansion. The main components in a heat pump are compressor, expansion valve, condenser and evaporator. The heat from the ground loop is transferred to the refrigerant in the evaporator. The refrigerant boils into a low pressure vapor and the temperature increases slightly. The vapor enters the compressor, where the pressure is increased, leading to a high temperature and high pressure vapor. Then the vapor enters the condenser. The refrigerant is at higher temperature than the room, which will lead to heat transfer from the refrigerant to the room. The vapor changes to a high pressure and a high temperature liquid. The liquid passes the expansion valve and the temperature is decreased. The refrigerant enters the evaporator to begin another cycle. The compressor is driven by electricity.

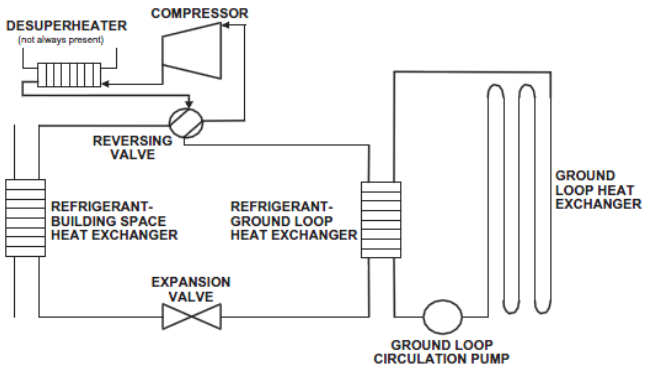

Figure 12: Schematic of a geothermal heat pump system including desuperheater (Self, 2012).

The ratio of heat output to the amount of energy input of a heat pump at given operating conditions is defined as the Coefficient of Performance (COP). The heat pumps performance are often described with the COP. Heat pumps deliver more useful thermal energy than the input net work, so this ratio yields an efficiency greater than one. The COP is given by Equation 6.

$$COP = \frac{Q_{load}}{W_{cycle}} = \frac{Q_{load}}{Q_{load} - Q_{source}} = \frac{T_{load}}{T_{load} - T_{source}}$$

Equation 6: COP for heat pump (Moran & Shapiro, 2006)

Where Q_{load} is the amount of useful energy discharged from the heat pump system and W_{cycle} is the net work provided into the system. Q_{source} is the energy quantity drawn from the surrounding atmosphere, for a geothermal heat pump the energy would be drawn from the ground. The COP depends on the temperature of the input water from the ground loop, which depends on geological conditions and technical conditions. The geological conditions will depend on the thermal and hydraulic parameters of the underground and local climate. The technical conditions will depend on the length and type of ground heat exchanger, material, type and quality of grouting. Other factors that affect the COP are the heating and cooling load, the type of heating system in the building and the relevant supply temperatures. The values for the COP are often given at different inlet temperatures to the evaporator and outlet temperatures of the condenser. For a inlet temperature to the evaporator of 0°C and a outlet temperature of the condenser of 35°C, values close to COP=5 can be reached. For outlet temperatures of 50°C, the COP can still reach 3.5. These results are based on measurements in Europe, mainly in the Swiss heat pump test centre in Toss (Sanner, 2003). The Water-Source Heat Pump Engineering Committee in USA recommends a COP of 3.1 for heating for ground loop systems (Sanner, 2003). As illustrated in Figure 13 the COP can have substantial higher ratings than 3.1.

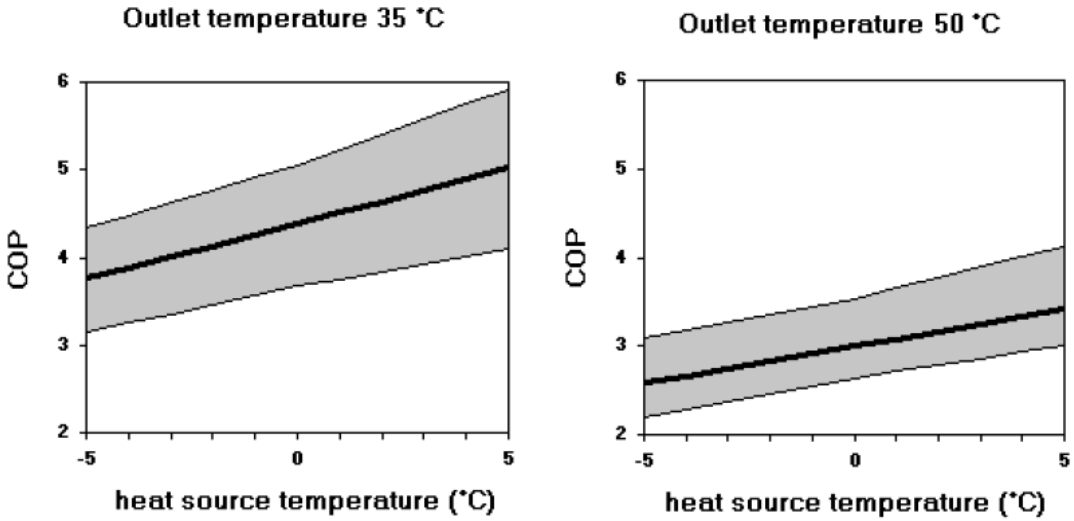

Figure 13: Values of COP for water heat pumps at different temperature conditions of the heat source temperature and outlet temperature of the condenser. Measured in the Heat Pump Test Centre in Toess (Kjellsson, 2009).

When comparing systems, the COP does not describe the performance over a period. The Seasonal Performance Factor (SPF) can be regarded as a mean COP for an entire heating season. The SPF takes not only one testing point into account, but also a period, e.g. a whole year. It is defined as the ratio of the heat output and the total amount of energy input during a whole season (Engineering Toolbox, 2011). It takes into account the variable heating demands and the variable heat source temperature over the year (IEA Heat Pump Centre, 2012). Usually, the SPF varies between 3.0-3.8 (Sanner, 2003). In cases where high quality standards for all components of a geothermal heat pump system are applied and also an optimum building heating system exists, values of SPF of 4.0 can be achieved. It is visible in Figure 13 the COP increase with increasing source temperature. So ground storages that are heated by a solar collector can raise the COP of the heat pump. The lower the load output temperature and the higher the source input temperature the more efficiently the heat pump will operate.

Existing geothermal heat pumps features makes them suitable only for operation with low-temperature heating systems. This limits the use of geothermal heat pumps to mostly new buildings, because many of the geothermal heat pumps are not designed to meet the high supply temperature demands of the older heating systems installed in many buildings all over Europe. The design temperature of the condenser is often around 45°C and return-temperature is around 40°. While the old heating systems often have the design temperatures of 80/60°C in the forward and the return pipes in the distribution systems (Kjellsson, 2009). In older buildings the radiators might be undersized to maintain the desired temperature. The above upper temperature limits in commercial heat pumps restricts their application to low-temperature heating systems such as fan-coils, low-temperature radiators or floor heating. Installation of heat pumps in existing buildings may require total replacement of the high-temperature system with a low-temperature heating system. It could be substituting the radiators with fan coils or other advanced systems and installing pipes with larger diameters (Sanner et al, 2003). From Equation 6 we can see that the efficiency of a heat pump is a function of difference between the temperature of the source and the temperature of the load. The smaller the temperature difference between the source and load temperature, the higher the COP will be. It is therefore favorable to use the lowest possible temperature distribution system.

5.3 Status of geothermal heat pumps

The main advantage of geothermal heat pumps is their ability to utilize soil and ground water temperatures between 5°C and 30°C, which is common at reasonable depths around the world. As of 2004 about 30 countries were using geothermal heat pump systems. The leading countries are USA, Sweden, Germany, Switzerland, Canada and Austria. By the end of 2004 the worldwide installed ground heat pump thermal capacity was around 12 GW which required an annual energy usage of 20TWh (RETScreen International , 2005). Research and practical demonstration on geothermal heat pumps are still in the exploring and experimental stage and many challenges need to be investigated, especially the enhanced heat transfer of ground heat exchangers and the combination of seasonal storages and geothermal heat pumps (Gao et al, 2008). According to Gao et al (2008) there were 2537 demonstration engineering projects about GSHP in China in 2005 and 129 of these projects were carried out in Shanghai. The growth of geothermal heat pump technology has been slower than for some other renewable and conventional energy technologies. This can be due to significant capital cost compared to other systems, non-standardized system designs, limited knowledge in the installation of geothermal heat pumps and limitations on use through government policies (Self, 2012).

6 Solar thermal collectors

6.1 Principles of solar thermal collectors

A thermal solar collector is an apparatus that gathers solar radiation and converts it into heat. The heat is transferred to a heat carrying fluid that transports it to hot water, space conditioning equipment or thermal energy storage. A typical solar collector consists of three main parts: Absorber, cover and insulation (Andresen, 2008). Not all of the collectors have cover or insulation, but to utilize waterborne heat in colder climate it is necessary to include these parts. The cover protects the absorber from being cooled down. It can also increase the efficiency, because the cover lets all the short waved radiation pass through, while it prevents all the long waved radiation from getting out. The cover is usually made of glass or plastic, but cover with low emitting coating or transparent insulation material can also be used. Low emitting coatings or transparent insulation materials will reduce the heat loss through the cover, but it will also reduce the transmission capabilities of the cover. Therefore, it will always be a matter of optimal solution for each case.

The absorber is often a thin metal plate which is colored black or has a selective surface. A selective surface absorbs visible light in the same way as a black surface, but it emits less infrared radiation. Therefore the heat loss is less in a collector with a selective surface, which will give a more energy efficient collector (Andresen, 2008). Typical selective surfaces consist of a thin upper layer, which is highly absorbent to shortwave solar radiation but relatively transparent to long wave thermal radiation. Selective surfaces are most useful when the collector surface temperature is much higher than the ambient air temperature. The absorber is the most important part in the collector because it transforms radiation to heat. The absorbed radiation sets the molecules on the surface in motion, and radiation energy is converted into thermal radiation.

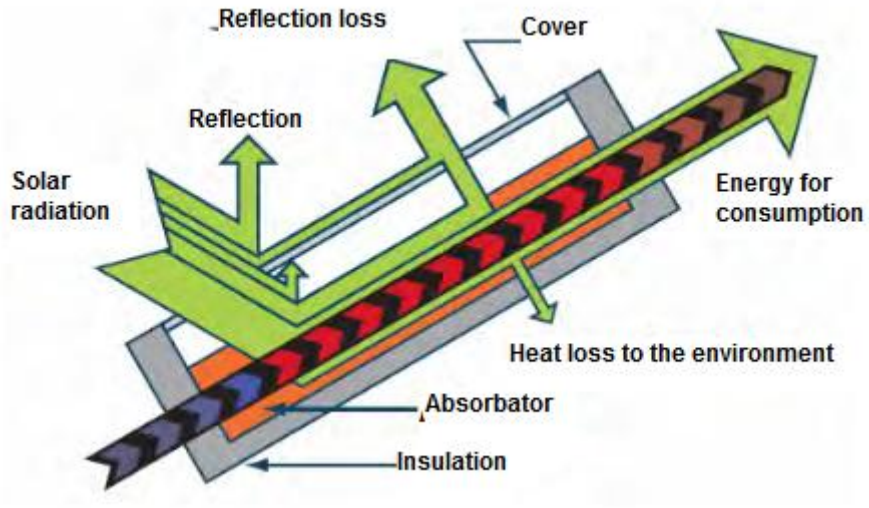

Figure 14: Principle drawing of a solar collector (Rindal & Salvesen, 2008).

6.2 Evacuated tube solar collectors

The proposed heating system at the GEL makes use of evacuated tube solar collectors, so it will be emphasized to present this kind of collector. In an evacuated collector the absorber is placed inside a vacuum-sealed glass tube. The vacuum envelope reduces convection and conduction losses, so the collector can operate at higher temperatures than the flat plate collectors (Kalogirou, 2004).

There are many different types of evacuated tube solar collectors. One of the most common type features a heat pipe placed inside a vacuum-sealed glass tube. The heat pipe is a sealed copper pipe which is attached to a black copper fin that fills the tube (Kalogirou, 2004). The black copper fin is the absorber. Inside the heat pipe there is a small amount of fluid. Due to the vacuum, the fluid will evaporate at very low temperatures. Solar heat will evaporate the liquid and the vapor will travel to the heat sink region where it condenses and releases its latent heat. At the top of each tube there will be a metal tip which acts as a condenser. The condensed fluid returns back to the heat pipe and the process is repeated. A manifold is mounted at the top and the fluid to be heated will flow through the manifold. The fluid picks up the heat from the tubes, then the heated liquid circulates through another heat exchanger and gives off its heat to a process or to water that can be stored in a storage tank. The efficiency of the evacuated tube solar collectors is higher at low incidence angles; this will give evacuated tube collectors an advantage over the flat plate collectors during day-long performances (Kalogirou, 2004).

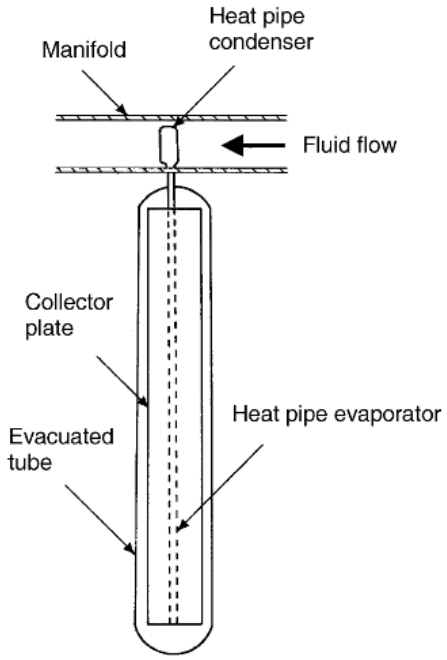

Figure 15: Schematic diagram of an evacuated tube collector (Kalogirou, 2004).

Another type is the all-glass evacuated tube collectors. The collector is based on a number of parallel-connected double glass tubes, which are open in both ends. The inner glass wall is treated with an absorbing selective coating. The collector fluid will flow from the bottom to the top inside of the inner tubes. Inside the inner tube there is another closed tube inserted, the purpose of this tube is to fill out a part of the tube volume so that less collector fluid is needed. In addition, it ensures a high

heat transfer coefficient from the inner glass tube to the collector fluid (Shah, 2005). Main advantage with this design is that is made completely of glass and it is not necessary to penetrate the glass envelope in order to extract heat from the tube, so there will not exist any leakage losses and it also less expensive than the single envelope (Kalogirou, 2004).

6.3 Thermal efficiency

In order to determine the thermal efficiency of a solar collector, it is necessary to define the heat flow equations in the system. Struckmann (2008) derives the efficiency equation for a flat-plate collector in one of many ways. The efficiency equation for an evacuated solar collector is in the same form, but the details regarding the heat losses and absorbed radiation will be different. This is due to the different physical structures of the collectors.

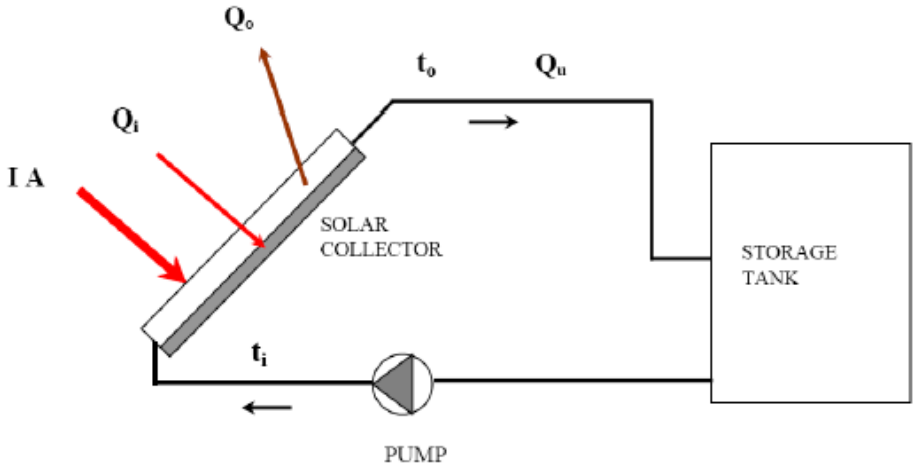

Figure 16: Heat flows in a typical solar system (Struckmann, 2008).

The amount of solar radiation received by the collector, Q_i [kW] is given by:

$$Q_i = I(\tau\alpha)A$$

Equation 7

Q_i Collector heat input [kJ]

I Solar radiation per square meter solar collector [kJ/hrm^2]

A Surface area of the solar collector [m^2]

τ Transmission coefficient of glazing [-]

α Absorption coefficient of plate [-]

$\tau\alpha$ is the product of the rate of the transmission of the cover and the absorption rate of the absorber. Some of the radiation is reflected back to the sky, another part is absorbed by the cover and the rest is transmitted through the cover and reaches the absorber plate as short wave radiation. This factor is included because it indicates the percentage of the solar rays penetrating the transparent cover and the percentage being absorbed.

The heat loss, Q_o, in a solar collector is given by:

$$Q_o = UA(T_c - T_{amb})$$

Equation 8

Q_o Heat loss [kJ]

U Collector overall heat loss coefficient [kJ/hrm^{2}K]

T_c Collector average temperature [°C]

T_{amb} Ambient temperature [°C]

The heat loss occurs since the collector absorbs heat and its temperature gets higher than the surrounding temperature. Heat is lost to the atmosphere by convection and radiation. The heat loss will also depend on the heat loss coefficient of the collector.

The useful energy gain, Q_u, under steady state conditions is proportional to the heat absorbed minus the heat lost to the environment. We can combine Equation 7 and Equation 8 to express useful energy gain:

$$Q_u = Q_i - Q_o = I(\tau\alpha)A - UA(T_c - T_{amb})$$

Equation 9

The useful energy gain can also be measured by the amount of heat carried away in the fluid passed through it:

$$Q_u = \dot{m}c_f(T_o - T_i)$$

Equation 10

$\dot{m}$ Mass flow rate of the fluid flowing through the collector [kg/hr]

c_f Specific heat of the fluid flowing through the collector [kJ/kgK]

T_o The outlet temperature of the solar collector [°C]

T_i The inlet temperature of the solar collector [°C]

It is difficult to measure or calculate the average temperature of the collector and therefore it is convenient to define a factor, F_R, which provide the ratio of the actual useful energy gain to the useful gain if the whole collector surface were at the inlet fluid temperature. F_R is expressed as:

$$F_R = \frac{\dot{m}c_f(T_o - T_i)}{I(\tau\alpha)A - UA(T_i - T_{amb})}$$

Equation 11

F_R Collector heat removal factor [-]

The inlet temperature of the collector, T_i, will be the lowest temperature through the whole collector, thus as we can see from Equation 9 the maximum possible useful energy gain occurs when the whole collector is at the inlet temperature. Another way to express the actual useful energy gain is to multiply the collector heat removal factor by the maximum possible useful energy gain:

$$Q_u = F_R A[I(\tau\alpha) - U(T_i - T_{amb})]$$

Equation 12

The collector efficiency is defined as the ratio of the useful energy gain to the incident solar radiation over a time period:

$$\eta = \frac{\int Q_u dt}{A \int I dt}$$

Equation 13

The instantaneous thermal efficiency is given by:

$$\eta = \frac{Q_u}{AI}$$

Equation 14

By combining Equation 12 and Equation 14 we obtain an equation for the thermal efficiency expressed by a straight line:

$$\eta = F_R\ \tau\alpha - F_R U \frac{T_i - T_{amb}}{I}$$

Equation 15

The heat loss coefficient U is not exactly constant, so a more exact expression is obtained by taking into account a linear dependency of U versus $T_i - T_{amb}$, so now the thermal efficiency can be expressed as:

$$\eta = F_R\ \tau\alpha - F_R U \frac{(T_i - T_{amb})}{I} - F_R U_{L/T} \frac{(T_i - T_{amb})^2}{I}$$

Equation 16

$U_{L/T}$ Thermal loss coefficient dependency on T [kW/m^{2}C^2]

Equation 16 can be simplified and rewritten as:

$$\eta = a_0 - a_1 \frac{\Delta T}{I} - a_2 \frac{\Delta T^2}{I}$$

Equation 17

When useful energy gain is simulated in simulation programs, Equation 17 is used to obtain the thermal efficiency. The three parameters, a_0, a_1 and a_2, defines the thermal efficiency. The parameters are based on measurements and are available for collectors tested according to ASHRAE

standards and rated by SRCC, and also for collectors tested according to the recent European Standards on solar collectors (Klein et al, 2006). The areas used for determining the values of a_0, a_1 and a_2 are different in the US and Europe. Typically, efficiency curves are provided for gross area in the US and for aperture area in Europe.

From Equation 16 we can draw some conclusions on how to improve the thermal efficiency. The thermal efficiency depends on the solar collector's optical properties and the differences between the inlet temperature and the ambient temperature. Keeping the solar radiation and ambient temperature fixed, it can be shown that the collector efficiency increases with decreasing inlet temperature of the working fluid (Yuehong, 2004). The ground heat exchangers may decrease the fluid temperature and thereby improve the solar collector efficiency. Glazing with high transmittance and absorber with high absorption will raise a_0, and thereby also raise the thermal efficiency.

6.4 Solar fraction and system efficiency

In order to analyze how well a system solar system works technically it is useful to calculate the solar fraction and the system efficiency. The solar fraction is defined as the amount of energy provided by the solar system divided by the total thermal load of the building:

$$SF = \frac{E_s}{E_{building}}$$

Equation 18: Solar fraction

E_s Total amount of solar energy provided to the heating [kJ]

$E_{building}$ Total heating demand of the building [kJ]

The system efficiency is defined as ratio of the total amount of useful solar energy gain and the total amount of solar radiation on the solar collector over a period of time:

$$\eta_{s\_sys} = \frac{E_u}{AG}$$

Equation 19: System efficiency

G Total solar radiation on the solar collector [kJ]

7 Stratified water storage tank

The mismatch of the exhaust and supply of energy generally occurs in systems with unstable resource and energy requirement, such as solar energy systems. Energy storages become important for sustainable utilization. A stratified water storage tank can be used as a buffer store. The buffer store can be used as short-term heat storage to balance peaks in heat delivery from the solar collectors. The solar collector is directly connected to the water storage tank. The heat distribution net can either be supplied by the buffer tanks or the borehole thermal energy storage. Due to the limited charging and discharging powers of borehole thermal energy storages, it is necessary with buffer storages. When the tank has sufficiently high enough water temperature it can deliver heat to the heating distribution system. If the tank temperature is too low, the solar heat will be utilized to heat the water. Water tank is a widely used energy storage system for civil use or industrial process. This is due to water has the characteristics of non-toxicity, high thermal capacity and suitable for wide range temperature requirement (Bauer, 2009).

In a stratified tank, the cold water is at the bottom and the hot water is at the top. A stratified tank differs from a fully mixed tank. In a fully mixed tank the hot water from the solar collector is allowed to mix with the cold water in the tank. Since the water is mixed, the supplied temperature to the load is lowered and the useful quality of energy is degraded. The inlet temperature to the solar collector will be higher in a mixed tank than in a stratified tank, so the amount of collected energy may be decreased. According to Han et al (2008) the energy storage efficiency and the system performance can be increased respectively by 6% and 20 % by using a stratified tank instead of a fully mixed tank. Therefore, in order to obtain the maximum efficiency of stored energy, thermal stratification technology is introduced and developed in recent 10 years (Han et al, 2008).

The principle of a stratified tank is that it is assumed that the inlet fluid will drop to a level where its density matches the density of the surrounding fluid. Due to the gravity and buoyant effect, water with different temperature will deposit to the corresponding height according to density difference. Hot water has a lighter density and will float to the top layer. Cold water has a heavier density and will float to the bottom layer. This phenomenon makes it possible to have stratification, with zones of different temperatures in one physical store. Then thermal stratification is built as a thermal barrier to separate the warm and cool fluids and maintain the stable vertical temperature or density gradient. A temperature gradient or thermo-cline is formed between the hot water at the top and the cold water at the bottom. Thermal stratification within the tank can be obtained by different methods:

(1) Heating of vertical walls, which leads to hot thermal boundary layers that draws the hot fluid into the upper part of the tank
(2) Heat exchange between the fluids contained in the tank by circulating through a heat exchanger. The heat exchanger can either be placed inside or outside of the tank.
(3) Direct inlet to the hot fluid layer in the tank at suitable heights

During the operation of the tank, the cold water is extracted at the bottom and directed into the solar collector. The cold water is heated and returned to the tank. Simultaneously, a second circuit extracts hot water from the top of the tank to supply the load. The return water from the load is injected back to the bottom of the tank. Turbulences can occur when the cold water flows downward, which can cause mixing and destruction of thermal stratification. Earlier research show

the degree of stratification depends mainly on tank configurations and operation conditions (Han et al, 2008).

The stratified tanks are traditionally divided into two heating types; indirect and direct heating mode. The indirect heat transfer type includes a heat exchanger on the inside or the outside of the tank. The following heat exchanger configurations are among the most common ones: (1) immersed tube or immersed coil in the tank, (2) external shell-and-tube exchanger and (3) mantle heat exchanger with a narrow annular jacket around the tank. For the indirect heating tank, the temperature difference between the cold and hot section makes it easy to keep the water in thermal stratification state. But the energy efficiency between the two separated media will be decreased due to the insufficient heat transfer.

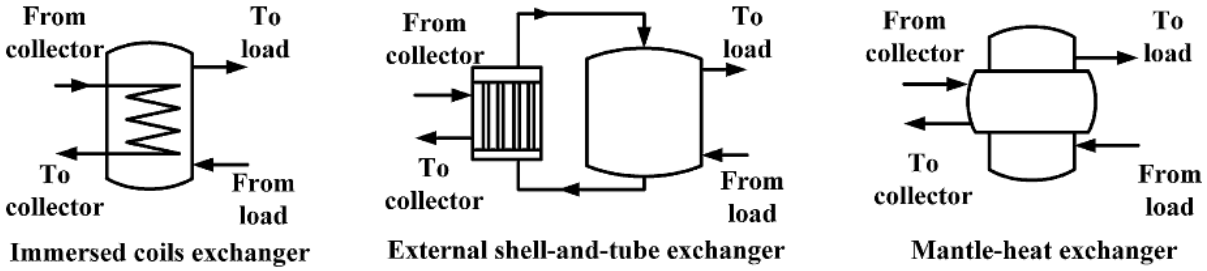

Figure 17: Three different types of heat exchangers. They can either be placed on the inside or on the outside of the tank (Han et al, 2008).

For the direct heating tank, thermal stratification will be more easily destroyed by water turbulence. There are several measures taken to slow down the turbulence generated by mixing of the hot and the cold water in the direct heating tank. A baffle plate can be inserted to control the flow pattern. Porous mesh can be inserted to slow down the water flow.

8 Weather conditions in Shanghai

By using the weather model in TRNSYS it was possible to obtain the solar radiation in Shanghai. Figure 18 shows the monthly global solar radiation on a horizontal plate in Shanghai. The figure shows the solar radiation is highest in July and is lowest in January. Figure 19 shows the monthly average temperature in Shanghai. It can be observed that the lowest outdoor temperature occurs when the solar radiation is weak, which challenge some parts of the proposed heating system in winter operation. Due to its huge area, China is divided into five climatic zones from north to south within the thermal design and engineering field. Shanghai belongs to the hot summer and cold winter zone (Gao et al, 2008). This means there is abundant solar energy in the summer and a large heat load in the winter, so the use of seasonal storages is very convenient. Shanghai is located in Yangtze River Delta in the eastern part of China at 31°12''N 121°30''E. Shanghai is located in the subtropical monsoonal climate. Winters are chilly and damp, and winds from Siberia causes temperatures to drop below 0°C. Summers are hot and humid with occasional thunderstorms.

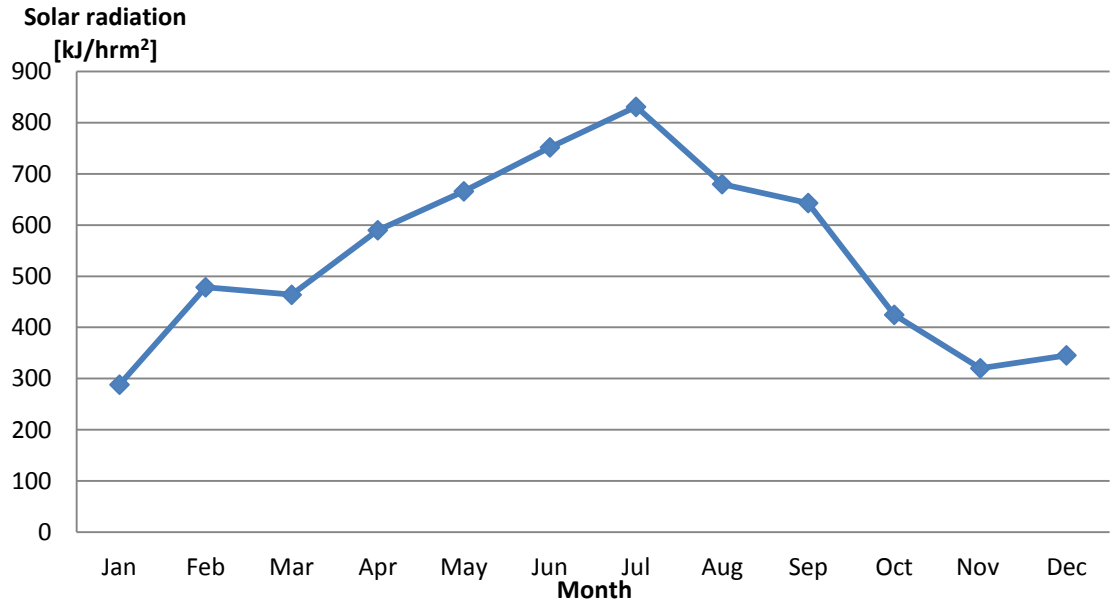

Figure 18: Monthly solar radiation on a horizontal plate in Shanghai. Weather data obtained from TRNSYS.

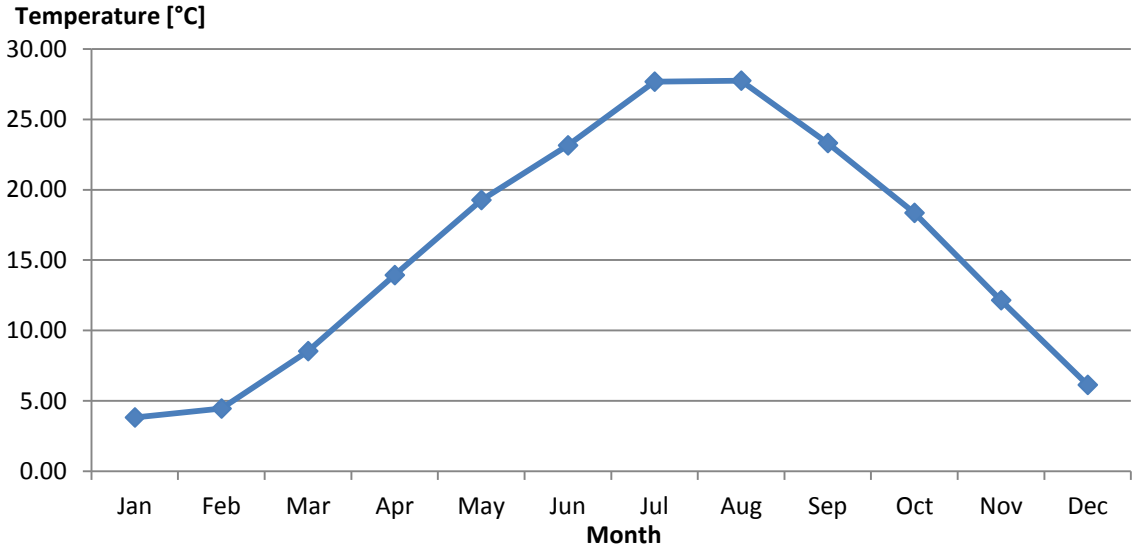

Figure 19: Monthly average temperature in Shanghai. Weather data obtained from TRNSYS.

9 TRNSYS

This chapter describes the simulation software that is used in this report and also the mathematical descriptions, parameters and functions of the model components in the simulation models.

9.1 Description of the software TRNSYS

To simulate the proposed heating system at the GEL with solar thermal collectors, borehole thermal energy storage and ground-source heat pump, the simulation software TRNSYS (Transient Systems Simulation Program) has been used. TRNSYS is a complete and extensible simulation program for the transient simulation of systems (Klein et al, 2006). The program is used by engineers and researchers to validate new energy concepts, such as solar heating systems. It can also be used for design and simulation of buildings and installations, including control strategies, occupant behavior and other alternative energy systems. TRNSYS was developed in 1974 by the Solar Energy Laboratory at the University of Wisconsin, USA, and has since then been developed continuously (Kjellsson, 2009).

The program consists of a suite of programs: A graphical user interface (Simulation Studio), a calculation program written in FORTRAN, a graphical user interface for buildings with several zones (TRNBuild) and an editor that can create stand-alone redistributable programs. In this work the Simulation Studio and TRNBuild has been used. In the Simulation Studio, there are several available model components for the user. TRNSYS simulates the performance of a system by breaking it down into individual components. These components are connected together via inputs and outputs. They are linked together to solve a specific task. For example, a simple solar heating system can be simulated using the components solar collector, water tank, pump, temperature controllers and auxiliary heating. The user can then find the performance of the system. In TRNBuild there are possibilities to model buildings with different thermal zones, walls and thermal properties of the walls.

One of the main advantages of TRNSYS is open modular structure. TRNSYS is programmed in FORTRAN and the source code of the kernel and the component models is delivered to the end user. It makes it possible and simple to extend existing models and to create own modules if the desired component is not available in the component library. This flexibility makes it possible to study systems and components in detail. One disadvantage related to the high flexibility and the high level of detail is that modeling of systems is time demanding compared to other less flexible and detailed systems. To prevent sources of errors it requires good knowledge of both the program and the system to be simulated

TRNSYS can simulate the whole energy flow of a system with respect to the climate, heat losses, transmission losses, ventilation, domestic hot water, demand for heating and cooling, etc. To obtain useful results, it is necessary that the mathematical model of the components is described in a realistic way. The mathematical models have been developed, validated and been used during a long time of a large number of users all over the world (Kjellsson, 2009). There are manuals provided for the program, where all the mathematical descriptions of the components are available. New components are added to the software all the time.

TRNSYS distinguishes between inputs and parameters. Inputs are time-dependent, while parameters are constant through the whole simulation. The output is the result of the internal calculations in the component module and can be used as input in other components. The components are defined by

properties that are given in the parameters. For example, the solar collector is defined by the parameters: area, intercept efficiency, efficiency slope, etc. The ground heat exchanger is defined by the borehole depth, number of boreholes, thermal conductivity, radius, etc. The components are calculated in subroutines of the main program and solved separately and sequentially (Kjellsson, 2009). Usually, in other component based simulation programs, all the equations are solved together at once. If the components form a loop in TRNSYS, the equations are solved by iteration.

A convergence tolerance limit defines the maximal number of iterations and the accuracy of the calculation results. This limit is user-specified. In this work, a tolerance limit of 0.001 has been used. The process with the calculations of all components and loops continues until the specified simulation time is over. The model uses a user-specified simulation step, which ranges from 0.01 seconds to 1 hour. If a loop is not converging within the tolerance limits, the last value is saved and a warning is printed. Too many warnings will lead to termination of the simulation. The convergence tolerances influence the consistency of the result of a loop and also the energy balances (Kjellsson, 2009). A tight limit tolerance will give a more consistent result and small errors in the energy balances, but will also give more computational time because of more iteration. There will always be a compromise between the accuracy in result and the computational time. It can be useful to check the simulation results carefully and compare them with measurements and/or separate calculations. This can be done by checking the total energy flows and energy balances in subsystems or by following the dynamic process in the system.

In TRNSYS there is an online plotter which can draw the output that might be of interest to follow, for example temperatures, mass flow, energy rate and so on. For the simulations there were plotters included in the simulation decks. To obtain the accurate simulation results, the components printers were used. The results were later processed in the software Microsoft Excel to calculate, sort out and output the results in an orderly manner. For integrating the results over a time period, integrators were used. At last, a control card is used to set the global information, like simulation time, simulation time step, tolerance integration and tolerance convergence. Some of the parameters were based on the system in the GEL, but some data was not available and had to be assumed. Unfortunately, it was not possible to check and compare the system with real measurements, since this heating system is only a proposed system.

9.2 Descriptions of the components used in simulations in TRNSYS

9.2.1 Weather Model

The component used for providing the weather data is a combined data reader and solar radiation processor. This weather model reads the weather data at regular time intervals from a data file and converts it to a desired system of units. It has the ability to calculate direct and diffuse radiation, the angle of incidence of beam radiation, the slope and azimuth of arbitrary number of surfaces.

Four different models for calculation of diffuse radiation on tilted surfaces are available in the weather model. The Perez diffuse radiation model is chosen as solar radiation processor to calculate sky diffusive radiation, accounting for circumsolar, horizon brightening and isotropic diffuse radiation by empirically derived "reduced brightness coefficients". These coefficients are functions of sky clearness and brightness (Xi, Lin, & Hongxing, 2011). According to Klein et al (2006) this radiation model is usually considered to be the best available model. For the simulations, the weather model gives input to the solar collector and to the heating demand of the building model. The weather model reads weather files from Meteonorm. Meteonorm is a program that consists of climate data from multiple monitoring stations in the world and several numerical models developed in international research programs (Meteotest, 2009). The solar radiation data in a lot of places can be determined with great accuracy with the help of this program. The data for the solar radiation are from the period of 1981 to 2000.

9.2.2 Evacuated Tube Solar Collector

The model of the evacuated tube solar collector assumes that the efficiency (η) versus a ratio of inlet temperature of the fluid minus the ambient temperature to radiation ($\Delta T/I$) curve can be modeled as a quadratic function (Klein et al, 2006). The efficiency of the solar collectors in TRNSYS is calculated by Equation 17 given in chapter 6.3:

$$\eta = a_0 - a_1 \frac{\Delta T}{I} - a_2 \frac{\Delta T^2}{I}$$

Where $\Delta T = T_i - T_a$. Where a_0 is the efficiency without heat losses, $a_1$is the first order of heat loss coefficient and a_2 is the second order of heat loss coefficient. The values of these parameters are results from standard test and must be provided by the user in TRNSYS. The manufacturer's data was provided in W/m^{2}K and had to be converted to kJ/hrm^{2}K to be used in the solar collector model.

Some of the parameters that have to be provided by the user are area and number of collectors that are connected in series. The incidence angle, the solar zenith angle and the azimuth angle changes with the position of the sun, so these inputs will be connected to the weather component. The weather component which registers climate data will give all the inputs for radiation, ambient temperature and various angles. The working fluid in this loop is water. The mass flow was calculated by Equation 20. The velocity was 1.5 m/s and radius of the pipes was 24 mm for the solar collector at the GEL.

$$\dot{m} = \rho A v = \rho_{water} \times \pi \times r^2 \times v$$

Equation 20: Mass flow rate

ρ Density of the working fluid [kg/m^3]

A Flow area [m^2]

v Flow velocity of the fluid [m/s]

The main characteristics for the solar collector model in the base case are given in Table 1.

Table 1: Main characteristics of the solar collector

Characteristics	Value	Comments
Number in series [-]	2	Inspected at the roof at the GEL
Collector area [m^2]	216	Inspected at the roof at the GEL
Fluid specific heat [kJ/kg*K]	4.19	Specific heat for water
a_0 [-]	0.734	Given by the producer
a_1 [kJ/hr*m^2*K]	5.5044	Given by the producer
a_2 [kJ/hr*m^2*K^2]	0.0432	Given by the producer
Mass flow [kg/hr]	9771.6	Based on available equipment at the GEL
Tilt angle	45°	Inspected at the roof of the GEL

9.2.3 Stratified water storage tank

The component models a stratified multi-node fluid storage tank. According to Klein et al (2006), this model provides very good accuracy and still keeping the parameter complexity and the computational effort reasonable. This is the most used tank model in the TRNSYS standard library. There are two outlets and two inlets. The two flow streams enter at fixed positions. The load flow from the ground storage enters at the bottom of the tank and the hot source flow from the solar collector enters at the top of the tank. Then the flow into the solar collector exits at the bottom and the flow into the ground storage exits at the top, as shown in Figure 20. The tank consists of N fully-mixed equal segments. The degree of stratification is determined by the value of N. No stratification effects are possible if N is equal to 1. The tank would then be modeled as a fully-mixed tank. In this simulation case N is chosen to be 5, to make use of the effects of stratification. Fluid streams flowing up and down from each segment are fully mixed before they enter next segment. It is assumed in the model that at the end of each time interval, any temperature inversions that exist are eliminated by total mixing of the appropriate adjacent segments (Klein et al, 2006).

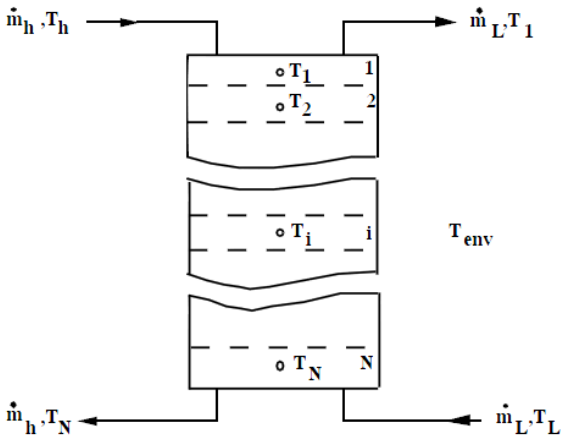

Figure 20: The schematic of the stratified water storage tank model in TRNSYS (Klein et al, 2006).

Following equations calculate the different energy rates of the water storage tank:

The rate of heat losses from the tank to the environment:

$$Q_{tank\ losses} = \sum_{i=1}^{N} UA_i\ (T_i - T_{amb})$$

Equation 21: Heat losses from the tank to the environment (Klein et al, 2006)

Q_{tl} Rate of energy loss from the tank to the surroundings [kJ/hr]

U Tank loss coefficient [kJ/hrm^{2}K]

A_i Surface area of the ith tank segment [m^2]

Ti Temperature of the ith tank segment [°C]

T_{amb} Temperature of the environment surrounding the tank [°C]

The rate of energy removed from the tank to supply the load:

$$Q_{load} = \dot{m}_L c_f (T_1 - T_L)$$

Equation 22: Energy removed from the tank to supply the load (Klein et al, 2006)

Q_{load} Rate at which sensible energy is removed from the tank to supply the load [kJ/hr]

$\dot{m}_L$ Fluid mass flow rate to the load [kg/hr]

c_f Specific heat of the tank fluid [kJ/kgK]

T_1 Temperature of the fluid exiting from the tank to supply the load [°C]

T_L Temperature of the fluid entering the tank from the load [°C]

The rate of energy transfer from the hot fluid stream coming from the solar collector to the tank is calculated by:

$$Q_{source} = \dot{m}_H c_f (T_H - T_N)$$

Equation 23: Energy supplied to the tank from the source (Klein et al, 2006)

Q_{source} Rate of energy input to the tank from the hot fluid stream [kJ/hr]

$\dot{m}_H$ Fluid mass flow rate from the heat source [kg/hr]

c_f Specific heat of the tank fluid [kJ/kgK]

T_H Temperature of the fluid entering the tank from the heat source [°C]

T_N Temperature of the fluid exiting the tank to the heat source [°C]

The main characteristics of the tank are given in Table 2.

Table 2: The characteristics of the stratified fluid storage tank

Characteristics	Value	Comments
Source (solar collector flow) specific heat [kJ/kgK]	4.190	cp for water
Load (storage loop flow) specific heat [kJ/kgK]	4.190	cp for water
Tank volume [m^3]	20	
Tank loss coefficient [kJ/hrm^2K]	2.5	

9.2.4 Borehole Thermal Energy Storage

In the performed simulations it is used U-tube ground heat exchangers with the heat carrier fluid circulating in the U-tube. When the heat carrier fluid is circulated through the ground heat exchangers, the fluid either rejects heat to or absorbs heat from the ground depending on the temperatures of the heat carrier fluid and the ground. For this system the heat carrier fluid is water. As described in chapter 4.3 the model assumes that the boreholes are uniformly placed within a cylindrical ground storage volume. There is conductive heat transfer to the storage volume and convective heat transfer within the pipes. The temperature is calculated from three parts: a global temperature, a local temperature and a steady-flux solution. The global and local solutions are solved with the use of an explicit difference method. The steady-flux method is obtained analytically. Finally, the temperature is obtained by superposing the solutions (Klein et al, 2006). This model is the most commonly used model in ground heat exchange applications and was developed by the Department of Physics in Lund University (Hellström, 1989). The model is limited to only simulate a storage volume with a cylindrical shape. The volume of the storage is defined in Equation 24.

$$V = \pi \times Number\ of\ boreholes\ \times Borehole\ depth \times (0.525 \times Borehole\ spacing)^2$$

Equation 24: Volume of the ground storage volume (Hellström, 1989)

At the GEL, there are three groups of boreholes. There are three boreholes in each group and these boreholes are connected in series, finally all of the groups are parallel connected. Totally there are nine boreholes. Current use of the boreholes is only for heat extraction with a geothermal heat pump, there is no heat storage during the summer. In the simulation there were nine boreholes. The real system at the GEL does not make use of insulation on the storage. This can be later simulated in TRNSYS, to see the effects of the insulation on the heat losses. The header depth is 1.5 meters because at depth less than 2 m the ground is highly influenced by the seasonal variations. There are not used any special filling in the GEL storage. Filling is usually placed in the space between the heat exchanger tube and the borehole wall and is used to provide better thermal contact.

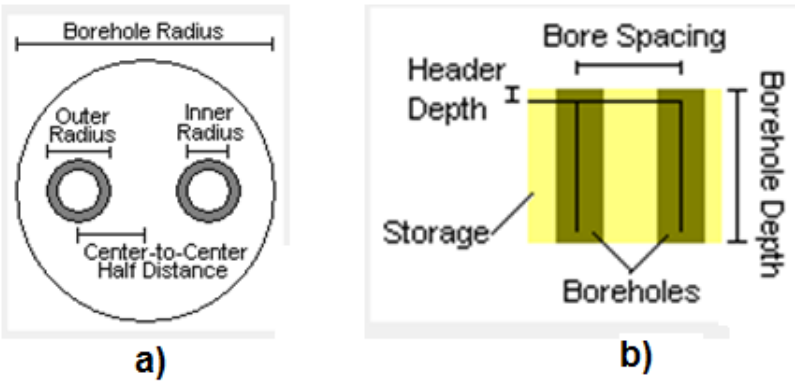

Figure 21 Figures describing the parameters of the boreholes. a) Borehole seen from above. b) Two boreholes seen from the side. (Klein et al, 2006)

The main characteristics of the ground, the boreholes and the ground heat exchangers in the base case are given in Table 3.

Table 3: The main characteristics of the ground storage in the base case

	Characteristics	Value	Comments
Ground	Initial temperature [C°]	18	Annual average air temperature in SH
	Thermal conductivity [kJ/hrmK]	5.22	
	Heat capacity [kJ/m^3/K]	2016	
Boreholes	Borehole radius [m]	0.15	
	Number [-]	9	
	Depth [m]	10	
	Number of boreholes in series [-]	3	
	Header depth [m]	1.5	
	Borehole flow rate [kg/hr]	1059.75	Measured in earlier experiments
	Borehole spacing [m]	5	
	Storage volume [m^3]	1948.3	
Ground heat exchangers	Inner radius of U-tube pipes [m]	0.013	
	Outer radius of U-tube pipes [m]	0.016	
	Number of U-tubes per borehole [-]	1	
	Pipe thermal conductivity [kJ/hrmK]	1.656	Pipe material is polyethylene
	Fluid specific heat [kJ/kgK]	4.19	cp for water
	Fluid density [kg/m^3]	1000	Density for water

9.2.5 Geothermal heat pump

Type 668 in TRNSYS models a water to water heat pump. The model is based on user-supplied catalogue data for the heating capacity (in kW) and power demand (in kW), based on the entering load and source temperatures. The model is able to interpolate data within the range of input values specified in the data files, but it is not able to extrapolate beyond the data range and will print a warning in TRNSYS if the conditions fall outside the data range. TRNSYS uses Equation 6 in chapter 5.2 to calculate the COP. The model uses following equations to calculate the different outputs:

The amount of energy absorbed from the source fluid stream in heating is given by Equation 25.

$$Q_{source} = Q_{load} - W_{input}$$

Equation 25: Energy absorbed from the fluid stream (Klein et al, 2006)

Q_{source} Energy absorbed from the source by the heat pump in heating mode [kJ/hr]

Q_{load} Amount of useful energy delivered to the load [kJ/hr]

W_{input} Power input into the heat pump [kJ/hr]

The outlet temperatures of the two liquid streams can then be calculated using Equation 26 and Equation 27.

$$T_{source,out} = T_{source,in} - \frac{Q_{source}}{\dot{m}_{source} c_{source}}$$

Equation 26: Source outlet temperature (Klein et al, 2006)

$$T_{load\ ,out} = T_{load,in} - \frac{Q_{load}}{\dot{m}_{load} c_{load}}$$

Equation 27: Load outlet temperature (Klein et al, 2006)

$T_{source,out}$ Temperature of liquid exiting the source side of the heat pump [°C]

$T_{source,in}$ Temperature of liquid entering the source side of the heat pump [°C]

$\dot{m}_{source}$ Mass flow rate of liquid on the source side of the heat pump [kg/hr]

c_{source} Specific heat of the liquid on the source side of the heat pump [kJ/kgK]

$T_{load\ ,out}$ Temperature of liquid exiting the load side of the heat pump [°C]

$T_{load,in}$ Temperature of liquid entering the load side of the heat pump [°C]

$\dot{m}_{load}$ Mass flow rate of liquid on the load side of the heat pump [kg/hr]

c_{load} Specific heat of the liquid on the source side of the heat pump [kJ/kgK]

9.2.6 Fan coil

The heating distribution system at the GEL uses fan coils to distribute heating to different parts of the building. Type 753 in TRNSYS models a heating coil using with three control modes. The heating coil model uses a bypass approach in which the user specifies a fraction of the air that bypasses the coil. The fan coil model assumes that the final air temperature is the same as the average temperature of the fluid in the coil (Pardo et al, 2010). The air stream passing through the coil is then remixed with the air that bypassed the coil. In the unstrained control mode of operation, the coil heats the air stream as much as possible given the inlet conditions of both the air and the fluid streams. Which means the flow is free-floating. There are also two other existing modes that can either control the outlet air temperature above a user specified minimum or to control the fluid outlet temperature above a user specified minimum. The unstrained control mode was used in the simulations. The flow was chosen to be free-floating because there is a room thermostat that controls the zone temperature by switching on/off the pump that supplies water to the heat sources (Zogou & Stamatelos, 2007).

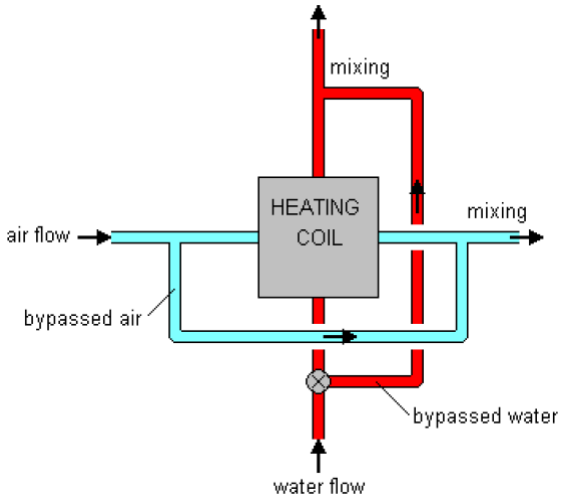

Figure 22: The schematic of the heating coil model in TRNSYS (Klein et al, 2006).

The energy transferred from the fluid to the air stream is calculated by:

$$Q_{fluid} = \dot{m}_{air}\left(1 - f_{airbypass}\right)\left(h_{air,coilout} - h_{air,in}\right)$$

Equation 28: Energy transfer from liquid to air in a fan coil (Klein et al, 2006)

Q_{fluid}	Energy transferred from the fluid stream to the air stream [kJ/hr]
$\dot{m}_{air}$	Total flow rate of air through the coil [kg/hr]
$f_{airbypass}$	Fraction of air bypassed [0...1]
$h_{air,coilout}$	Enthalpy of air exiting the coil before mixing [kJ/kg]
$h_{air,in}$	Enthalpy of air entering the coil [kJ/kg]

9.2.7 Pump and fan

The working principles of the pump and fan model is the same, so these models will be described in the same chapter. This pump or fan model computes a mass flow rate using a control function, which is either 0 or 1, and a user-specified maximum flow capacity. Pump or fan power may also be calculated as a linear function of the mass flow rate. The outlet flow rate and the power used are either both zero or both at their maximum value.

The outlet mass flow rate is calculated by Equation 29.

$$\dot{m}_o = \gamma \dot{m}_{max}$$

Equation 29: Mass flow rate for pump

$\dot{m}_o$	Outlet mass flow rate [kg/hr]
γ	Control function ($0 \leq \gamma \leq 1$)
$\dot{m}_{max}$	User-specified maximum flow capacity (when γ =1) [kg/hr]

Linear relationship between the flow rate and power consumption is assumed. The electricity consumption of the pump or the fan is given by Equation 30.

$$P = \gamma P_{max}$$

Equation 30: Electricity consumption for pump

P	Power consumption of pump or fan [kJ/hr]
γ	Control function ($0 \leq \gamma \leq 1$)
P_{max}	User-specified maximum power consumption (when γ =1) [kJ/hr]

The main characteristics of the pump are given in Table 4.

Table 4: Main characteristics of the pump.

Characteristics	Value	Comments
Rated power [kJ/hr]	2684	
Total pump efficiency	0.6	The overall pump efficiency includes the inefficiencies due to the motor and shaft friction

9.3 Base case

Table 5 presents the main characteristics of the components used in the simulations. The values of the characteristics were used as inputs and parameters to the base case in the simulations. Parameters and inputs were varied one at a time, while the remaining parameters and inputs were kept constant.

Table 5: Main characteristics of the base case.

Solar collector		
Characteristics	**Value**	**Comments**
Number in series [-]	2	Inspected at the roof at the GEL
Collector area [m^2]	216	Inspected at the roof at the GEL
Fluid specific heat [kJ/kg*K]	4.19	Specific heat for water
a_0 [-]	0.734	Given by the producer
a_1 [kJ/hrm^{2}K]	5.5044	Given by the producer
a_2 [kJ/hrm^{2}K^2]	0.0432	Given by the producer
Mass flow [kg/hr]	9771.6	Based on available equipment at the GEL
Tilt angle	45°	Inspected at the roof of the GEL

Water tank		
Characteristics	**Value**	**Comments**
Source (solar collector flow) specific heat [kJ/kgK]	4.190	cp for water
Load (storage loop flow) specific heat [kJ/kgK]	4.190	cp for water
Tank volume [m^3]	20	
Tank loss coefficient [kJ/hrm^{2}K]	2.5	

Ground storage		
Characteristics	**Value**	**Comments**
Ground		
Initial temperature [C°]	18	Annual average air temperature in SH
Thermal conductivity [kJ/hrmK]	5.22	
Heat capacity [kJ/m^3/K]	2016	
Boreholes		
Borehole radius [m]	0.15	
Number [-]	9	
Depth [m]	10	
Number of boreholes in series [-]	3	
Header depth [m]	1.5	
Borehole flow rate [kg/hr]	1059.75	Measured in earlier experiments
Borehole spacing [m]	5	
Storage volume [m^3]	1948.3	

Ground heat exchangers		
Inner radius of U-tube pipes [m]	0.013	
Outer radius of U-tube pipes [m]	0.016	
Number of U-tubes per borehole [-]	1	
Pipe thermal conductivity [kJ/hrmK]	1.656	Pipe material is polyethylene
Fluid specific heat [kJ/kgK]	4.19	cp for water
Fluid density [kg/m^3]	1000	Density for water

Pumps		
Characteristics	**Value**	**Comments**
Rated power [kJ/hr]	2684	
Total pump efficiency	0.6	

10 Simulations and results

In this chapter the simulations and results of the different operation modes will be presented. The weather conditions for the simulations is described in chapter 8 and the weather model that generates the weather conditions is described in chapter 9.2.1. The parameters and inputs for the components in the base case are given in Table 5.

10.1 Simulations of the solar thermal ground storage model – Operation mode 1

The proposed storage system was simulated in TRNSYS. In order to simulate the storage system, a simulation deck was built up in TRNSYS. Table 6 provides an overview of the main components used in the storage model.

Table 6: Overview of the main components in the ground storage model.

Component	Name in TRNSYS	Type number in TRNSYS	Description of the model is given in chapter
Evacuated tube solar collector	Evacuated tube solar collector with specified outlet temperature	538	9.2.2
Stratified water storage tank	Storage tank; Fixed inlets, Uniform losses	4a	9.2.3
Borehole thermal energy storage	Vertical U-tube ground heat exchanger	557a	9.2.4
Pumps	Variable speed pump	110	9.2.7

The mathematical equations and the descriptions related to these components are described in chapter 9. The storage model consisted of two loops, the solar collection loop and the ground storage loop, respectively blue and green ring in Figure 23. Two pumps were used, one pump for each loop. One controller is used to control the operation time of the solar collector. The printers, integrators and plotters are omitted from the screenshot.

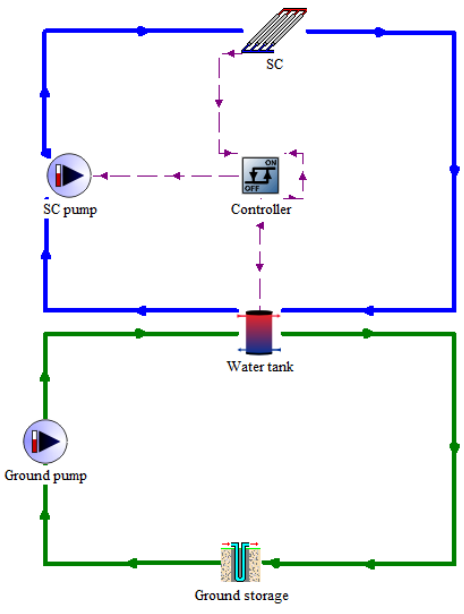

Figure 23: Screenshot of the ground storage simulation model in TRNSYS.

10.2 Energy flows of the ground storage

The main focus of the simulation of the storage system was to find how much heat can be stored in the storage during storage season and to find the final ground temperature. After obtaining the results of the base case, it was done further simulations to explore the system. The energy flows and the energy balances were followed systematically to study how the efficiencies, amount of energy and heat transfer rates varied with different conditions of the boreholes and also to validate the model and to study the behavior of the system.

To show which values that were obtained through the simulation, Figure 24 and equation 31-34 describe the energy flow of the system. The heat store, heat loss, temperature and heat injection of the borehole storage were studied. The heat loss and temperature of the tank were studied. The thermal efficiency and temperature of the solar collector were studied.

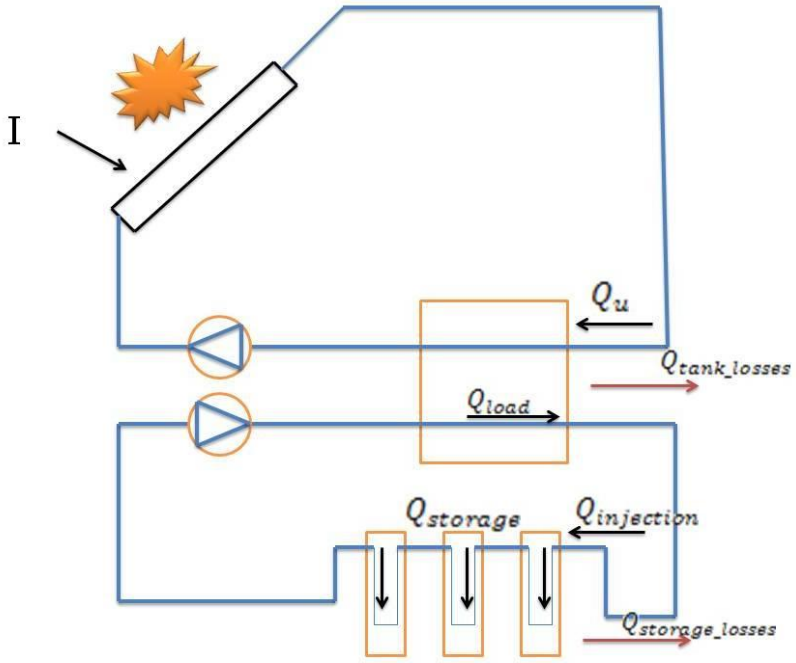

Figure 24: Energy flows of the storage model.

Following equations describe relationships between the different energy flows:

$$I = \frac{Q_u}{\eta\, A}$$

Equation 31

↓

$$Q_u = Q_{load} + Q_{tl}$$

Equation 32

↓

$$Q_{load} = Q_{inj}$$

Equation 33

↓

$$Q_{inj} = Q_{store} + Q_{sl}$$

Equation 34

I	Radiation on tilted surface [kJ/hrm^2]
Q_u	Useful solar energy gain [kJ/hr]
Q_{load}	Rate at which sensible energy is removed from the tank to supply the load [kJ/hr]
Q_{tl}	Rate of energy loss from the tank to the surroundings [kJ/hr]
Q_{inj}	The rate at which heat is added to the ground storage volume from the fluid [kJ/hr]
Q_{store}	The actual rate at which heat is stored in the ground storage volume [kJ/hr]
Q_{sl}	The rate at which heat is lost to the ambient through the ground storage volume [kJ/hr]

All these heat transfer rates can be obtained separately in TRNSYS, so equations 31 - 34 were used to check the consistency of the model.

10.3 Results of the base case

The results from simulation of the base case are presented in this section. The useful energy gain from the solar collector, Q_u, is supplied to the tank. Q_u depends largely on the thermal efficiency of the solar collector, which depends on the inlet and outlet temperatures of the collector. The tank will have some heat losses to the environment, Q_{tl}, due to temperature differences between the tank and the environment. There are also heat losses in the storage to the surrounding ground, Q_{sl}. Q_{store} is the output of main interest. This parameter tells how much heat that can be stored in the storage. The initial temperatures in the storage match approximately the temperatures in the surrounding ground. Initial ground temperature is 18°C.

The energy rates are integrated with respect to time with the help of an integrator in TRNSYS. Table 7 displays the total amount of energy gains and energy losses from May to October.

$$E = \int Q \, dt$$

Equation 35: Total amount of energy

From the results in Table 7, the storage efficiency and the tank efficiency can be calculated. The ratio of heat loss to heat injection was defined to describe the characteristics of the borehole storage. The storage efficiency is E_{sl}/E_{inj} =37.6%, which means a big amount of the energy injected is lost to the surrounding ground outside of the storage volume and to the environment. The tank efficiency is E_{tl}/E_u = 16.8%. The average thermal efficiency of the solar collector obtained from the simulation is found to be 27.4%.

Table 7: Absolute amount of energy gains and energy losses for the base case

Outputs [MJ]	Results
E_u	113988
E_{tl}	19168
E_{sl}	34418
E_{inj}	91473
E_{store}	57055

Figure 25 shows that the ground storage temperature increases as thermal energy is injected to the storage. As seen in Figure 25 the soil temperature in the end of the storage season is only 32.57°C. Since we wish to use the borehole storage for direct heat exchange, the storage temperature should be around 40 °C (Pavlov & Olesen, 2009).

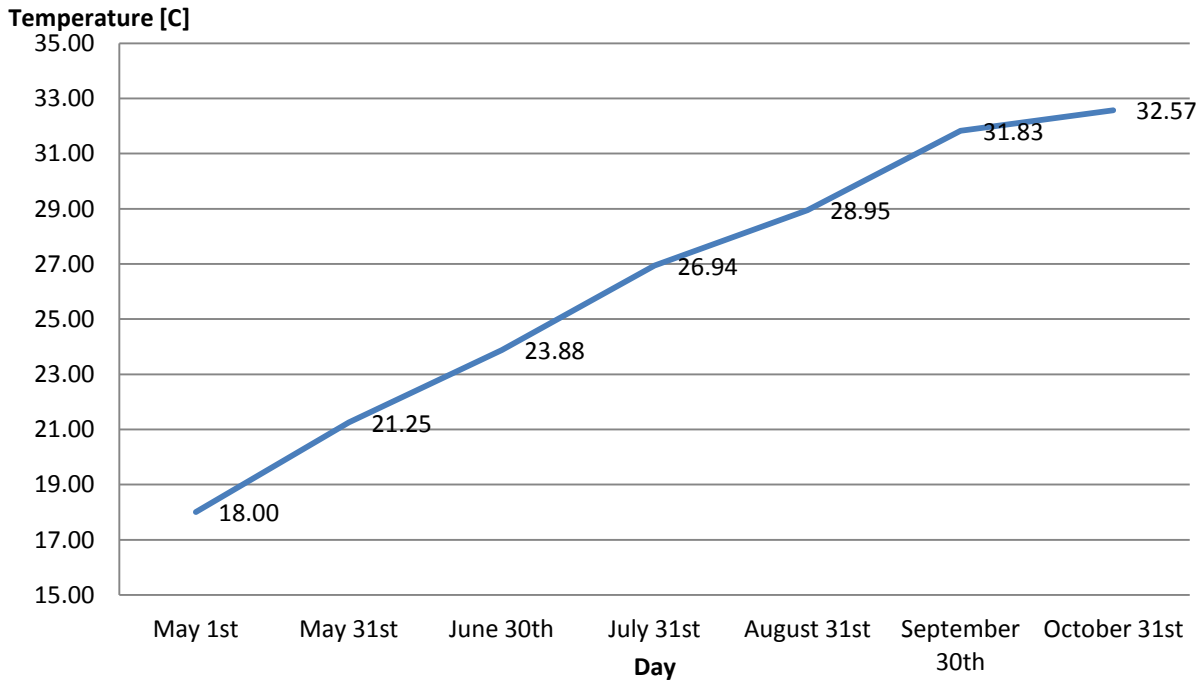

Figure 25: Ground storage temperature during storage season

A typical graph for the operation of the base case in the storage season is presented in Figure 26 for the first 10 days of July. Around 20% of the solar radiation is converted into useful solar energy gain. In the graph Q_{load} has the same changing tendency as Q_{store}, this is because Q_{sl} is constant. This is due to the calculation methods of the simulation software. The heat losses of the top, bottom and side areas of the ground storage volume are generating peaks every 40 hours, while the rest of the time these outputs are zero. This is due to the frequency at which the solution for a single borehole is superimposed on the total bore field and how often that solution is superimposed upon the far field. To avoid the peaks, the storage losses are divided evenly on all the operation hours.

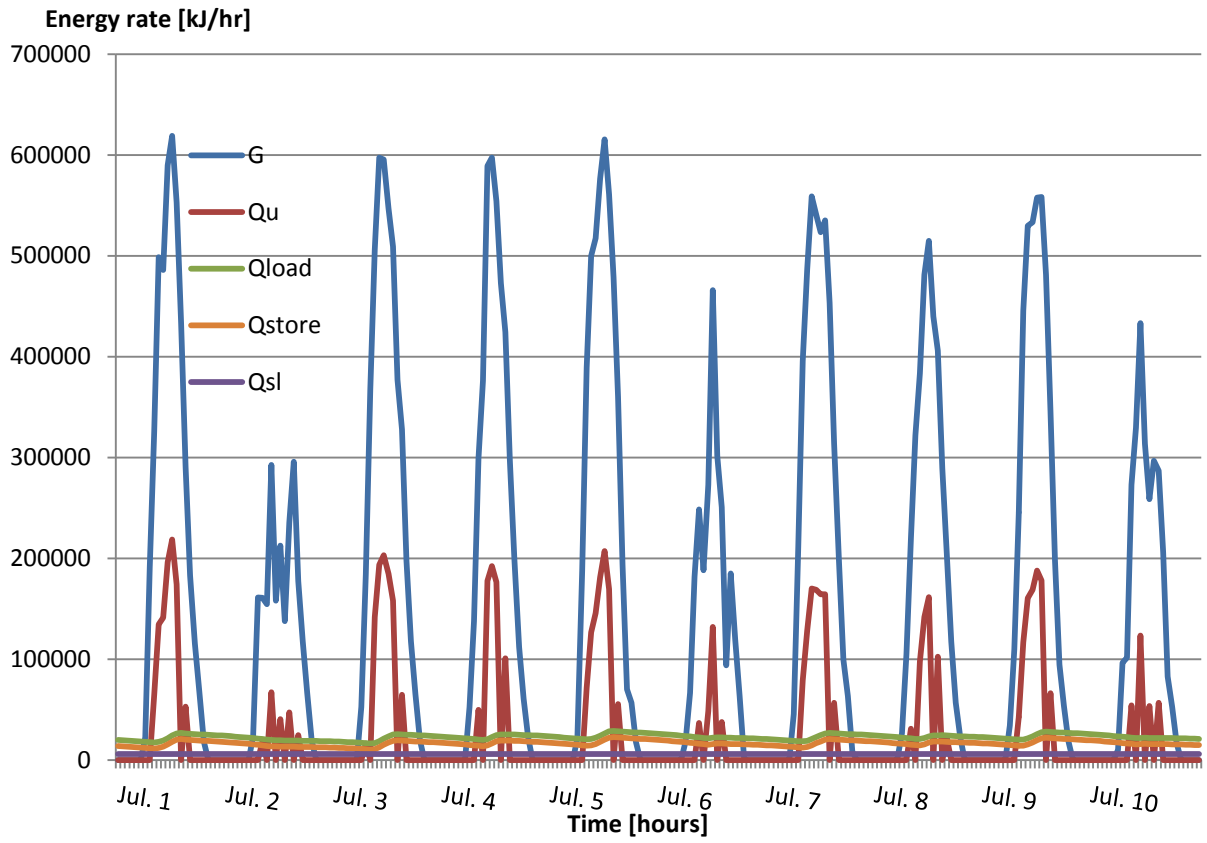

Figure 26: Simulation of gains and losses of the base case for 10 typical days in July.

Figure 27 shows the amount of energy that is collected by the solar collector and the amount of the energy that is actually stored in the ground storage. During the 10 days of July, 4020 MJ is stored in the storage of 6752 MJ that is collected by the collector. E_{load} and E_{tl} added together equals E_u. This balance is only correct for simulation of 10 days. For simulation of 1 day the balance is not correct because of the solution of the storage losses in the simulation software.

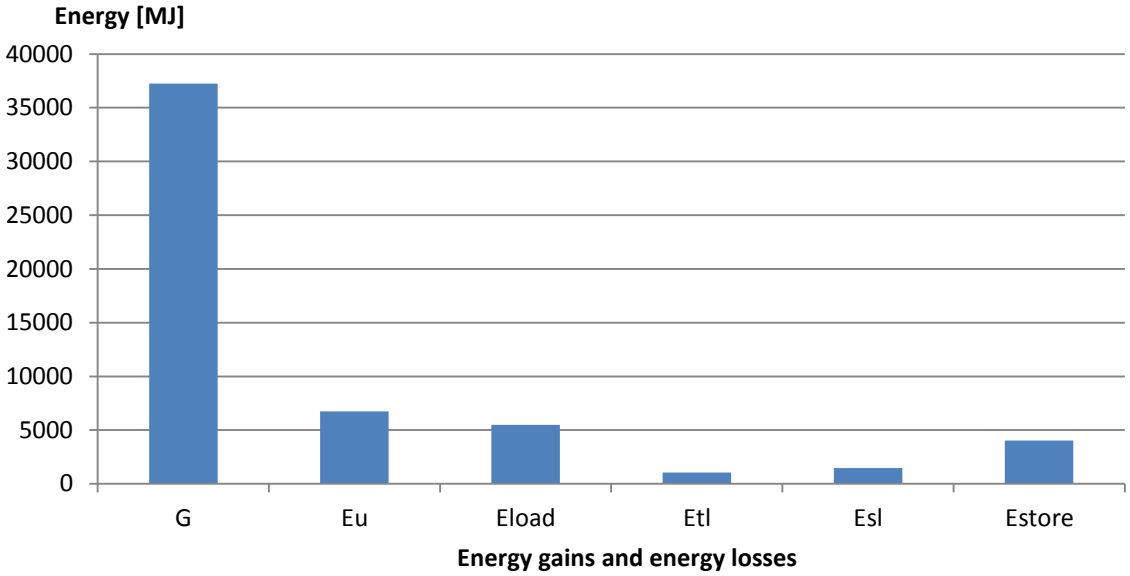

Figure 27: Overview of the total amount of energy gains and losses for 10 days in July.

10.4 Simulations of design parameters with influence on the system performance of the ground storage model

In this section the design parameters with influence on the system performance and behavior will be studied by varying the different parameters. Each parameter will be taken into consideration separately so as to examine the influence on system efficiency. In order to do such an analysis the base case of GEL became the reference of the possible comparisons. The significance of the parameters in the system will be described. The results of the total amount of energy gains and losses were collected to calculate the system efficiencies. Different efficiencies were defined to compare the results of the varied parameters.

The ratio of the stored energy in the ground storage related to the useful solar energy gain is called F_{StU}. This ratio describes the percentage of collected solar energy that can be converted to storable heat. The amount will depend on the design of the collector, the amount of radiation, the ambient temperature and the temperature of the fluid used to transfer the energy. The ratio is calculated by following equation:

$$F_{StU} = \frac{E_{store}}{E_u}$$

Equation 36: Ratio of stored energy to useful solar energy gain

The ratio of the stored energy in the ground storage related to the energy removed from the tank to supply the load is called F_{StL}. This ratio is larger than F_{StU} because it excludes heat loss from the water tank. F_{StL} is calculated by following equation:

$$F_{StL} = \frac{E_{store}}{E_{load}}$$

Equation 37: Ratio of stored energy to energy injected

The ratio of the heat losses in the water tank related to useful solar energy gain is called F_T. This ratio describes how well the tank can store the solar thermal energy that is injected in to the tank. The ratio is defined as:

$$F_T = \frac{E_{tl}}{E_u}$$

Equation 38: Ratio of water tank losses to useful solar energy gain

The ratio of the heat losses in the storage related to useful solar energy gain is called F_{LU}. The advantage of a storage system is reduced by the unavoidable loss of heat. This ratio is defined as:

$$F_{LU} = \frac{E_{sl}}{E_u} = 100\% - F_{SU} - F_T$$

Equation 39: Ratio storage losses to useful solar energy gain

The ratio of the heat losses in the storage related to the useful solar energy gain is called F_{LL}. This ratio does not include the tank losses. This ratio will describe the storage losses isolated. The ratio is calculated by following equation:

$$F_{LL} = \frac{E_{sl}}{E_{load}} = 100\% - F_{SL}$$

Equation 40: Ratio of storage losses to injected energy

The system efficiency, η_{s_sys}, and the thermal efficiency, η, of the solar collector were also calculated from the results of the simulations. The equations for calculation of these efficiencies have earlier been described in chapter 6.4.

10.4.1 The influence of the solar collector area

The solar collector area is the area of the solar collector that is exposed to the sun. Four different collector areas were used for the simulations, so as to investigate the influence of the collector area to the storage temperature, total useful solar energy gain and total thermal energy stored in the ground. While the collector area increases, the energy stored in the ground will also increase. But that could occur until a specific collector area, since the ground storage temperature will also increase and after a while perhaps the amount of storage losses will be larger than the amount of stored energy. Therefore, we wanted to check if the amount of stored thermal energy is increasing with the collector area. In addition to the collector of 216 m^2 of the base case, there were also made simulations for areas of 250, 300 and 350 m^2.

Table 8: Results of simulation for varied collector area.

Results	Solar collector area			
	216 m^2/Base case	**250 m^2**	**300 m^2**	**350 m^2**
F_{StU}	50.0%	49.7%	48.9%	47.8%
F_{StL}	62.4%	61.9%	61.4%	61.0%
F_T	16.8%	16.9%	18.8%	21.5%
F_{LU}	30.2%	30.6%	30.7%	30.6%
F_{LL}	37.6%	38.1%	38.6%	39.0%
η_{s_sys}	20.0%	19.2%	18.0%	16.9%
η	27.4%	26.5%	25.2%	24.1%

The systems with larger collector areas operate at higher temperatures which will lead to lower collector efficiencies. The results in Table 8 show that F_T increase with larger collector area, this is because the tank losses increase with higher tank temperature.

Figure 28 shows the total amount of useful solar energy gain through the storage season increases with the collector surface. This is an expected result, since a larger collector area would imply that a larger amount of solar radiation is captured by the collector and transformed into useful energy gain.

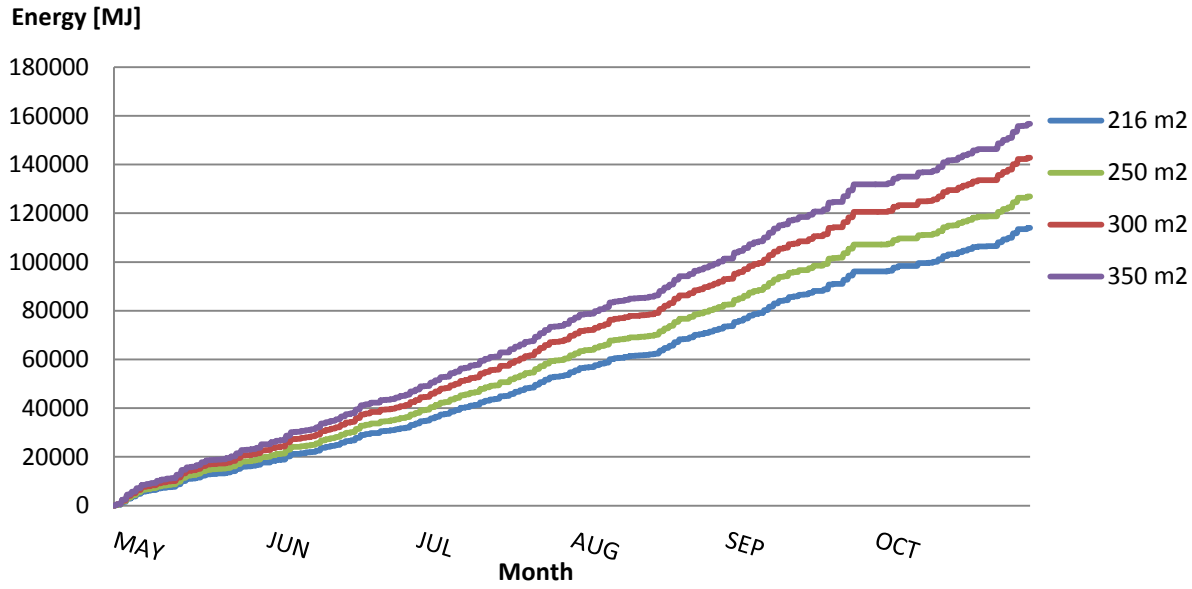

Figure 28: Total useful solar energy gain summed over each month.

Figure 29 represents the amount of heat stored in the storage, which equals the injected heat deducted the losses in the storage. These results confirm that the stored heat is increasing with the collector area, since the collected solar energy also increases. Although the storage losses also increase with solar collector due to higher storage temperature, the total amount of stored energy is still increasing with collector area.

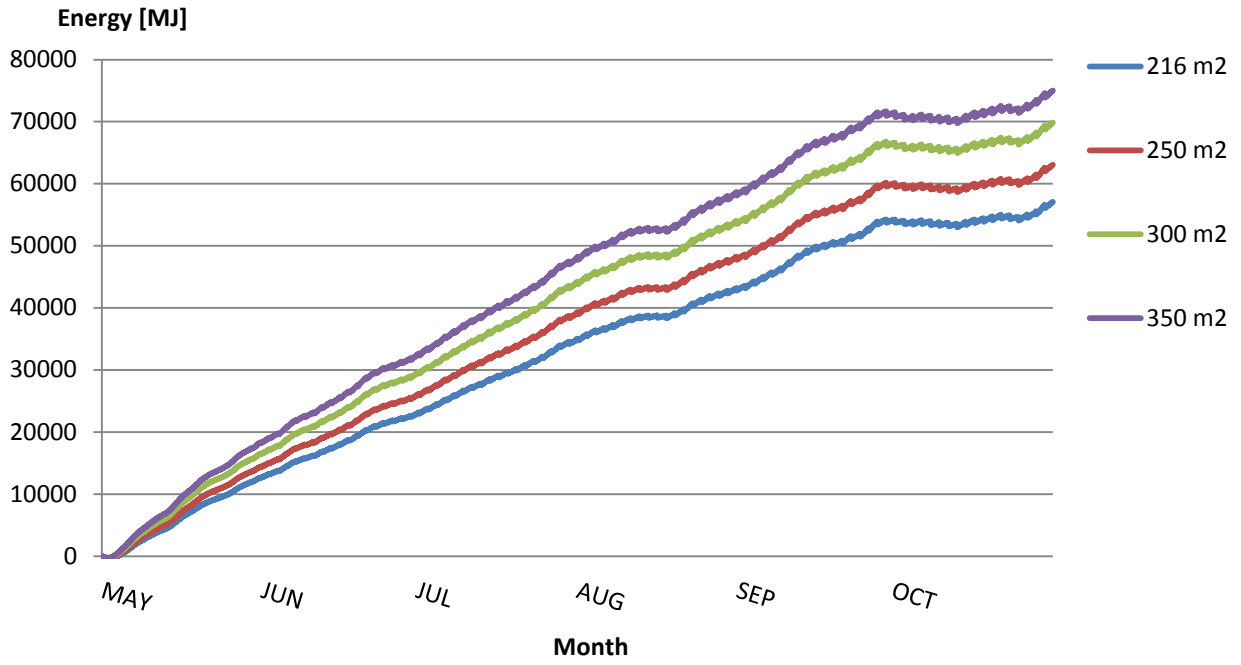

Figure 29: Total thermal energy stored in the ground storage summed over each month.

Figure 30 presents the storage temperature at the end of every month in the storage season. It is seen that when the collector area is larger, the ground temperature is higher. The ground temperature increases with increased solar collector area, because the outlet temperature of the solar collector is increased. This is because when the area increases the amount of solar radiation hitting the collector surface also increases.

When the storage temperature is higher, the heat loss from the storage surfaces to the surrounding ground is larger. Also, the heat loss from the collector to the surrounding is larger because the return temperature is higher, which leads to decrease of the efficiency of the solar collector, as illustrated in the results of thermal efficiency and system efficiency in Table 8.

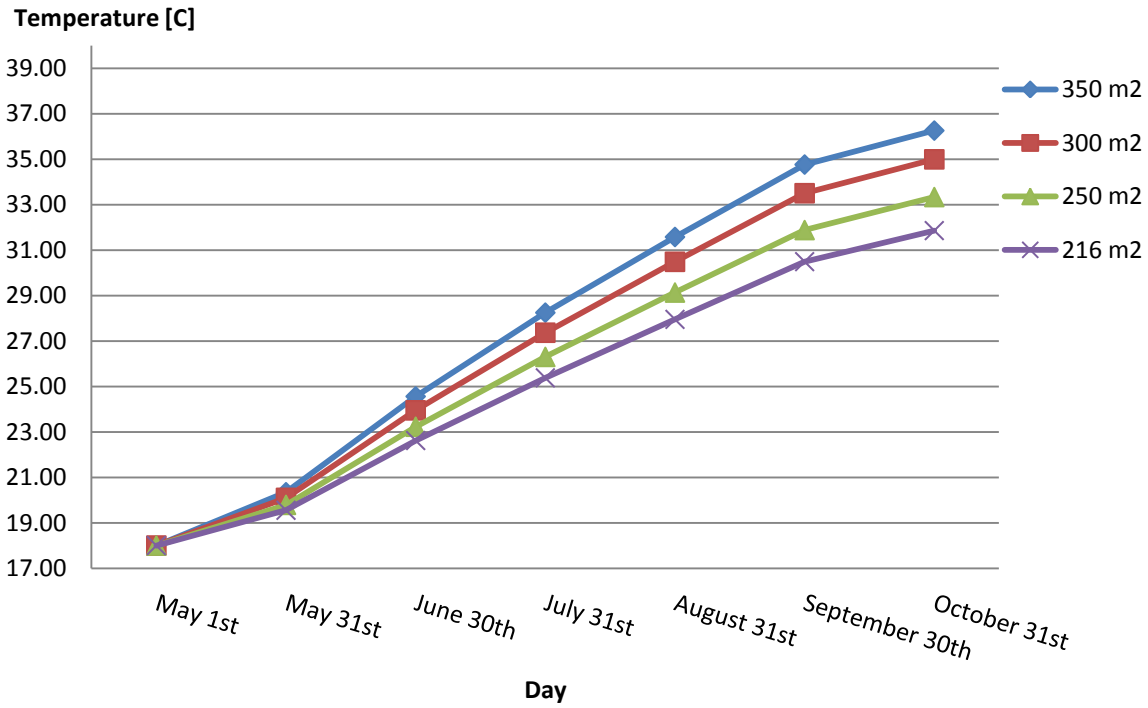

Figure 30: Storage temperature for varied collector area.

10.4.2 The influence of the flow rate of the solar collector

The flow rate through the solar collector was examined by varying the velocity of the flow through the collector. The mass flow rate is calculated by Equation 20. There are several factors that determine the mass flow. The mass flow of the heat carrier fluid has to be so large that the collector is sufficiently cooled. This will ensure a low average temperature of the collector, resulting in high efficiency for the collector. At the same time, the mass flow cannot be too large so the collector is unable to raise the outlet temperature to the desired level. For the simulations of the mass flow rate, the cooling of the collector and the desired outlet temperatures were not taken in consideration, because the purpose of the simulations were just to examine the different effects on the efficiencies with different flow rates.

Table 9: Results of simulations of different velocities of the flow through the solar collector.

	Velocity [m/s]				
	0.5	**1**	**1.5/Base case**	**2**	**2.5**
Flow rate [kg/hr]	3257	6514	9771	13029	16286
Results					
F_{StU}	49.8%	49.8%	50.1%	50.6%	50.7%
F_{StL}	61.5%	61.9%	62.4%	63.2%	63.6%
F_T	16.9%	16.9%	16.8%	16.7%	16.5%
F_{LU}	31.1%	30.7%	30.2%	29.5%	29.1%
F_{LL}	38.5%	38.1%	37.6%	36.8%	36.4%
η_{s_sys}	22.3%	21.3%	19.9%	17.9%	16.2%
η	25.8%	27.2%	27.4%	27.3%	27.5%
Operating hours [h]	1096	968	895	845	803

The results of the simulations in Table 9 show that the lower the flow rate the lower the thermal efficiency, η. The solar collectors operate at higher inlet temperatures for lower flow rates. Because of the higher temperatures more heat is lost to the ambient environment, thereby leading to lower thermal efficiencies, as displayed in Table 9. The temperature difference between inlet and outlet of the collector is also higher for lower flow rates. Equation 10 shows the mass flow rate is inversely proportional to the temperature difference, so when the mass flow increases, the temperature difference decreases. On the other hand, the solar collector system efficiency, η_{s_sys}, decreases with increasing flow rate. This is because η_{s_sys} is dependent of the total solar energy gain over a period. As we can see the solar collector has more operating hours with lower flow rates, which means the total solar energy gain is also bigger. The result of η presented in Table 9 is an average of all the thermal efficiencies calculated at every time step and is therefore not that dependent of the total solar energy gain.

There is a controller to control the water pump in the solar collector system. The pump is only turned on when the temperature difference between the inlet and outlet of the solar collector is high enough or else it is turned off. So the controller decides the operating hours of the solar collector.

The operating hours was one of the results of the simulation. As seen in Table 9 the operating hours is higher for lower flow rates, this is due to higher temperature differences for these flow rates. Since the working periods will be longer, the useful energy gain from the collector will also be larger for lower flow rates. Figure 31 shows that the lowest velocity, 1.5 m/s through the collector, will give the largest amount of useful energy gain. Decreasing the flow rate will slow down the flow velocity, giving it more time to be in contact with the hot solar collectors, thus the temperature out of the system is increased so the temperature difference between inlet and outlet is increased, and thereby also increasing the energy gain. The outlet temperature decreases as the water velocity increases since the fluid is exposed to less time of radiation.

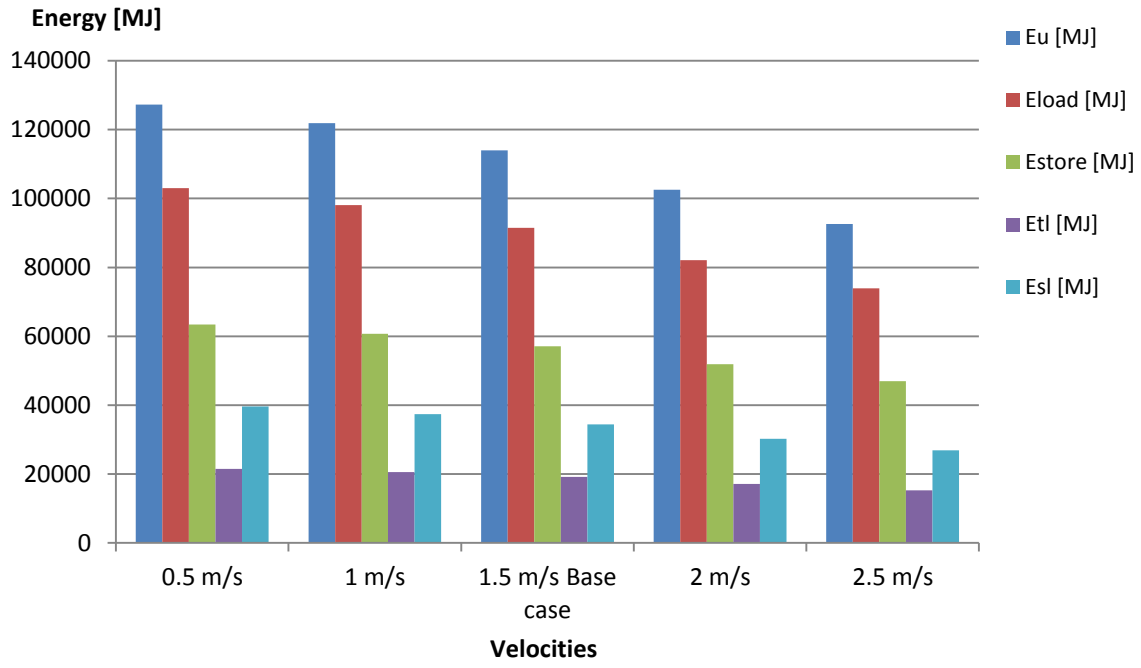

Figure 31: Total energy gains and energy losses through the storage season with varied velocities

10.4.3 The influence of the volume of the ground storage

The heated ground volume comprises the volume of the storage. The storage volume has a cylindrical shape. Number of boreholes, depth and spacing taken together allow the storage volume to be calculated. The volume of the ground storage was one of the most important parameters to investigate. To investigate its effects on the system performance, the parameters number of boreholes, spacing and depth were varied. The sizing of the ground storage depends on the energy demand, the operation time for a year of the heat pump and the desired temperature in the storage. Experiences from earlier projects show that the major investment of solar heating systems combined with seasonal storage is the cost of building the storage, for example drilling of the boreholes, refill of boreholes. As drilling costs increase with depth of the borehole, the length and the number of boreholes are important (Pavlov & Olesen, 2009). The costs associated with the depths typically form 30-50% of the total system costs (Rawlings et al, 2004). Therefore it is very important to size the system correct. Shallow boreholes are more beneficial in relation to the energy demand of the circulation pumps. This is because the boreholes are connected in parallel and the pressure drop the circulation pump must overcome is reduced.

10.4.3.1 The influence of the borehole depth

The borehole depth was varied between 10-50 meters, which are common depths in borehole thermal energy storages for small scale use. The volume increases with bigger depths. All other parameters were kept constant. In these simulations, it was assumed that the thermal conductivity was constant through the whole ground.

Table 10: Results of simulation with varied borehole depth.

	Depth				
	10 m/Base case	**20 m**	**30 m**	**40 m**	**50 m**
Volume [m^3]	1948	3897	5844	7793	9741
Results					
F_{StU}	50.1%	61.7%	66.3%	68.8%	70.3%
F_{StL}	62.4%	69.2%	71.6%	72.9%	73.6%
F_T	16.8%	9.5%	6.7%	5.2%	4.3%
F_{LU}	37.6%	30.8%	28.4%	27.1%	26.4%
F_{LL}	30.2%	27.4%	26.3%	25.6%	25.3%
η_{s_sys}	19.9%	24.0%	26.0%	27.3%	28.2%
η	27.4%	30.0%	31.6%	32.9%	33.9%

The results in Table 10 shows the magnitude of F_{LL} is decreasing with increasing storage sizes, since heat losses are increasing with the storage envelope surface (proportional to the square of a length), while stored energy is increasing with the storage volume (proportional to the cube of a length). So when the storage volume is increased the amount of stored energy will increase faster than the amount of heat losses. Refer to Equation 5 that describes the heat losses of the ground storage and Equation 4 that describes the maximum amount of stored energy.

It is visible in Figure 32 that the storage temperature rises with decreasing volumes. The return temperature to the tank is higher because of higher temperature in the ground for smaller storage volumes. Since the return temperature to the tank is higher, the temperature in the tank will rise, leading to larger temperature differences between the environment and the tank. Larger temperature difference between the tank and the environment will increase the tank losses. Decreased depths will increase the relative storage losses and the tank losses. Initially the storage temperature is at its undisturbed ground temperature, in this case 18°C. When the injection of heat begins, the storage will be charged to a higher temperature. The storage temperature will become higher than the temperature of the surrounding ground and the storage losses will increase. The relative storage losses will be larger for smaller volumes that operate at higher storage temperatures. Lower storage temperature will also give lower inlet temperature to the solar collector, which will raise the collector efficiency. Low storage temperature limits collector heat losses and low return temperature improves solar collector efficiencies.

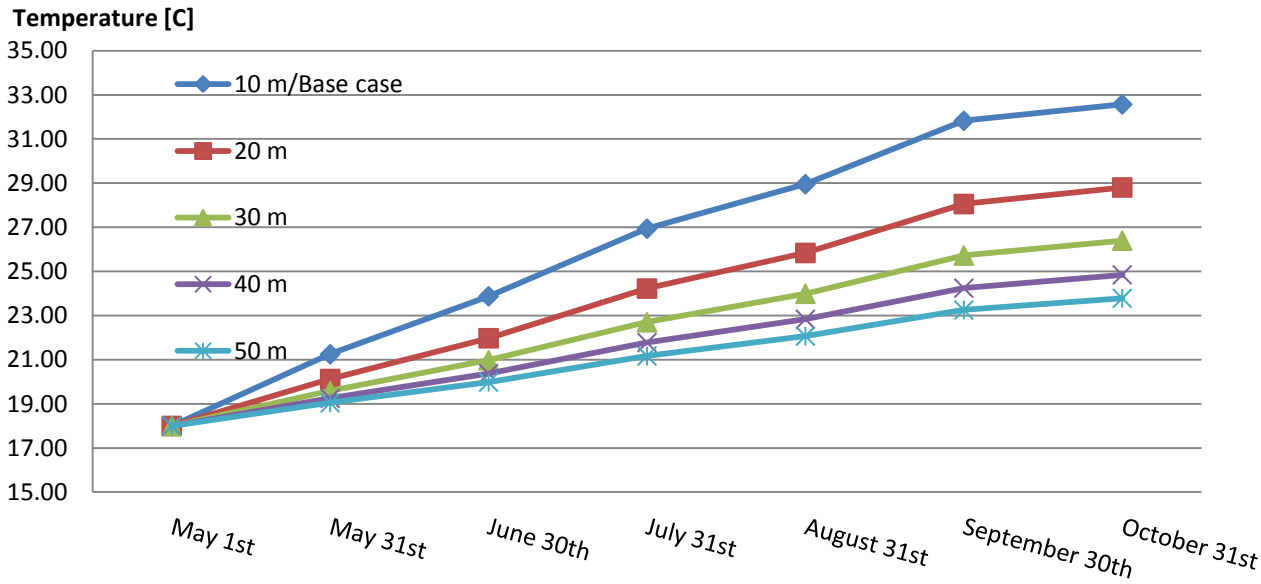

Figure 32 Ground storage temperatures with varied borehole depths.

Since the storage has a cylindrical shape, the losses can be divided into three parts. Figure 33 displays the storage losses of the top, side and bottom surfaces of the storage. By changing the depth, only the surface areas on the side will increase while the top and the bottom surface areas will stay constant. The heat losses of the storage unit are roughly proportional to the area exposed to the surroundings. Therefore the loss on the sides will increase with bigger depths, since the side areas would be larger and the heat loss increase with the surface area. While the top and bottom losses will decrease with bigger depths, since the storage temperature decreases with bigger volumes, depicted in Figure 33. The absolute amount of heat losses is bigger with increased depth, but still the storage efficiencies are better for these storages because the absolute amount of useful energy gain is bigger.

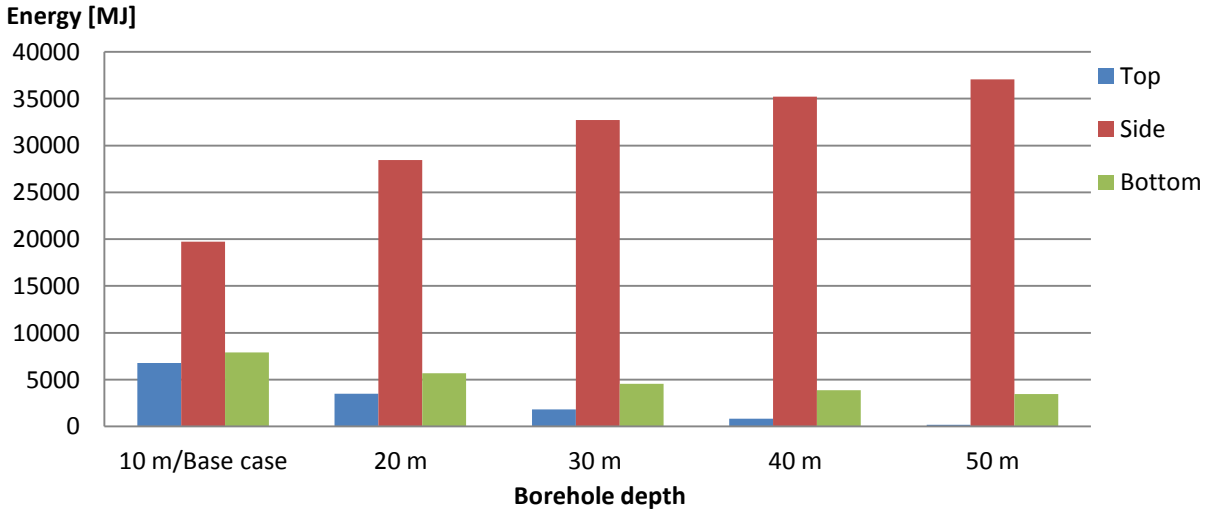

Figure 33: Storage heat losses through top, side and bottom surfaces of ground storage volume with varied borehole depth.

10.4.3.2 The influence of the borehole spacing

The borehole spacing is defined as the distance between two boreholes. In this case, the borehole spacing was examined while keeping the number of boreholes constant. In earlier realized projects, the spacing is usually varied between 2-5 meters (Bauer, Heidemann, & Steinhagen-Müller, 2009). For the simulations, the spacing is varied between 2 - 6 meters. As the spacing is reduced, the volume of the storage will also reduce. All the other parameters were kept constant.

Table 11: Results from simulation with varied borehole spacing at the same number of boreholes.

	Borehole spacing				
	2 m	**3 m**	**4 m**	**5 m/Base case**	**6 m**
Volume [m^3]	312	701	1247	1948	2806
Results					
F_{StU}	21.8%	33.3%	42.7%	50.1%	56.6%
F_{StL}	29.5%	42.9%	53.8%	62.4%	70.2%
F_T	22.1%	18.9%	17.5%	16.8%	16.5%
F_{LU}	52.0%	44.3%	36.6%	30.2%	24.1%
F_{LL}	70.5%	57.1%	46.2%	37.6%	29.8%
η_{s_sys}	17.8%	19.1%	19.7%	19.9%	20.1%
η	26.0%	26.8%	27.3%	27.4%	27.5%

Reducing the spacing will lead to higher temperature of the borehole storage, shown in Figure 34. The higher temperature is due to the smaller volume. A smaller storage volume operates at a higher storage temperature (Ataer, 2006). The storage temperature decreases with increasing storage volume, because the collected solar energy needs to heat a bigger space. Higher storage temperature will lead to higher operating temperature in the whole system, which will lead to lower F_{StL} and higher storage losses. The larger the storage volume, the more energy can be stored, shown in Figure 35. For spacing of 2-3 meters, the losses in the storage are bigger than the stored energy. The spacing has a bigger influence on the storage losses than the tank losses. Because the temperature change in the storage is bigger than the temperature change in the tank for different spacing.

The collector efficiency increases with spacing and storage volume. Increasing the spacing from 2 to 3 meters increases the collector efficiency. Increasing the spacing more than 4 meters has a very small effect on the collector efficiency.

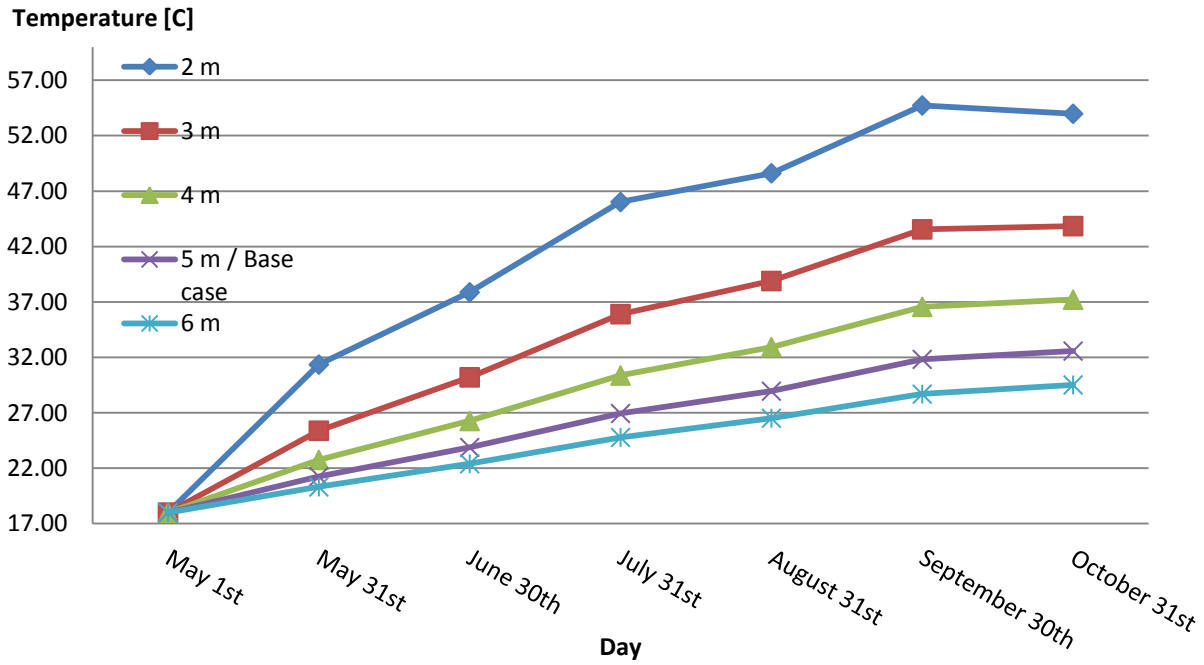

Figure 34: Storage temperatures with different borehole spacing at the same number of boreholes.

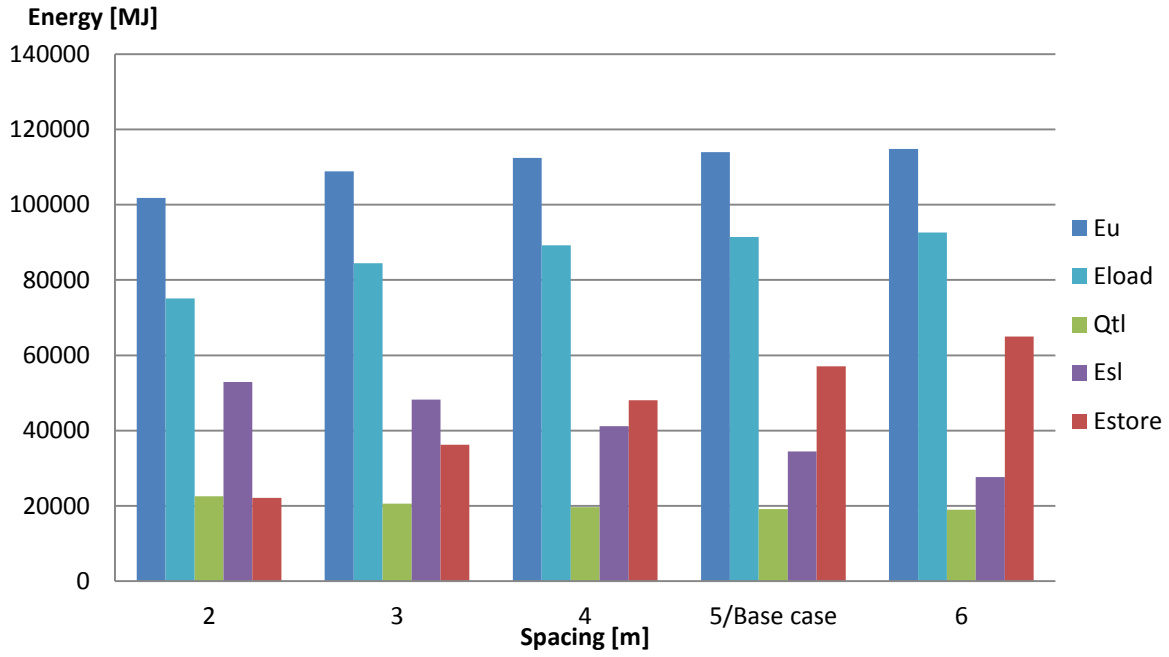

Figure 35: Total energy gains and energy losses through the storage season with different borehole spacing at the same number of boreholes.

10.4.3.3 The influence of the number of boreholes

We wanted to test the effects of the heat transfer by changing the number of boreholes without changing the storage volume. Increasing the number of boreholes will increase the heat transfer area. In this simulation the volume was kept constant by increasing or reducing the number of boreholes and spacing. By keeping the volume constant, we could study the effects isolated. There were also done some simulations without keeping the volume constant and the number of boreholes was varied; the effects on the system were almost the same as in other cases where the volume is changed. The number of boreholes and the spacing were decided according to volume of the base case that was kept constant at 1948 m^3. By varying the spacing between 2-6 meters, the number of boreholes is found by Equation 24. Five cases were simulated; case A with 56 boreholes and 2 m spacing, case B with 25 boreholes and 3 m spacing, case C with 14 boreholes and 4 m spacing, case D with 9 boreholes and 5 m spacing and case E with 6 boreholes and 6 m spacing.

Table 12: Results from simulation with different spacing and number of boreholes at the same storage volume.

		Case A	**Case B**	**Case C**	**Case D/Base case**	**Case E**
Varied parameters	Spacing [m]	2	3	4	5	6
	Number of boreholes [-]	56	25	14	9	6
Results	F_{StU}	47.5%	49.2%	50.0%	50.1%	50.8%
	F_{StL}	50.8%	54.5%	58.4%	62.4%	66.5%
	F_T	5.9%	8.6%	12.4%	16.8%	22.4%
	F_{LU}	46.0%	41.0%	35.6%	30.2%	24.6%
	F_{LL}	49.2%	45.5%	41.6%	37.6%	33.5%
	η_{s_sys}	26.7%	24.6%	22.2%	19.9%	17.7%
	η	32.4%	30.5%	28.9%	27.4%	26.2%

By keeping a constant volume and only change the number of boreholes and spacing, it is observed that having more boreholes the heat transfer to the ground will increase. The results in Figure 37 show that there are bigger temperature differences between the inlet temperature and the outlet temperature of the heat carrier fluid in these storages. Which means the heat carrier fluid transfers a larger amount of heat to the ground. The larger the temperature difference the larger the heat transfer. The parameter, number of boreholes, has a big influence on the heat transfer to the ground. Case A, which has the highest number of boreholes, has the largest temperature difference. This is due to the hot water has to circulate though more boreholes and by that give more heat to the ground. The heat transfer area increases with the number of boreholes. Case A has also the smallest spacing, which is very favorable for heat storage, because the boreholes will thermally influence each other and thereby raise the heat transfer. The heat transfer area increases with number of boreholes and reduced spacing. The storages with more boreholes reach higher storage temperatures, depicted in Figure 36, because more heat is transferred into the ground.

F_{LU} and F_{LL} are decreasing for lower numbers of boreholes because there are fewer losses in these storages. The results show that the storage losses are increasing with increasing number of

boreholes, while the tank losses are decreasing with increasing number of boreholes. The increasing storage losses are due to higher temperature in the storage. But the solar collector efficiency is higher and the tank losses are lower with increasing number of boreholes, because the return temperatures are lower, as displayed in Figure 37, which will make the solar collector inlet temperature and average tank temperature lower. The closer the boreholes are to each other the lower outlet temperature. The return temperatures are lower since the heat transfer is better in these storages.

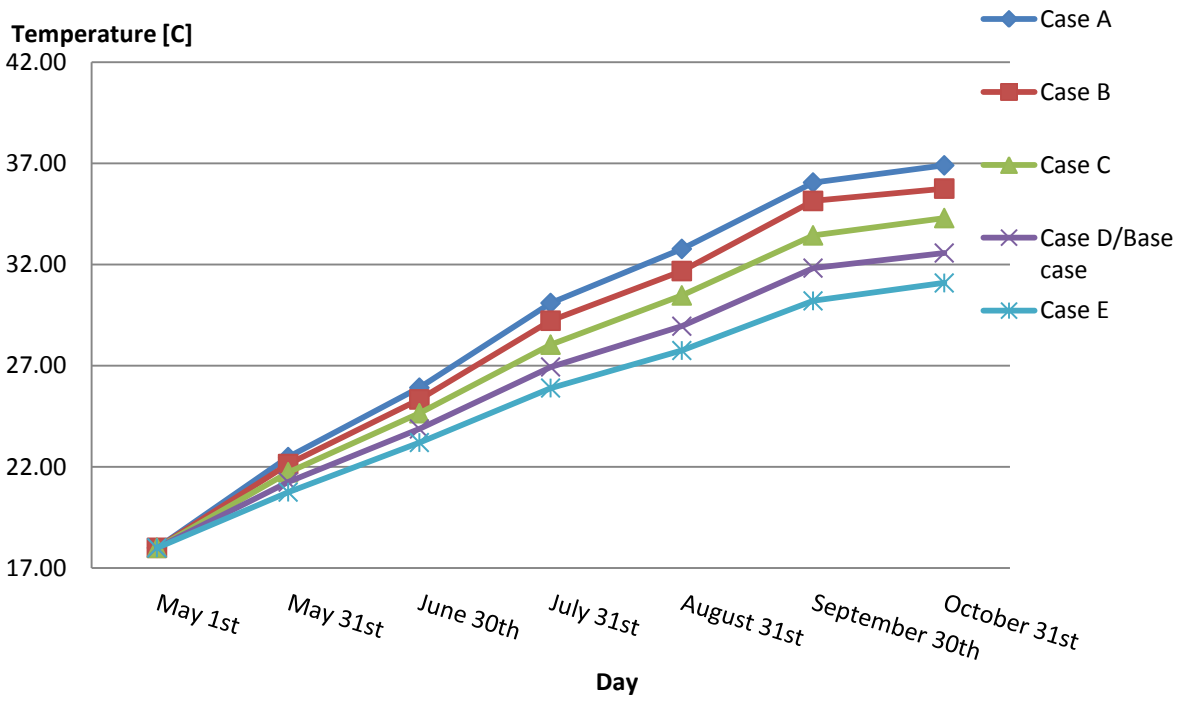

Figure 36: Ground storage temperature with varied spacing and number of boreholes.

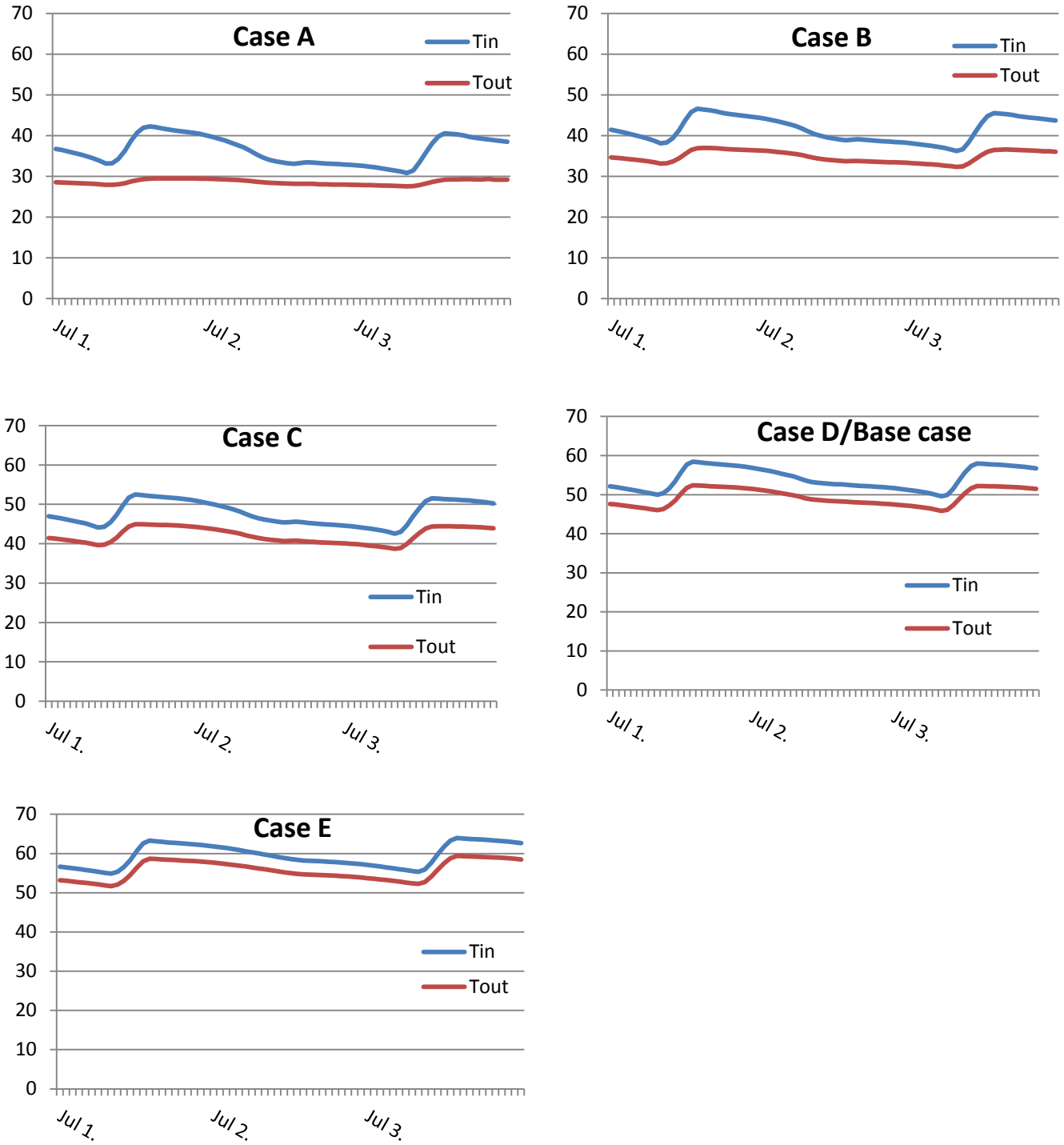

Figure 37: Inlet and outlet temperature of the heat carrier fluid circulated through the ground storage for some typical days in July.

10.4.3.4 Optimization of number of boreholes and spacing

We wanted to optimize the number of boreholes and spacing for the given storage volume in the base case. Decreasing and increasing the spacing with very small changes will provide a more exactly overview of the effects and the influence these parameters. Table 13 displays the number of boreholes as a consequence of altered borehole spacing.

Table 13: Varied spacing and number of boreholes at the same storage volume.

Spacing	Number of boreholes
0.5	900
1	225
1.5	100
2	56
2.5	36
3	25
3.5	18
4	14
4.5	11
5	9
5.5	7
6	6
6.4	5

The amount of stored heat in the storage is at its highest when the spacing is 2 m, as seen in Figure 38. At the end of October, the amount of stored heat is 72424 MJ. This is because for smaller spacing the temperature is too high so the storage losses are higher than the stored heat. For bigger spacing and reduced boreholes the heat transfer area is smaller, so the heat transfer will be smaller. When the spacing is bigger than 2 m, the stored heat is reducing. For spacing smaller than 2 m, the storage losses are bigger than the stored heat in the storage. For spacing of 2 meters, the amount of storage losses and the amount of stored heat are almost equal. But still this configuration can store more heat than configurations with larger spacing, because the total useful solar gain is bigger.

The configuration with spacing of 2 m and 56 boreholes appeared to be the most efficient configuration for the storage volume of 1948 m^3 with borehole depth of 10 m. This configuration can store the biggest amount of heat. The reduction of tank losses is very limited for spacing smaller than 2 m. The increase in useful solar gain is also very limited for spacing smaller than 2 m. The storage temperature graph starts to flat out for spacing of 1-2 meters. The results in chapter 10.4.3.3 showed that the storage efficiencies, F_{StU} and F_{StL}, are higher for decreasing boreholes and increased spacing. However, the total amount of stored heat in the ground storage has the greatest importance. Even though the storage efficiencies are higher for increasing boreholes and reduced spacing, but the total amount of stored heat is bigger for spacing of 2 m and 56 boreholes. This is due to the solar collector efficiency is higher so the collected solar energy is higher.

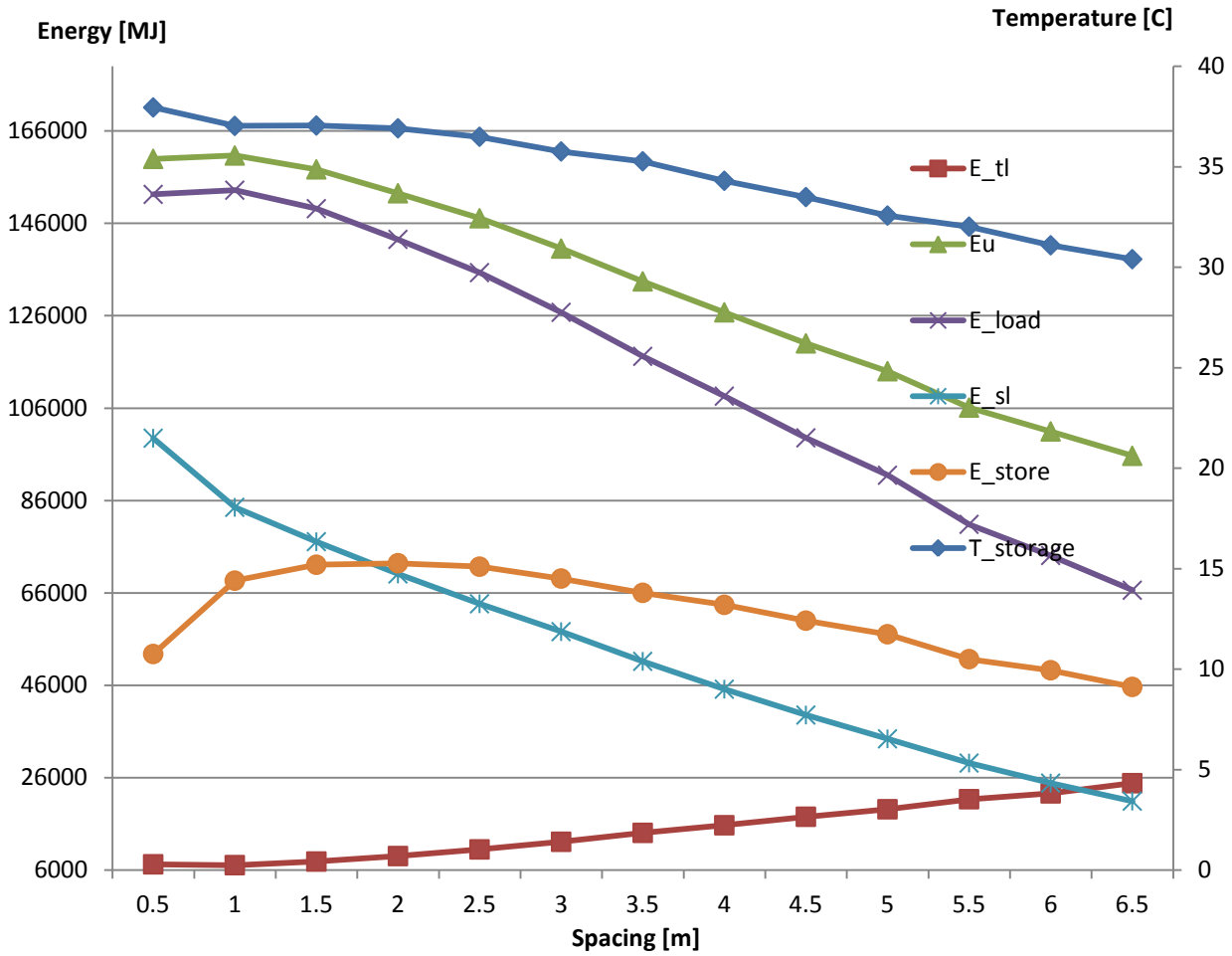

Figure 38: Optimization of number of boreholes and spacing.

10.4.4 The influence of the storage insulation

To see the effects of insulation on top of the storage there were executed simulations with different insulation thicknesses. The main focus of the simulations was to see the effects on the heat losses on different surface areas of the ground storage and storage efficiencies. Use of an insulation layer will obviously reduce the heat losses of the ground storage, but it was interesting to see the effects of different thickness of the insulation. Effect of interest was the improvement of the storage efficiencies compared to increasing thickness of insulation. An insulation layer with thermal conductivity of 1.0 kJ/hrmK was used in the simulation. The insulation thickness was varied between 0 - 0.8 meters. The insulation was placed on the top of the storage.

Table 14: Results of simulations with different insulation thickness.

	Insulation thickness				
Result	**0 m/Base case**	**0.2m**	**0. 4m**	**0.6 m**	**0.8 m**
F_{StU}	50.1%	51.2%	51.9%	52.3%	52.6%
F_{StL}	62.4%	63.8%	64.7%	65.3%	65.7%
F_T	16.8%	16.9%	16.9%	16.9%	16.9%
F_{LU}	30.2%	29.0%	28.3%	27.8%	27.5%
F_{LL}	37.6%	36.2%	35.3%	34.7%	34.3%
η_{s_sys}	19.9%	19.9%	19.9%	19.9%	19.9%
η	27.4%	27.3%	27.4%	27.4%	27.4%
Temperature in the storage in the end of October [°C]	32.57	32.89	33.09	33.21	33.30

The results in Table 14 show that the tank efficiency stays the same through the simulations. The storage insulation has a limited effect on F_T, because there is only a small change in storage temperature, so the tank temperature will almost stay the same. The same applies for η_{s_sys} and η. Obviously, the storage insulation has largest effect on the top losses and leading to reduction in top losses, as illustrated in Figure 39. This will increase F_{StU} and F_{StL}. Observed from the results, the improvements on the storage efficiency get smaller and smaller with increasing insulation thickness. The side losses and bottom losses have a small increase, because there is a small increase in the storage temperature, as presented in Table 14.

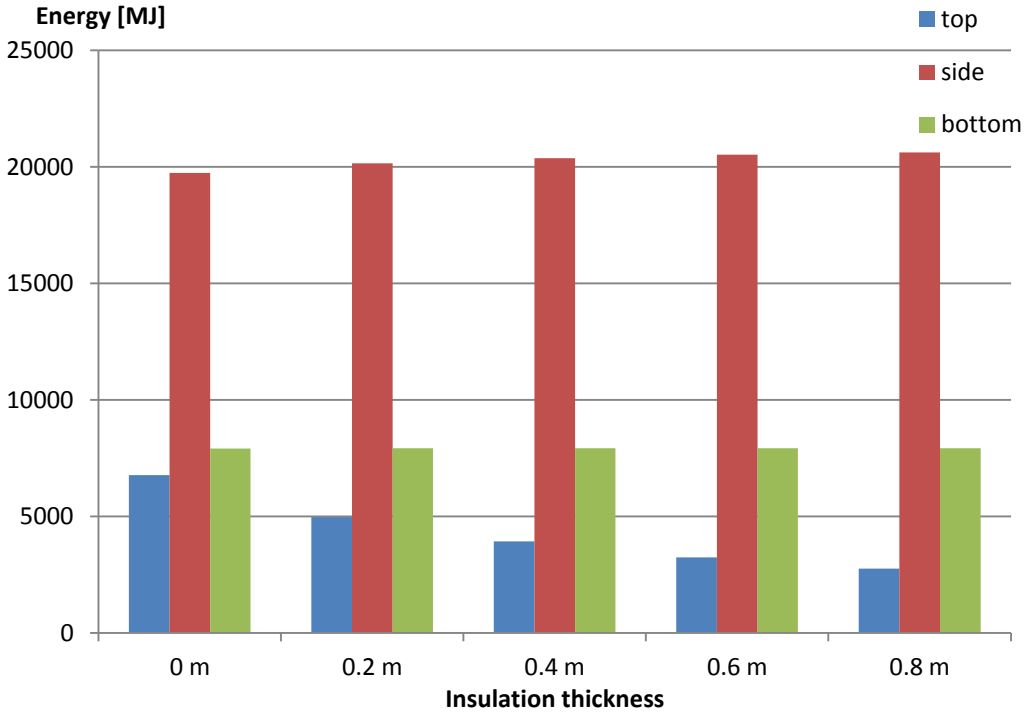

Figure 39: Storage heat losses through the top, side and bottom surfaces of the ground storage volume with varied insulation thickness on the top of the storage volume.

10.4.5 The influence of the water tank volume

The volume of the water tank was varied investigate the influence on the solar collector efficiency and the tank losses. The water tank is used as a buffer store. In available literature there are different recommendations for the volume of the buffer tank. Kovacs et al (2002) recommend a volume of 75-125 l for every square meter of evacuated tube collector area (0.075-0.125m^3/m^2). The water tank volume in the base case lies within in this range. Usually, these recommendations are aimed at domestic water heating and not solely for space heating. This is due to the most widespread application for solar systems are domestic water heating. The practice of sizing for space heating systems is very similar for to those of systems for domestic water heating (Martínez, Velázquez, & Viedma, 2004). For space heating systems it is required a bigger solar collector area.

Table 15: Results from simulations with varied water tank volume.

	Water tank volume					
Result	**5 m^3**	**10 m^3**	**15 m^3**	**20 m^3/Base case**	**25 m^3**	**30 m^3**
F_{StU}	58.0%	55.6%	52.9%	50.1%	47.7%	45.7%
F_{StL}	62.5%	62.5%	62.6%	62.4%	62.4%	62.5%
F_T	9.9%	11.7%	14.0%	16.8%	19.3%	21.5%
F_{LU}	34.8%	33.4%	31.6%	30.2%	28.8%	27.5%
F_{LL}	37.5%	37.5%	37.4%	37.6%	37.6%	37.5%
η_{s_sys}	15.5%	17.6%	18.9%	19.9%	20.7%	21.4%
η	25.4%	26.2%	27.1%	27.4%	27.9%	28.2%

Smaller tank volume gives less stratification, because there is less height to stratify the temperature. Less stratification will give higher solar collector inlet temperature and thereby decrease the collector efficiency. Figure 40 shows the influence of tank volume on the energy gains and the energy losses of the system. The storage losses are not very affected by the volume of the water tank because the storage temperature does not change a lot. Figure 40 depicts the total amount of stored heat has a maximum at tank volume of 20 m^3. Thus, bigger stores do not increase system performance significantly and can even decrease the stored energy in the ground storage as a result of the increasing heat loss of the water tank as the volume increases. The volume of the water tank has biggest influence on the tank losses and the solar gain. When the tank volume increases, the surface area will also increase which will lead to increase in tank losses. Increase in tank volume will also lead to better temperature stratification in the tank, so the solar collector inlet temperature will decrease which will increase its efficiency, which is displayed in Table 15.

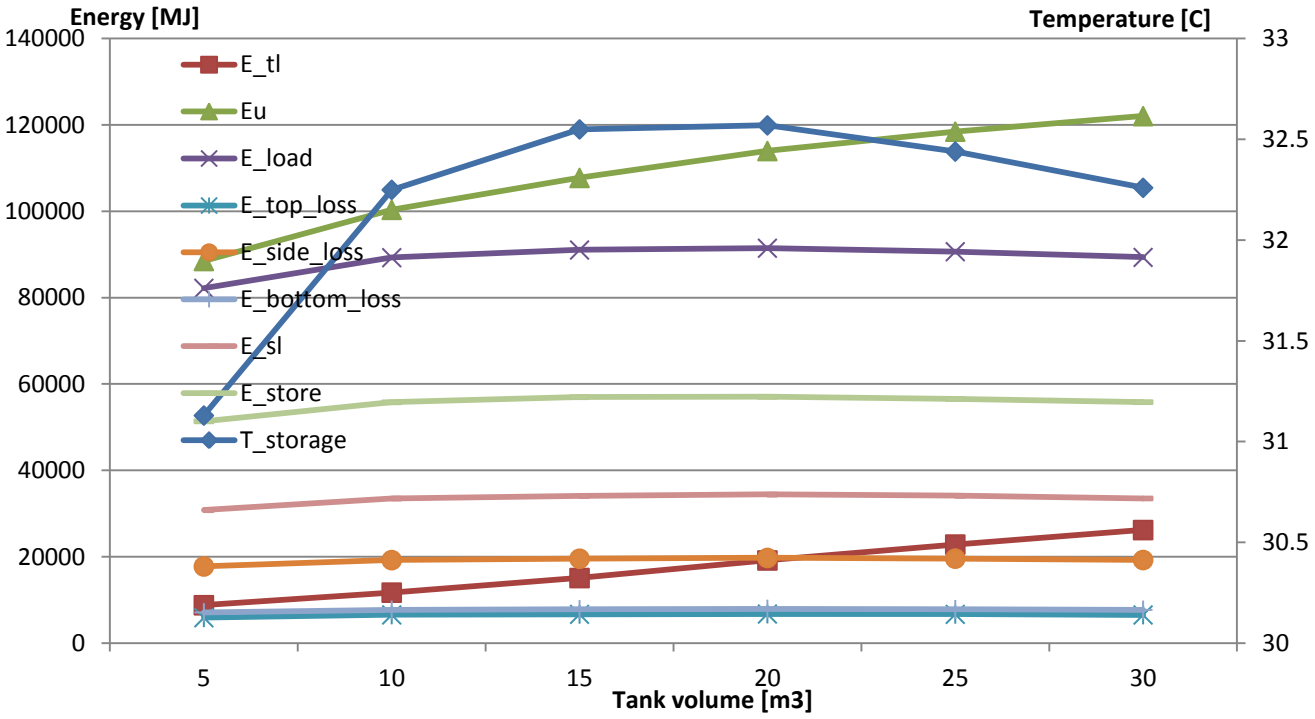

Figure 40: Energy gains and losses and storage temperature with varied tank volume

10.5 Summarization of the simulations results of the solar thermal ground storage model

In this paragraph the most important observations of the system behavior and performance regarding the different parameters will be summarized and concretized.

10.5.1 The impact of size of storage volume and solar collector area

After simulations of different storage volume it is clearly that the heat loss from the storage unit depends on the size and shape of the storage unit and the storage temperature during a cycle. The relative heat losses during a cycle increases with the temperature difference between the storage temperature and the undisturbed temperature in the surrounding ground. Decreasing the volume leads to higher storage temperatures, thus higher heat losses. To compensate for the high losses in high temperature storages, these kinds of storages could be built in a much bigger scale. Heat losses increase with surface area and heat storage increase with volume, so to minimize the heat losses the surface area to volume ratio should be kept as low as possible. Another element is that the larger the storage volume, the more solar energy can be collected.

Simulations of different collector areas showed that increasing solar collector area leads to higher storage temperatures and higher return temperatures thus lower collector efficiency. The simulations showed that the solar collector efficiency is very dependent on the return temperature from the ground storage. Less solar useful solar energy gain leads to less stored energy in the BTES, which will lead to lower storage efficiency.

The sizes of the ground storage volume and the solar collector area depend on the objective of the usage of the ground storage. If the objective is to keep the ground storage at a high enough temperature in order to supply the whole heating demand and minimize the use of auxiliary heating, then the solar collector area needs to be big. Because increased solar collector area will increase the storage temperature. The volume of the storage needs to be relatively small to achieve higher storage temperatures. If the objective is to use the solar collector to keep the ground temperature at a suitable level for use with heat pumps, so the evaporator do not get too high inlet temperatures, then the solar collector area needs to be smaller. The volume of the storage needs to be relatively large to achieve lower storage temperatures.

Since we want to use the ground for direct heat exchange, the soil temperature needs to be higher than 30°C, so it is possible to directly use the water in the fan coil. So we want to choose the smaller volumes in relation to the solar collector area. When the ground temperature has dropped to a suitable level, the heat pump can be utilized. At the same time, larger volumes can store more heat, because the relative storage losses are less. So if we want to store a certain amount of heat and still keep a high soil temperature, the storage volume must increase to compensate for the storage losses and the solar collector area must increase to raise the soil temperature. However, capital cost can be excessive for building a big storage volume and installing a big solar collector area (Gentry et al, 2006).

10.5.2 The impact of outlet temperature and storage temperature on heat capacity

Another observation is that for a given ground storage volume and storage temperature, the storage capacity will depend on the outlet temperature of the storage. The lower the outlet temperature is, the higher the storage capacity of the system becomes, because the temperature difference

between the inlet and outlet temperature is larger. By transferring as much heat as possible to the storage/soil the temperature difference will be as large as possible. Improving the heat transfer in the soil will lead to optimization of the whole system. The heat transfer between the soil and the heat carrier fluid depends on the arrangement of the boreholes, the number of boreholes and the position of the boreholes. Also, the outlet temperature gives the lowest temperature level in the system and respectively the minimum discharge temperature of the borehole storage. Therefore, high outlet temperatures reduce the storage capacity of the store. High return temperatures are due to improper design of the system (Pavlov & Olesen, 2009). Similarly, for a given outlet temperature, storage capacity will increase with the storage temperature. However, higher storage temperature will always reduce the efficiency of the system, because it will give a reduced collector efficiency and tank efficiency.

10.5.3 The impact of borehole configuration

According to theory, see chapter 4.5, the borehole configuration for heat extraction requires bigger spacing between the boreholes since interaction is undesirable. For the proposed system we want to include storage of thermal energy during summer, therefore interaction is favorable, so the boreholes should be placed in a compact pattern with low spacing. As seen from the results, the configuration with spacing of 2 m and 56 boreholes can store the biggest amount of heat. For smaller spacing than 2 m the storage losses are too high. For spacing bigger than 2 m the heat transfer area is too small. The results show that a compact pattern is better suited for storage of heat.

After discussing with my supervisor it was decided it was more interesting to continue to work on case A with 2 m spacing and 56 boreholes. It is because this storage showed most promising efficiencies for the use of storing thermal energy and reaches a high soil temperature during storage season. We wanted to test further how this borehole configuration works during heating season, especially with a heat pump. Case A represents a compact configuration with small spacing, short boreholes and many closely spaced boreholes. So far the simulations have confirmed the theory that compact storages work well in storages. Even though most of the simulations were performed for the base case, most of the results also apply for case A. For example the effect of bigger solar collector area, bigger storage volume, etc. also applies for case A. There were also performed some similar simulations for case A. The reason that we used the base case for the simulations of operation mode 1 was because we wanted to test if it was possible to use the existing borehole configuration at the GEL for the proposed heating system. After the simulations it showed that the base case was not the most efficient system for storing thermal energy. Also, the soil temperature was not high enough to be used in direct heating with the ground. For the rest of the thesis, base case 2 is referring to case A. Except from the number of boreholes and spacing, all other parameters are kept the same in base case 2.

10.6 Simulations of operation conditions of the storage model

It was performed simulations for different operation times of the ground storage operation mode. The purpose of the simulations was to study the electricity consumption of the pumps, the end temperature of the storage, the heat losses and gains of the ground storage at different length and start of operation times. The pumps will have smaller electricity consumption at shorter storage season. The operation time of the solar collector pump will also depend on the solar radiation because of the controller. Longer duration of the storage season would imply higher end temperature of the storage. At the same time there will also be more heat loss in the storage with longer storage season. It was interesting to see how much the end temperature would increase and how much the heat loss would increase compared to how much the heat gain would increase. The main objective was to see the changes of these outputs.

A COP was defined for the storage to compare the system performance of different starting months of the storage season. The COP is defined as the ratio between the energy stored in the storage during the storage season and the total electricity use in the system during the storage season. The electricity is consumed by one circulation pump in the solar collector loop and one circulation pump in the BTES loop.

$$COP_{store} = \frac{E_{store}}{El_{sc} + El_{BTES}}$$

Equation 41: COP for ground storage

E_{store} The actual amount of energy that is stored into the ground storage volume [kJ]

El_{sc} Electricity use for the circulation pump in solar collector loop [kJ]

El_{BTES} Electricity use for the circulation pump in the BTES loop [kJ]

Figure 41 presents the total amount of energy losses and energy gains according to the starting month of the storage season. From the graph we can see that E_u and E_{inj} almost have the same changing tendency and the difference between these two energy amounts is small. This is because the difference between these two energy amounts is the tank losses, and the changes in these losses are very small. E_{store} is very different from E_{inj} since E_{sl} has big changes according to different starting months. The storage losses increase with the length of the operation time, because the storage temperature increases. Obviously, the starting month October has lowest amount of stored heat in the storage, due to the short period of storage. It can also be observed that almost all collected solar energy is stored into the storage during this month. This is because the storage losses and tank losses are very small since the end temperature is low. Figure 42 shows the end temperature for every month according to the starting month of the storage season. The graph shows that the longer the storage period, the higher the end temperature. We can also see that by starting the storage season in July, the soil temperature can reach a much higher temperature than the other months during the first month. This is due to high solar radiation in July. The simulations software uses the equations in chapter 9.2.7 to calculate the electricity consumption of the circulation pumps. The total electricity consumption for the circulation pumps in the solar collector loop and the borehole thermal energy storage was simulated according to different starting month, as illustrated in Figure 43 and Figure 44. As expected, the electricity demand increased with the

length of storage season. From the result of the COP in Table 16, we can see that the COP is highest for the starting month October. This because the electricity use is relatively small compared to the heat stored. For the starting month April the COP is lower, because there are more heat losses in the storage over a longer time period due to the temperature rise.

There are several factors that influence the choice of the starting month. The end temperature of the soil is very important, because the temperature needs to be higher than 30°C so the storage can be used in direct heating. The higher the temperature the longer time the direct heating can provide with heat. Longer operation time of the direct heating mode means less use of the heat pump, so electricity will be saved. We can see from the results that if the starting months are September or October the end temperatures are below 30°C, so these months are not suitable choices. We wanted highest end temperature as possible, so the operation time of operation mode 3 (described in chapter 3.2.3) is longest as possible. Starting month April has the highest end temperature, but the storage efficiency is not very good, since the storage losses are higher than the stored energy. The COP for May is higher than the COP in April. So the starting month May, the same as in the base case, is the most appropriate choice.

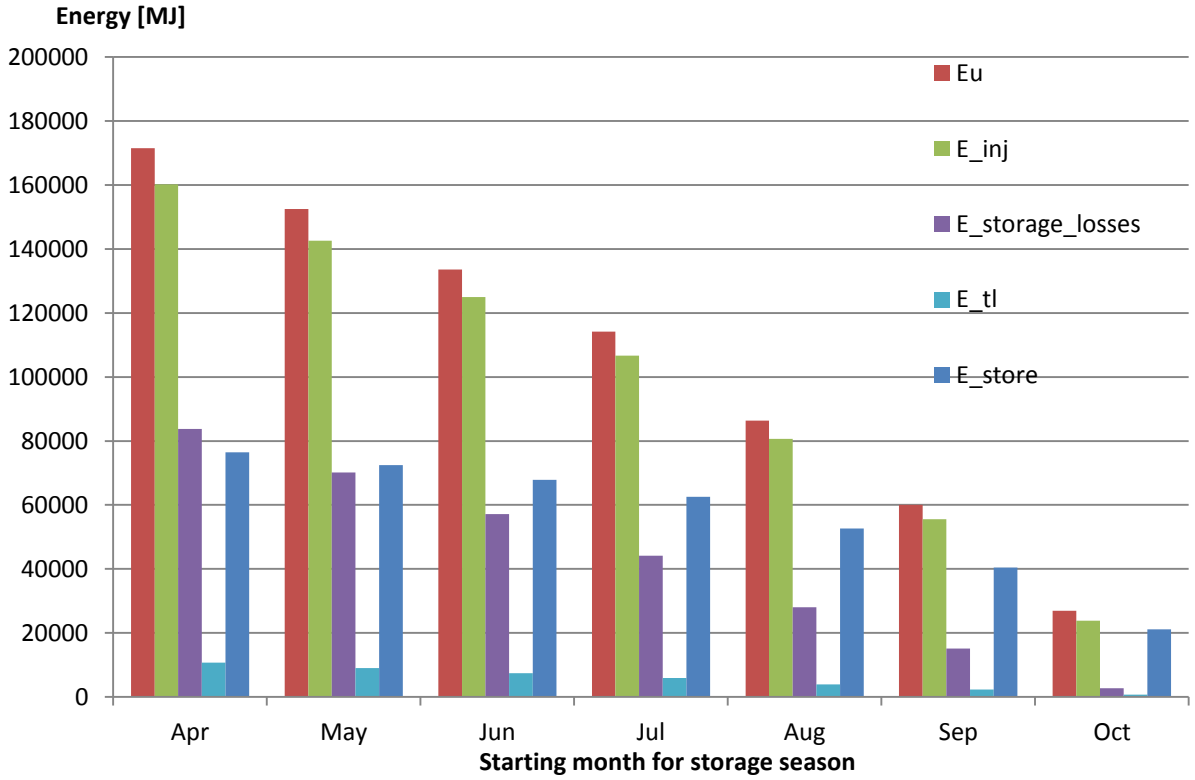

Figure 41: Total energy gains and losses according to different starting months of storage season.

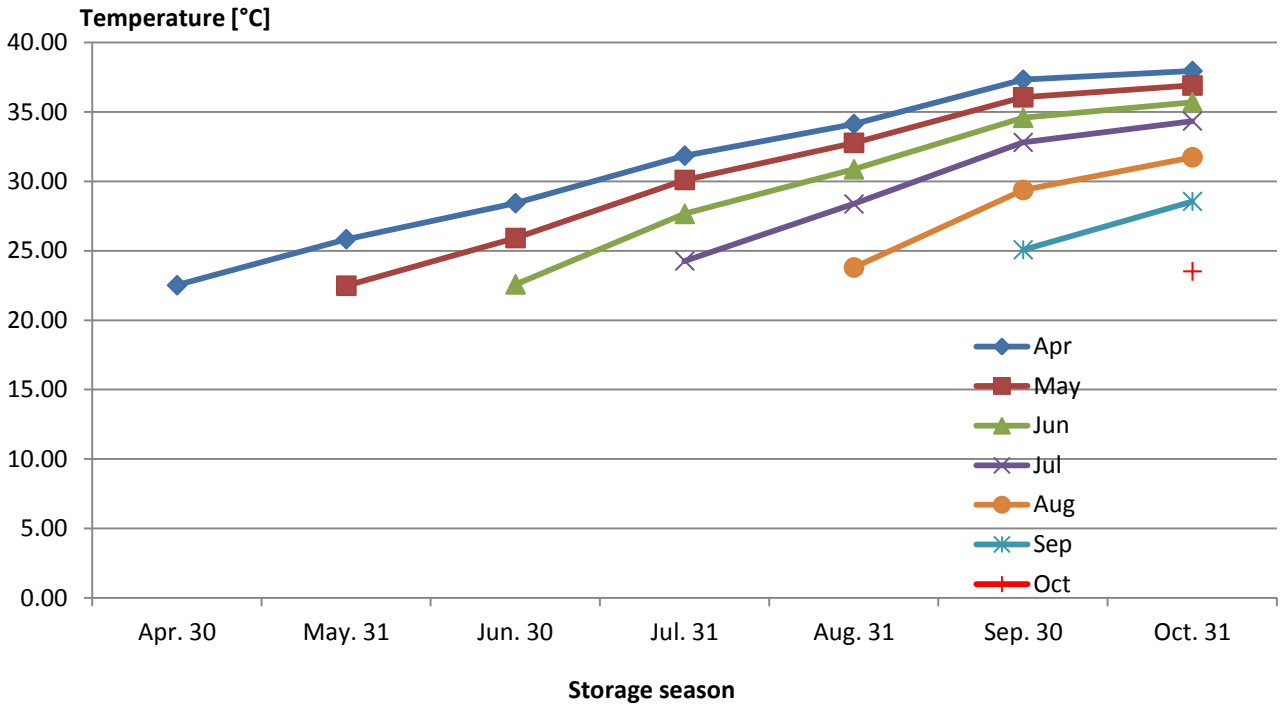

Figure 42: Storage temperature according to different length of storage season.

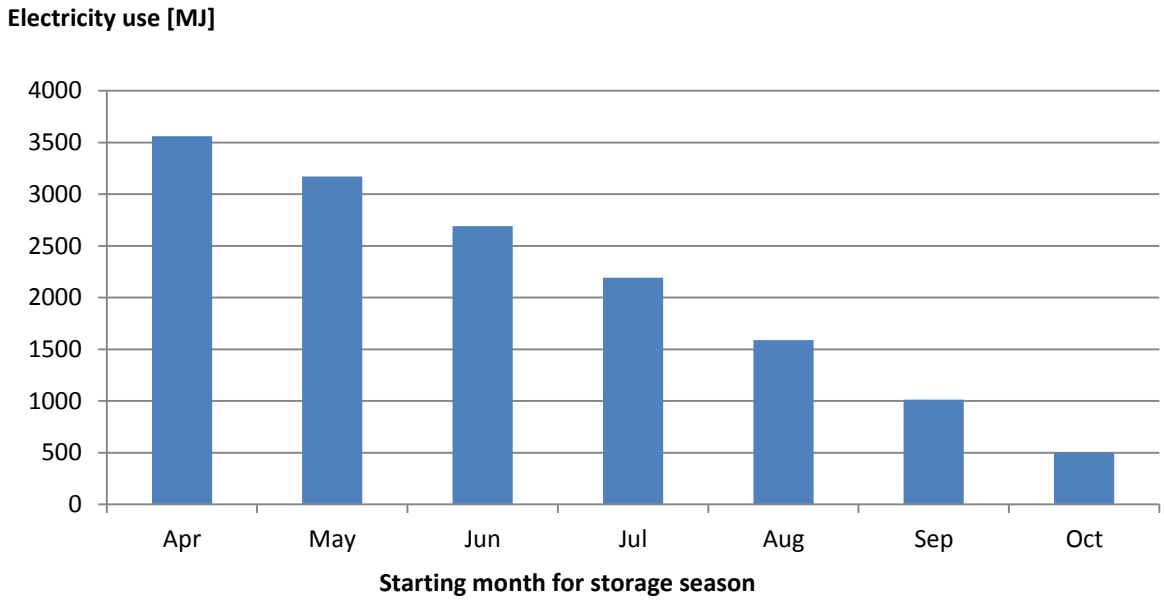

Figure 43: Electricity use for the circulation pump in the solar collector loop according to different starting month of storage season.

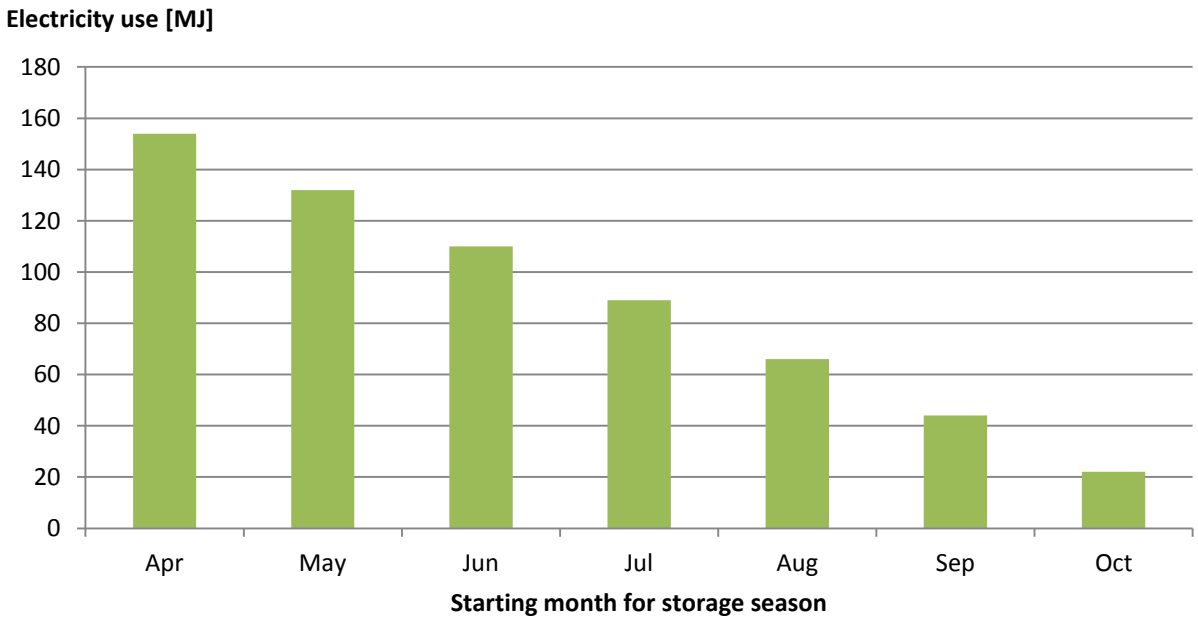

Figure 44: Electricity use for the circulation pump in the BTES loop according to different starting month of storage season.

Table 16: COP_{store} for different starting month of the storage season.

Starting month	COP_{store}
April	20.57
May	21.93
June	24.21
July	27.43
August	31.79
September	38.29
October	40.58

10.7 Simulations of the reference building

The heat demand of the ground floor of the GEL was simulated in TRNSYS. The simulations were later used as the heating load in the simulations of the heating modes. Normally, the first floor is used by students as work place. The simulated work place area comprises 816.5 m^2 and work place volume comprises 3429.2 m^3. The work place is planned to be used by around 30 students. To perform the simulation the work place area is characterized by its building materials, internal gains, dimensions, distribution and orientation. Type 56 was used to model the transient thermal behavior of the building. There are four different kinds of construction elements: external walls, floor, windows and roof. The whole floor was treated as a simple zone with a single inside air temperature.

The parameters in Table 17 are included in the TRNSYS software package through the TRNBuild tool specifically designed to simulate the thermal behavior in a multi-zone building area. The TRNBuild software reads in and processes a file containing the building description and generates two files that will be used by the type 56 during a TRNSYS simulation. The heat gains from the occupants and lighting in the building were specified and included in the simulations.

The thermal properties of the building shell and frame are summarized in Table 17.

Table 17: The thermal properties of the building shell and frame at the GEL.

Buildings shell component	Total thickness [m]	U-value [W/m^2K]	Layers	Layer thickness [m]	Conductivity [kJ/hrmK]	Capacity [kJ/kgK]	Density [kg/m^3]
External walls	0.332	0.228	Aluminum	0.002	729.972	0.840	2700
			Mineral wool	0.250	0.216	0.750	100
			Concrete	0.080	5.400	0.920	2400
Floor	0.215	0.441	Ceramics tiling	0.010	15.552	1.100	2000
			Adhesive layer	0.005	2.52	1.050	1400
			Cement mortar	0.020	3.348	1.050	1800
			Concrete	0.100	5.400	0.920	2400
			Insulation	0.080	0.144	0.800	40

10.7.1 Space heating

Energy and power demand of the reference building was calculated by simulation in TRNSYS. By defining the zone temperature in TRNSYS the model is allowed to calculate the amount of energy required to keep the zone at that temperature. It is a calculation of the ideal heating, which shows the smallest amount of energy that is needed in order to keep the zone temperature that is specified.

10.7.1.1 Energy demand

Table 18 provides an overview of the energy demand for space heating of the reference building in different units.

Table 18: Simulation results of the energy demand of the reference building.

	Specific energy demand [kWh/m^2]	Total energy demand [kWh/year]	Specific energy demand [MJ/m^2]	Total energy demand [MJ/year]
Energy demand	33.4	27233.0	120.1	98038.8

10.7.1.2 Power demand

Table 19 provides an overview of the power demand for space heating of the reference building.

Table 19: Simulation results of the power demand of the reference building.

	Average power demand [W/m^2]	Peak power demand [W/m^2]	Average power demand [kJ/hrm^2]	Peak power demand [kJ/hrm^2]
Power demand	11.3	31.0	40.7	111.6

Figure 45 shows the heat power demand for every month. The figure shows that the peak power demand occurs, in January, at the same time with the adverse environmental conditions. This is because the largest temperature difference between outdoors and indoors temperature occurs at these conditions. The heating season will last from the beginning of November to the end of March, since there are only heating demand in these months.

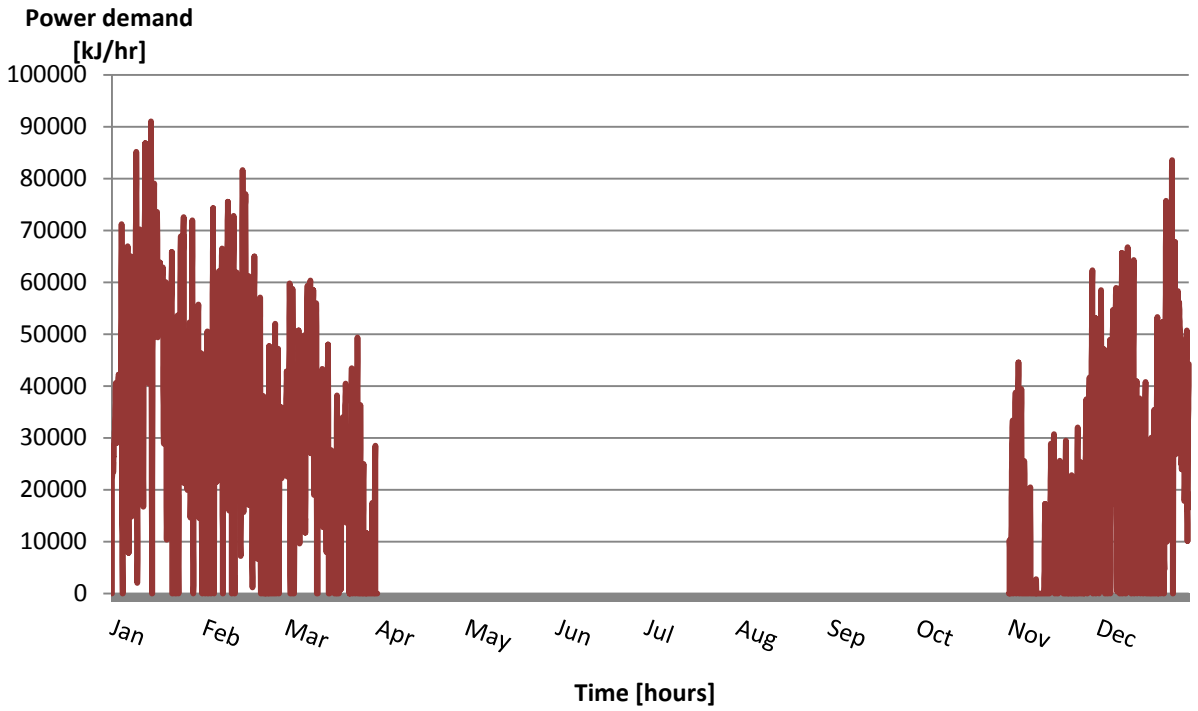

Figure 45: Annual heat power demand profile for the first floor (816.5 m^2) at GEL. Results obtained from TRNSYS.

10.8 Simulation of the different heating modes

The different heating modes have been described in chapter 3.2. Operation modes 2 - 4 represent the heating modes. In this chapter the three different heating modes will be simulated to study the heating performance. The heating load for the simulations will be based on the reference building. All of the systems use a fan coil to distribute heat into the reference building. The fan coil model calculate the outlet air conditions based on the water and air entering conditions and then directs this air stream to the building model. The air stream will change the zone temperatures in the building and an iterative process is commenced in TRNSYS.

The operation modes are simulated separately due to limitations in time and simulation software. To connect all the operation modes together will require a lot of temperature controllers and equations to control the valves. It was not focused on best control strategy to improve system efficiency, since the objective of the work was to study the behavior and the cooperation of the ground storage with the heating system. Naturally, when all the operation modes work together the return temperatures will be different. Due to the separate simulations it may weaken the dynamics of the system. However, the simulations will still show the behavior of the heating system in work with the different operation modes. The simulations will also show a roughly and reasonable presentation of the heat delivered to the load. The principles of each heating operation modes are shown and simulated.

The space heating system is the same for all of the systems; it is only the heat sources that are different. The solar direct heating system uses a solar collector model as heat source and a water tank model. The ground storage direct heat exchange uses a borehole storage model as heat source. The geothermal heat pump model uses a geothermal heat pump model and a borehole storage model as a heat source.

Heat pumps or solar collectors connected to a system are highly dependent on the temperature of the incoming flow. To gain sufficient accuracy of such heat sources a time step of few minutes is required (Persson, Perers, & Carlsson, 2011). For the simulation of the heating systems a time step of one minute is used.

For all of the systems, control strategies are implemented to regulate both the heat source and the space heating system. On the demand side of the model, the indoor temperature of the building is regulated by a thermostat set to 20°C with a ±2°C dead band. Which means the set temperature is 20°C, but the temperature is allowed to float between 18-22°C. One of the objectives is to observe how often the different systems can make it possible for the room temperature to reach the set temperature. It could also be possible for the heating modes to help raise the temperature and make use of auxiliary heating to cover the rest, but it is not covered in this study. Only when the set temperature is reached, it is regarded as coverage of the heat demand.

The air change will have a big impact on the indoor air quality. Higher number of air changes will give better indoor air quality, but at the same time the fan will use more energy to provide air. Higher air change will also give higher air velocity into the building, which can cause feeling of drafts for the user and also higher velocity will give cooler temperatures which can cause discomfort. In the simulations the air mass flow was set to 20000 kg/hr which gives an air change of 5 h^{-1}. According to ASHRAE recommended air change for offices is 4 - 10 h^{-1} (Mumma, 2003). The air mass flow was an input into the fan coil.

The air change is calculated by following calculation:

$$AC = \frac{\dot{m}_{air}}{\rho_{air} V}$$

Equation 42: Air change

AC	Number of times the air within a defined space is replaced [1/h]
$\dot{m}_{air}$	Air flow rate [kg/hr]
ρ_{air}	Density of air [kg/m^3]
V	Space volume [m^3]

As depicted in Figure 45 in chapter 10.7.1.2 the heating season starts from November 1st and lasts until March 31st. The heating season lasts for 3624 hours. The simulation period was from November to March. Some of the simulation results will be presented for shorter periods to easier show the results. The end temperature of the soil after the storage season was found in earlier simulation in chapter 10.4. This temperature will be used as start temperature for the heating season.

For the heat pump calculations the length of the boreholes of base case 2 were found to be too short and the volume too small to be used in combination with the heat pump. This will be explained further in chapter 10.8.6.

10.8.1 Heating scheme

Table 20 presents the heating scheme of the proposed heating system. The table summarizes the operation modes that were thoroughly described in chapter 3.2. Operation mode 1 is the storage mode and the simulations for this mode were presented in chapter 10.3 and 10.4. Operation modes 2-4 are the heating modes. As mentioned earlier, the heating modes have preferred order. Solar direct heating is the first choice, direct heat exchange with the ground is the second choice and the geothermal heat pump is the third choice.

Table 20: Heating scheme for the proposed heating system.

Operation mode	Solar Collector	Borehole	Heat pump
1. **Solar underground thermal storage:** Solar radiation absorbed by the solar collectors is transferred into the water storage tank, and then injected into the ground through the interaction between the borehole heat exchangers and the ground. This mode takes effect during the non-heating/storage season (May-October).	Solar collectors are in operation to produce heat for recharging of boreholes.	Heat injection. Gives increased temperatures to the borehole.	Not in operation.
2. **Solar direct-heating mode:** Solar collector is used to produce heating. Heat is exchanged inside of a solar water storage tank.	Heat production at temperatures higher than 30°C.	No heat extraction.	Not in operation.
3. **Heating mode by borehole direct heat exchange:** Borehole is used to provide heating by direct heat exchange. This mode takes effect when the solar collectors cannot produce sufficiently high temperatures to be used for the heating system.	Not in operation.	Heat extraction. Used for direct heat exchange with the heating system in the building. Heat exchange at temperatures higher than 30°C.	Not in operation.
4. **Heating mode by heat pump:** Heat pump is used to provide heating and borehole is used as a heat source for the heat pump. This mode takes effect when the borehole does not have high enough temperatures to be utilized in direct heat exchange.	Not in operation.	Heat extraction.	Heat pump starts to operate at temperatures below 30°C.

10.8.2 Simulation of solar direct heating model – Operation mode 2

There are three closed loops in the simulation of the solar direct heating mode, as illustrated in Figure 46. The red loop is the solar collector loop. The solar collector is connected to the water tank and transfers heat to the tank. The hot water exchanges heat with the air in the fan coil unit in the blue loop. The heated air is directed into the building in the green loop. There were two pumps in this model. One pump is connected to the solar collector and one pump is connected to the liquid side of the fan coil. The electricity use will be for the pumps. An ON/OFF differential controller with hysteresis effect is used to model the practical operation of the solar collector pump subjected to temperature control.

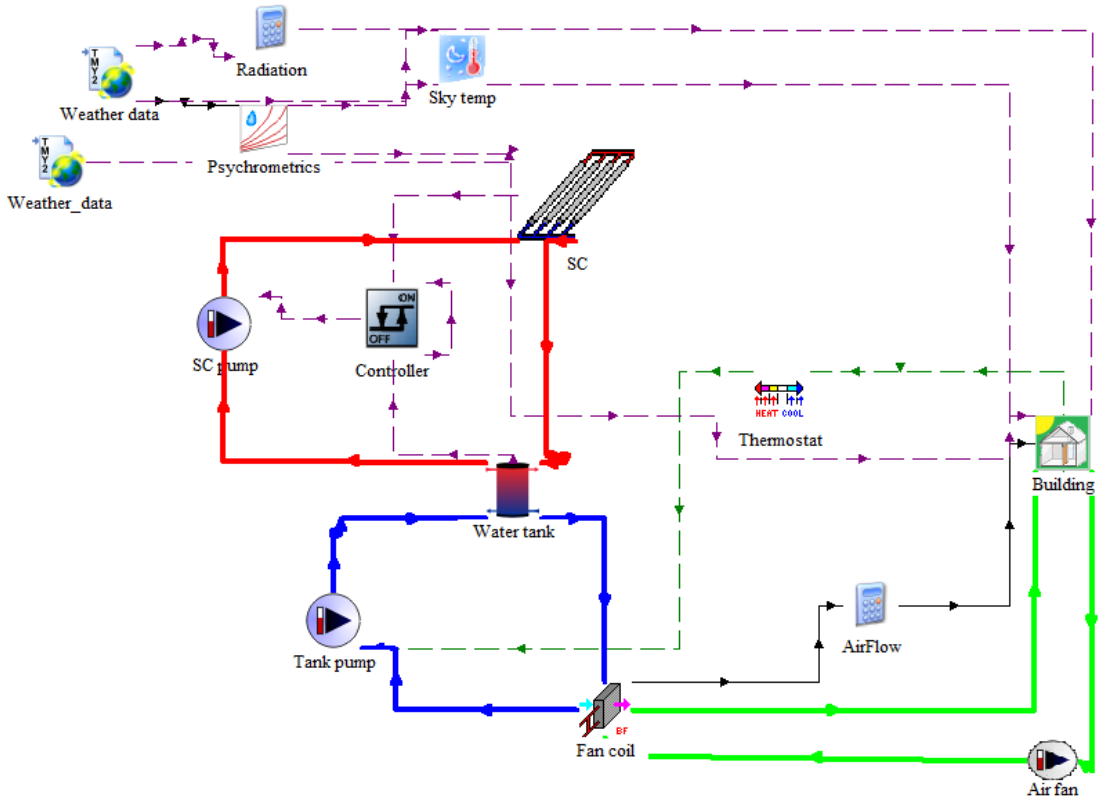

Figure 46: Simplified sketch of the project file components in TRNSYS. Solar direct heating mode with solar collector and water tank.

Table 21 provides an overview of the main components in TRNSYS used in the solar direct heating model.

Table 21: Overview of the main components in the solar-direct heating model

Component	Name in TRNSYS	Type number in TRNSYS	Description of the model is given in chapter
Evacuated tube solar collector	Evacuated tube solar collector with specified outlet temperature	538	9.2.2
Stratified water storage tank	Storage tank; Fixed inlets, Uniform losses	4a	9.2.3
Two pumps	Variable speed pump	110	9.2.7
Fan	Variable speed fan	111b	9.2.7
Reference building	Multi-zone building	56	10.7

10.8.3 Analysis of the simulations of the operation mode 2

The parameters are kept the same as in the base case 2, described in chapter 10.5.3. The objective of this simulation was to find out how much of the heat load can be covered by the solar direct heating mode.

A typical graph of the winter operation during the coldest period is presented in Figure 48. The figure shows the operation for the first 20 days in January, when the ambient temperature occasionally drops below 0°C and heating is necessary. It can be observed that the solar collector outlet varies between 10-50°C. The solar collector outlet is highly dependent on the solar radiation. During winter the solar radiation is much lower than during the summer. As illustrated in Figure 18 in chapter 8 the solar radiation in January is almost 70% lower than the solar radiation in July. Since the solar radiation is at its lowest during January, the solar heating cannot cover a large part of the load. When the solar collector outlet temperature is below approximately 30°C, it is not able to heat the room temperature up to the set temperature. When the tank temperature drops below 30°C, the other heating operation modes should be utilized.

As the temperature of the solar collector increases, the room temperature also increases. During higher temperatures the control signal starts to cycle on/off, because the thermostat tries to keep the room temperature at 20°C ±2°C. As seen in Figure 47 the fan coil outlet temperature varies frequently between 20°C and higher temperatures when the collector outlet temperature is high enough to maintain the set temperature. This is because the water pump is turned on and off. When the collector has temperatures around 50°C, the room may be higher than 22°C, so the pump will be switched off. The fan coil outlet temperature should be above 30°C, so the provided air temperature feels comfortable. The fan coil outlet temperature can keep temperatures above 30°C when the room temperature is heated to around 20°C.

We can see from Figure 49 January has the highest heat load and also the lowest energy supplied from the solar collector, which leads to a low solar fraction. The heat load is dependent on the ambient temperature. January has the lowest average ambient temperature, refer to Figure 19 in chapter 8, which will cause the largest difference between the indoor and outdoor temperature. This month is normally the coldest, which gives the highest heating demand. The solar fraction is low because of the low solar radiation in January. The graph of the solar fraction is closely related to the curve of solar radiation, see Figure 50. The solar fraction has almost the same changing tendency as the solar radiation curve, except in November. The solar fraction is higher in November than December even though November has lower solar radiation than December. This is because November has a relatively small heat load. There are many cloudy and rainy days in November which gives low solar radiation, but the average ambient temperature is high in this month which gives a smaller heat load.

From the simulations of the whole heating season (November-March), we can see that the solar collector can cover a big part of the heating load and keep a room temperature of 20°C. For the colder periods when the set temperature is not reached it is necessary to make use of the other operation modes, either direct heat exchange with the ground or the geothermal heat pump. Using equation 18 the solar fraction for the whole period is found to be 0.37.

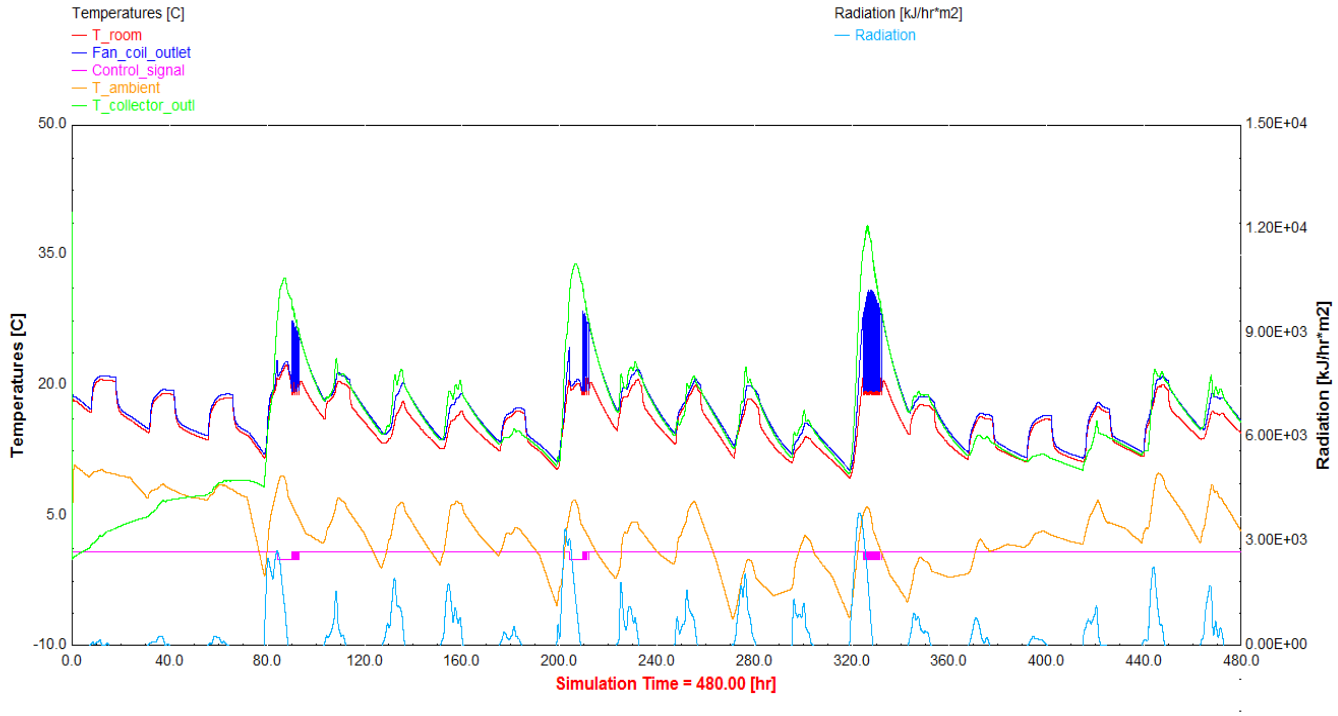

Figure 48: Simulation of the solar direct heating mode during the first 20 days of January. Room thermostat is set to 20°C.

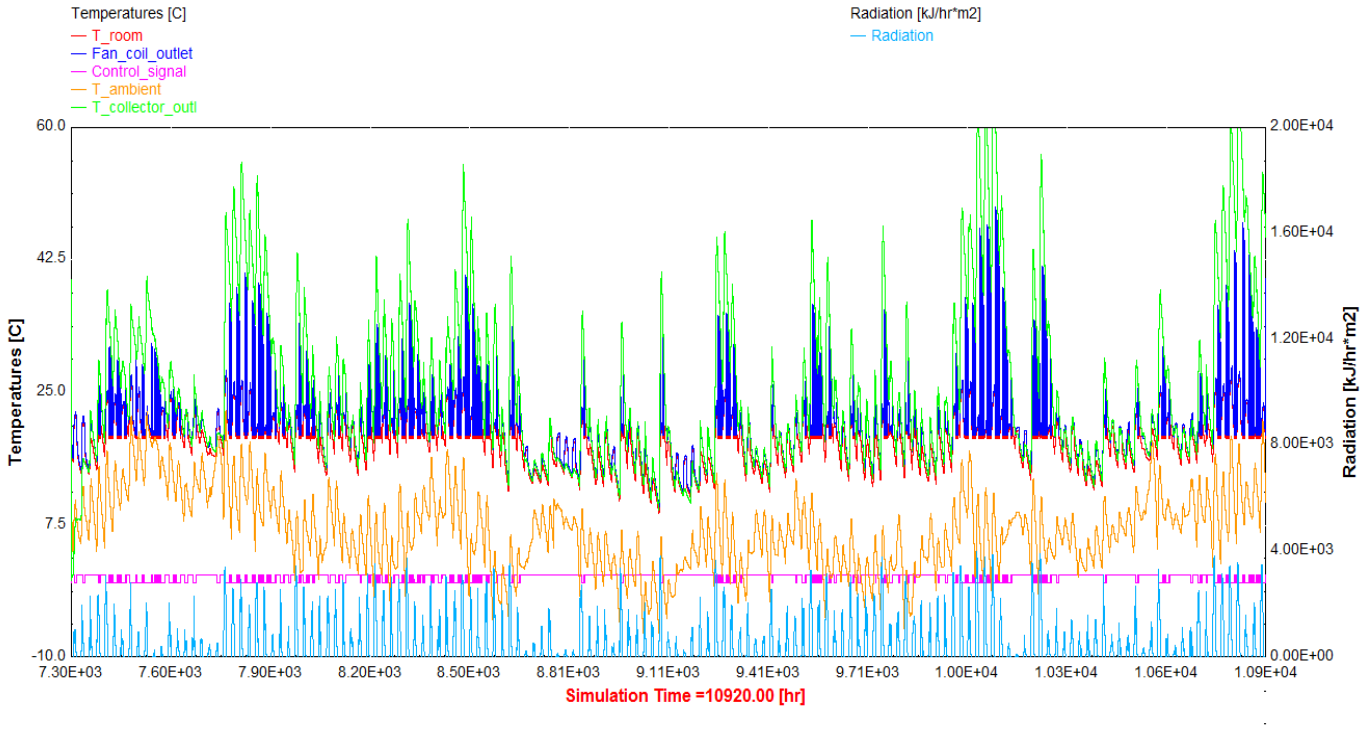

Figure 47: Simulation of the solar direct heating mode during the whole heating season from November to March. The months start at following hours:
November – 7926 hr, December – 8016 hr, January – 8760 hr, February – 9504 hr, March – 10248 hr

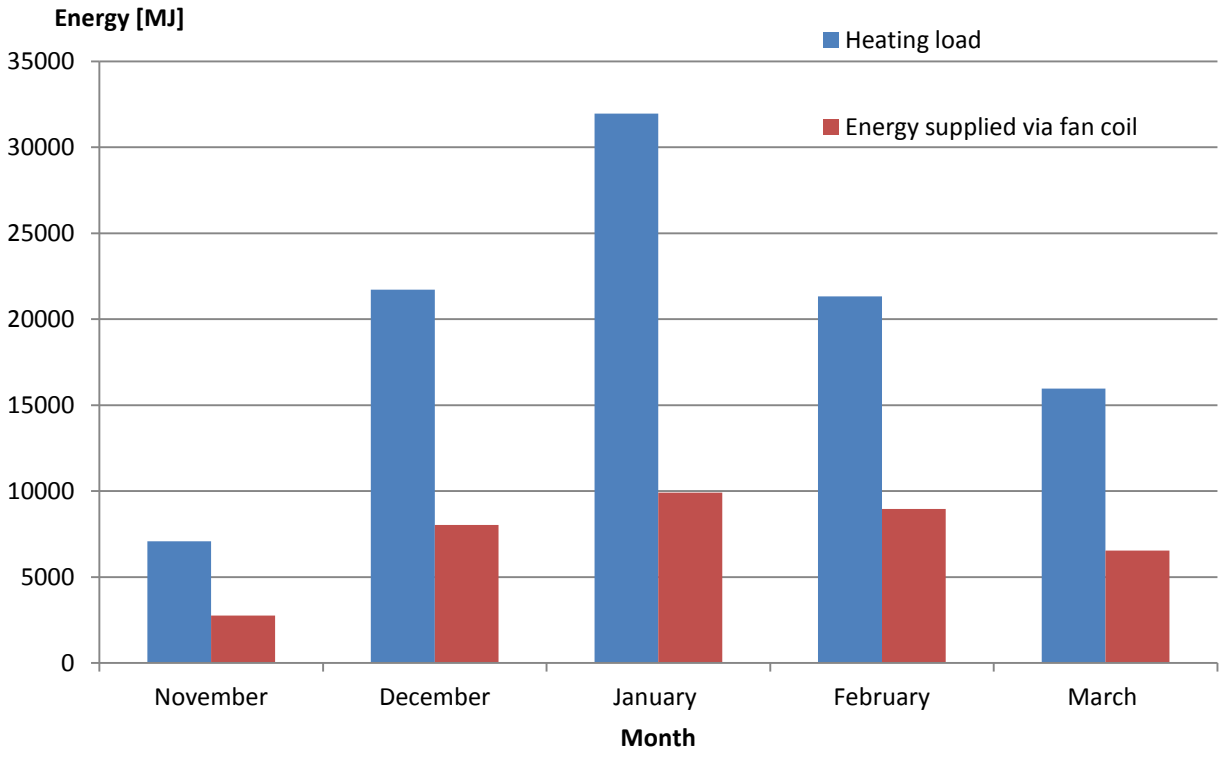

Figure 49: The heating load of the reference building and the energy supplied by the fan coil in the heating season.

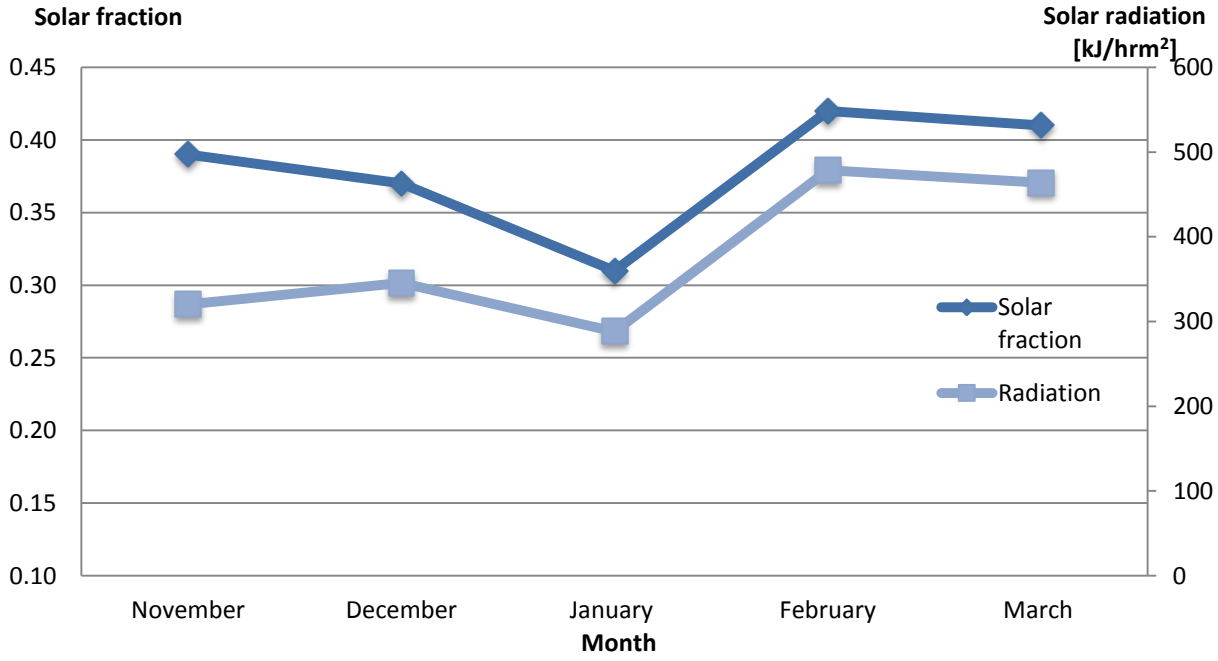

Figure 50: The solar fraction (Energy supplied by the coil/Heating demand) in the different months of the heating season .

10.8.4 Simulation of direct heat exchange with the boreholes model – Operation mode 3

The direct heat exchange model contains two loops as shown in Figure 51. The ground storage volume exchanges heat with the fluid side of the fan coil in the blue loop. The hot air is directed into the building in the green loop. The electricity use will be for the circulation pump that is connected to the storage.

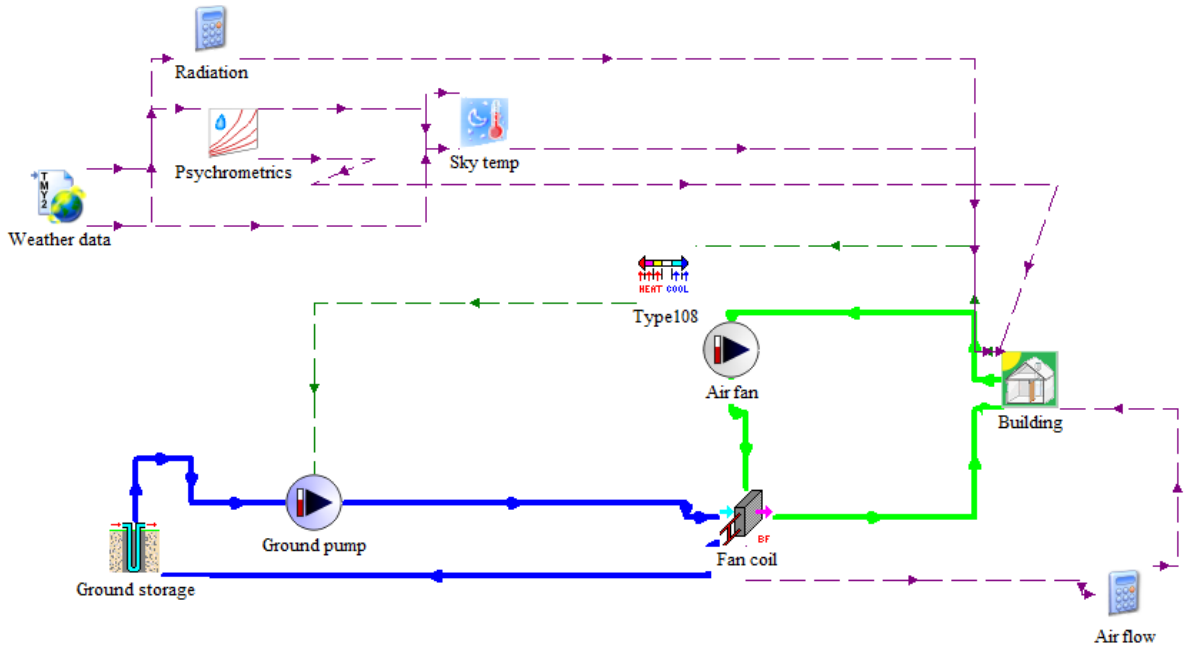

Figure 51: Simplified sketch of the project file components. Direct heat exchange with the ground storage.

Table 22 provides an overview of the main components in TRNSYS used in the direct heat exchange model.

Table 22: Overview of the main components in the direct heat exchange model.

Component	Name in TRNSYS	Type number in TRNSYS	Description of the model is given in chapter
Borehole thermal energy storage	Vertical U-tube ground heat exchanger	557a	9.2.4
Pump	Variable speed pump	110	9.2.7
Fan	Variable speed fan	111b	9.2.7
Reference building	Multi-zone building	56	10.7

10.8.5 Analysis of the simulations of operation mode 3

The parameters in the simulations were the same as in the base case 2. The storage consists of 56 boreholes and the spacing between the boreholes is 2 m. The objective of this simulation was to find out how much of the heating load can be covered by the direct heat exchange of the boreholes and how long time the heating can keep the room at set temperature. From the results of the simulation of the storage season, the results showed that the temperature in the end of the storage season would be 37°C. So the start temperature in the soil of the heating season is 37°C.

Figure 52 presents the room temperature after operation mode 3 has been turned on. Figure 52 shows that when the soil temperature drops below 30° C, the direct heat exchange with the ground is not able to maintain the set temperature of 20° C. This is due to the fact that the storage temperature is lower than the minimum temperature required for space heating, 30°C. The black line in the figure shows the difference in room temperature when the soil temperature is higher or lower than 30°C. To the right of the black line the room temperature is stable. For a short period in the beginning of the heating season the ambient temperature is high, so heating is not required. The ground provide some heat after the ground temperature drops below required temperature, so that the room temperature is a little bit higher than the ambient temperature, but it is not enough to maintain a stable temperature of 20 °C. So the room temperature varies a lot with the ambient temperature. Heat transferred from the storage to the room is 24934 MJ. This will cover around 25% of the heat demand.

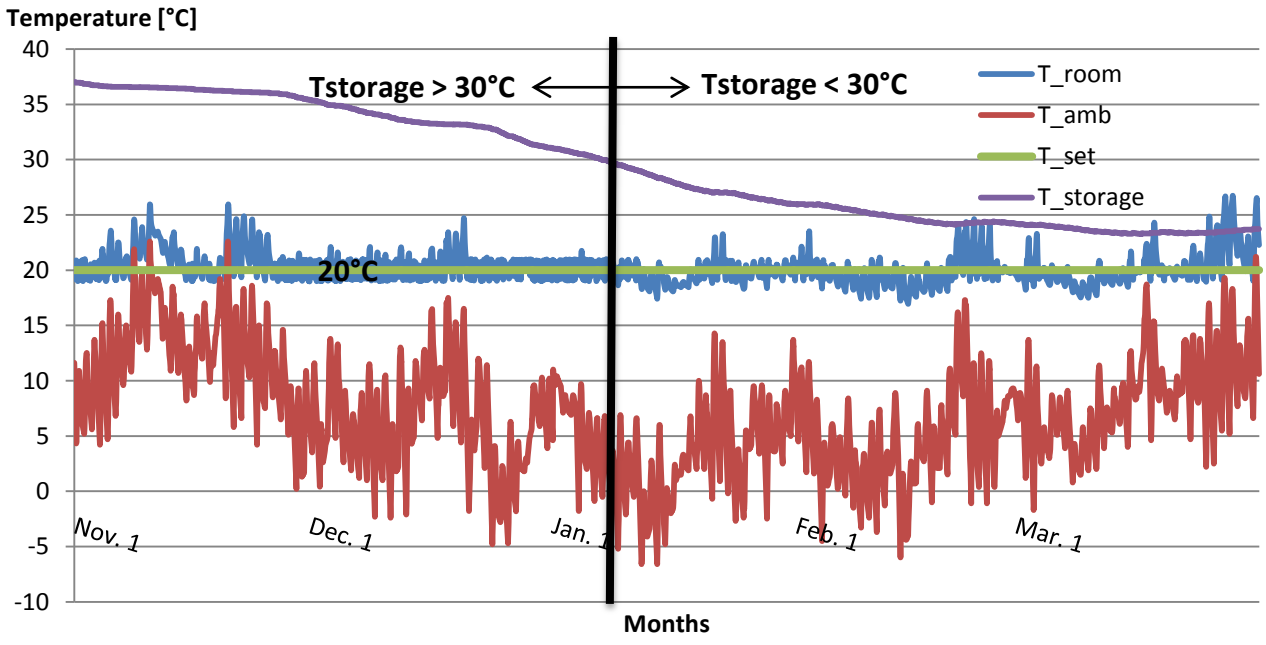

Figure 52: Simulations of direct heat exchange with the ground for the whole heating season.

10.8.6 Simulation of geothermal heat pump model– Operation mode 4

There are three closed loops in the simulation of the geothermal heat pump mode as illustrated in Figure 53. The ground storage transfers heat to the evaporator in the red loop. The heat pump exchanges heat with the liquid side of the fan coil in the blue loop and the heat directed into the building in the green loop.

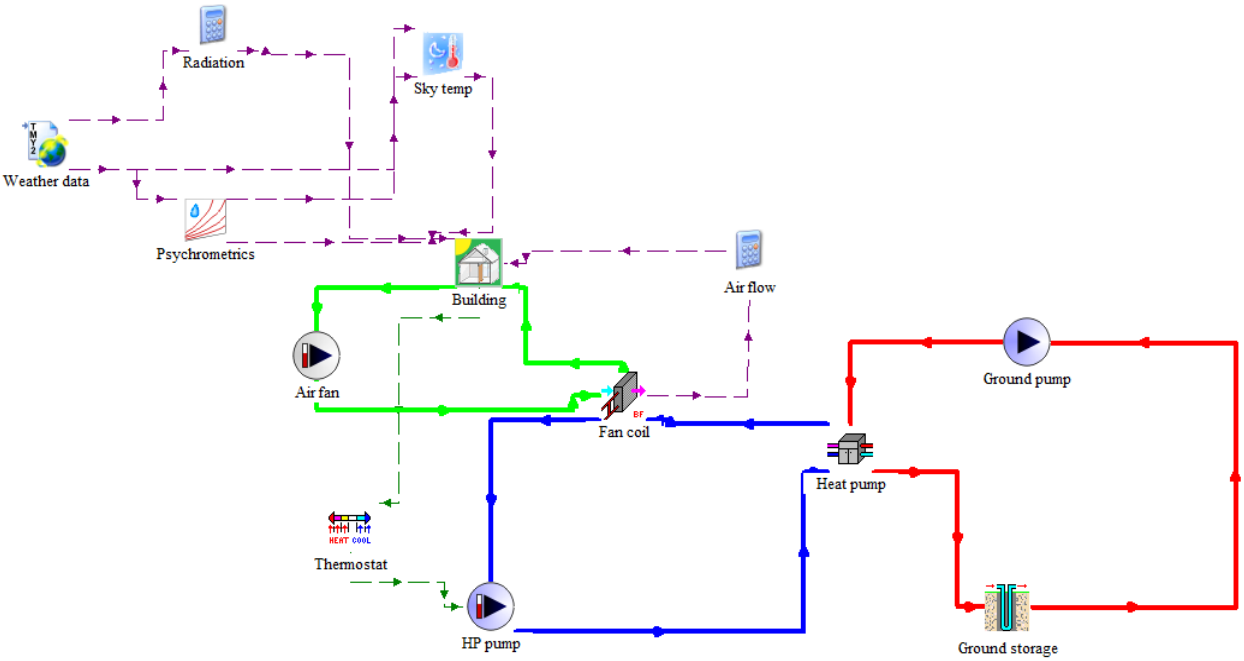

Figure 53: Simplified sketch of the project file components. Geothermal heat pump with the ground storage as a heat source.

Table 23 provides an overview of the main components in TRNSYS used in the geothermal model.

Table 23: Overview of the main components in the geothermal heat pump model.

Component	Name in TRNSYS	Type number in TRNSYS	Description of the model is given in chapter
Borehole thermal energy storage	Vertical U-tube ground heat exchanger	557a	9.2.4
Two pumps	Variable speed pump	110	9.2.7
Fan	Variable speed fan	111b	9.2.7
Reference building	Multi-zone building	56	10.7
Heat pump	Water to water heat pump	668a	9.2.5

10.8.7 Analysis of the simulations of operation mode 4

The parameters were kept the same as in the base case 2. The objective of this simulation was to find the compatibility of the ground storage with the heat pump. The temperature in the boreholes is an indicator of performance of the heat pump system and one interesting objective is to analyze this temperature. Another model of a traditional geothermal heat pump system without solar collectors was used under the same environmental conditions and load characteristics as references for comparison of COP and electricity use.

Figure 54 illustrates the ground temperature, the inlet and outlet temperature of the evaporator during the heating season. The evaporator inlet temperature together with the condenser outlet temperature determines the heating performance of water-to-water heat pump. According to Xi, Lin and Hongxing (2011) when the condenser outlet temperature is kept constant, like in this case, the COP will decrease with the evaporator inlet temperature. In the simulations the fluid temperature drops below 0°C. The working fluid becomes too low for proper performance. Since the simulations shows that the fluid temperature drops below 0°C, it can lead to completely frozen boreholes. If the ground heat exchangers are too short, the temperature of the fluid entering the evaporator is too cold and can damage the heat pump. The storage temperature decreases very fast because of too short boreholes. It will lead to unstable temperatures.

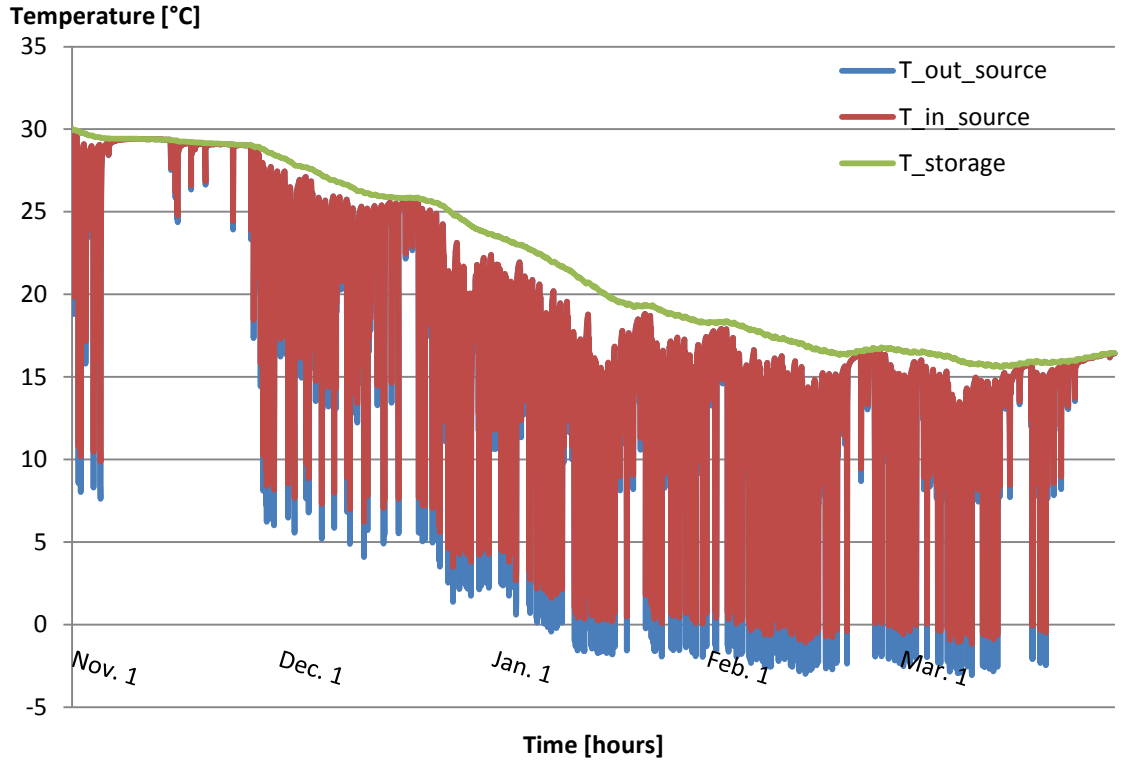

Figure 54: Inlet and outlet temperature of the ground storage with borehole depth of 10 meters.

The estimation by the steady-state calculations, see appendix B, shows that the temperature increase in the soil during summer and the temperature decrease in the soil during winter are not balanced. The big temperature decrease during winter is due too short boreholes and too small volume. The heat transfer rate is bigger in the heating season than the storage season. Since the temperature difference is 4 times higher in heating season than in storage season, we tried to balance the heat extraction and injection by increasing the volume by 4 times in heating season. This can be done by increasing the depth to 40 meter. Since the storage volume is increased, the soil temperature will decrease. To find the approximately ground temperature in the bigger volume, we used Equation 43. This equation will find an average temperature between the original volume and the new volume, by using the original temperature and the average mean temperature in the soil in Shanghai when there is no storage.

$$\rho c_f V_1 (T_{30} - T_a) = \rho c_f V_2 (T_a - T_{18})$$

Equation 43: Estimation of ground temperature

ρc_f Storage heating capacity of the soil [kJ/m^{3}K]

V_1 Volume in the base case 2 with borehole depth of 10 m [m^3]

T_{30} Original storage temperature of 30°C in base case 2 after using operation mode 3 [°C]

V_2 New increased volume with borehole depth of 40 m [m^3]

T_a Average temperature [°C]

T_{18} Average mean temperature in the soil in Shanghai of 18°C [°C]

The estimate of the ground temperature was found to be 20.4°C. The calculations of the temperature are shown in appendix C. This is just an average temperature between the mean temperature in the soil and the temperature after storage of heat, with storage volumes taken in consideration.

Heat transfer rate from the storage is given by equation:

$$Q_{load} = \rho c_p V (T_{fin} - T_{fout})$$

Equation 44: Heat transfer rate from the storage

Q_{load} Heating load of the building [kJ]

ρc_f Specific heating capacity of the soil [kJ/m^{3}K]

V Ground storage volume [m^3]

T_{fin} Inlet temperature of the fluid [°C]

T_{fout} Outlet temperature of the fluid [°C]

As we can see from the equation is that if the heat load stays the same and the volume increase then the temperature decrease/difference will be smaller.

Figure 55 shows the inlet and outlet temperature of the storage after increasing the borehole depth to 40 meters. It shows that for a bigger volume, the inlet and outlet temperatures are more stable and higher. Deeper depth has more stable temperatures, because it is not very influenced by the surface temperature. The heat pump has big enough capacity to provide heating for the whole heating season, but the heat pump is only needed when the other operation modes cannot provide sufficient heating. As shown in Figure 55 the ground temperature keeps decreasing at the beginning of December. The descending tendency of the temperature does not cease until the beginning of March, when higher ambient temperature alleviates the heating load and solar radiation is higher. Space heating was activated at the beginning of November. The heat load is very small and high ground temperature is observed for the same reason at the end of the heating period.

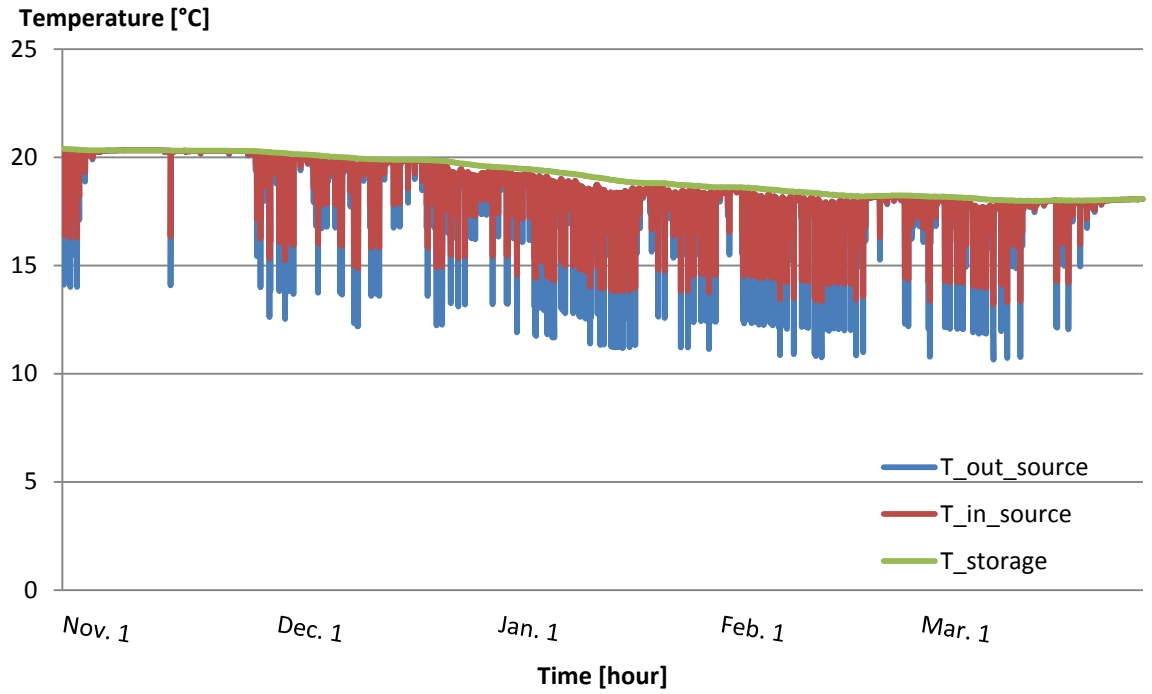

Figure 55: Inlet and outlet temperature of the ground storage with borehole depth of 40 meters.

We wanted also to test the difference in electricity use and the COP between a heat pump with a heated and unheated storage. In an unheated storage, the soil temperature is equal to the annual mean soil temperature in Shanghai, which is 18°C. The COP for the heat pump with heated storage for the whole heating period was found to be 4.5. The COP for the heat pump with unheated storage for the whole heating period was 4.2. Since the temperature inlet of the evaporator is raised, the COP is also raised. In this case the COP is calculated for the whole heating season performance. As we can see the COP is dependent on the temperatures in the system and the borehole depth.

10.9 Summarization of the results of the heating modes

There are totally three operation modes during heating season and the results for each operation mode are listed in Table 24.

Table 24: Simulation results for each mode in heating season

Operation mode	Supplied heat [MJ]	Percentage of the load
Mode 2	36203	37%
Mode 3	24934	25%
Mode 4	36901	38%

From the results it can be concluded that the solar direct heating mode and geothermal heat pump supplies almost the same amount of the heat demand. Operation time of the heat pump is significantly reduced because of the use of other heating modes. Operation mode 2 and operation mode 3 can cover 37% and 25% of the load respectively, so operation mode 4 must cover the remaining heat load, which accounts for 38% of the load.

10.10 Evaluation of electricity use in the different operation modes

The use of electricity is calculated as the total sum of the electricity demand in the heat pump, solar collector circulation pumps and ground storage circulation pumps. The electricity used in the reference system is calculated in the following way:

$$\sum E_{el} = E_{pS} + E_{pSC} + E_{pDX} + E_{HP} + E_{pHP}$$

Equation 45: Electricity use in the entire system

$\sum E_{el}$ Total use of electricity in the system [MJ]

E_{ps} Electricity used by the pumps in operation mode 1 [MJ]

E_{psc} Electricity used by the pumps in operation mode 2 [MJ]

E_{pbDX} Electricity used by the pumps in operation mode 3 [MJ]

E_{HP} Electricity used by the heat pump in operation mode 4 [MJ]

E_{pHP} Electricity used by the pumps in operation mode 4 [MJ]

The benefits of the solar collector and ground storage can be described as: Maximum benefit of solar energy and ground storage = Decreased use of electricity= Use of electricity in system without solar collectors – Use of electricity in system with solar collectors

The savings of electricity is defined as the difference in use of electricity between systems with and without solar collector and ground storage. When comparing different systems with and without solar collector and ground storage, the savings of electricity shows the potential benefits of solar heat in the geothermal heat pump systems. The main electricity input to the system is the electricity to the heat pump. The heat pump needs electrical energy to run the compressor. The remaining

input is the electricity to the circulation pumps. The use of electricity to the circulation pumps depend on type, size, system and operation time (Kjellsson, 2009). The operation time of the pump in the solar collector loop will depend on the radiation. Most importantly is that the energy consumption of the circulation pumps must not exceed the energy saving of the heat pump. The electricity consumption of the fan connected to the fan coil in the heating distribution system in the building is not included in the analyses. This is regarded to be the same for both systems and of less importance to quantify.

Table 25: Electricity use for system with and without solar collector

	Electricity use [MJ]
Base case 2	
Operation mode 1	
SC pump	3170
Borehole pump	132
Operation mode 2	
SC pump	739
Tank pump	549
Operation mode 3	
Borehole pump	903
Operation mode 4	
Heat pump	5375
Source pump	174
Load pump	41
Total electricity use	11083
Case without solar collector	
Heat pump	14410
Source pump	481
Load pump	109
Total electricity use	15000
Comparison between with and without solar collector	
Electricity saved	3916
Percentage saved when using solar collector in a geothermal heat pump system	26.1%

Table 25 shows an estimate of the electricity use for the different operation modes. The electricity use for the heat pump and the circulation pumps in the different operation modes could be obtained from the simulations. The equations used in TRNSYS to calculate the electricity consumption of the heat pump and the circulation pumps are found in chapter 9.2.5 and 9.2.7 respectively. To find the electricity used for operation mode 2 and 4, the intended coverage percent was found and then multiplied with the total electricity use for the whole season of operation mode 2 and 4 respectively. To find the elecetricity used in operation mode 3, the electricity use is found for the whole period before the ground temperature reaches 30°C. The results show that 26.1% of the electricity use can be saved by combining the solar collector with the ground storage. This saving could be increased by implementing more efficient control strategies of the circulation pumps. The borehole pump in the operation mode 1 is running constantly, instead the pump could be switched off when the solar collector is off. The load pump in operation mode 4 is also operating under always-ON conditions, it could be introduced some form of control strategy. An optimum control strategy for the circulation pumps must exist, however it has not been systematically investigated in this research. From the results it can be concluded that operation mode 3 has the smallest electricity consumption, this is because there is only one circulation pump in operation in the whole system.

Without storage of heat during the summer, the temperature in the ground will be around 18 °C. This will increase the work of the compressor, because the compressor needs to work with a higher temperature lift. At the same time, the electricity use of the circulation pumps in the storage season will be saved. The COP of the heat pump for the whole operation time depends on the whole system, as well as the operation and especially on the temperatures in the ground, the depth of the borehole and the power of the heat pump. After increasing the volume in the simulations, the ground temperature was reduced. So the inlet temperature to the heat pump was not very different in the case with and without solar collectors. Therefore, the majority of the energy saving will not be due to the small raise in the COP. The majority of the energy savings is due to the reduced operation time of the heat pump, because there are other heating opportunities.

11 Conclusion

The goal of this work was to evaluate a proposed heating system at the Green Energy Laboratory (GEL) in Shanghai. Emphasis was placed on studying the behavior of the ground storage with regard to parameters of influence.

Over the years there has been a large interest in SAGSHP because it can be an environmentally friendly substitute for the traditional space heating systems. Traditional geothermal heat pumps have very good and stable efficiencies, because at depths below 8 meters the ground has almost a constant temperature. However, if the annually heat extraction from the ground is larger than the naturally recharging in the summer, the ground temperature will subsequently sink and the performance of the heat pump will be weakened. Therefore, solar collectors and ground storage could be good measures to avoid this effect. There are several ways of combining the collectors with the geothermal heat pump. The connections depend on the usage of the solar collector, energy performance and climate conditions. The solar collector can be used for domestic hot water heating in the summer, for heating the building and for recharging the ground storage in the summer. Due to the complexity of these systems it is hard to draw any conclusions about general design. The design will vary from place to place. It was also found out from the literature reviews that the borehole configuration depends on the use of the boreholes.

After several simulations of parameters that have influence on the size of the storage it was shown that the sizing of the storage is critical. The system performance is directly linked to the size. Smaller volumes operate at higher storage temperatures, but they also have higher relative heat losses. By varying the solar collector area, it was shown that increasing solar collector area gives higher storage temperatures and higher return temperatures. The solar collector efficiency is highly dependent on the return temperature of the storage. By improving the heat transfer in the ground, the return temperature becomes lower and the solar collector efficiency will also be improved. Conclusion that could be drawn from the simulations is that the size of the ground storage and the solar collector depends on the use of the storage. A big solar collector and a relative small storage volume give high storage temperatures and allow the system to be used in a direct system and supply the whole heating demand. A small solar collector area and a relative big storage system give lower storage temperature which is suitable for the use of heat pump.

Simulations showed that if the purpose of the boreholes is to store heat, then the boreholes should be placed in a compact pattern with low spacing. A high number of boreholes with low spacing are most suitable for storage of heat. This is due to high number of boreholes increases the heat transfer area and the heat transfer to the ground is increased. Small spacing will increase the thermal interaction between the boreholes, which is favorable for storage of thermal energy. For the given storage volume at the GEL, it was found that a ground storage with 56 boreholes and 2 meters spacing showed the most promising performance for thermal energy storage. It was decided to continue to work on this specific case, because it had a high storage efficiency and reached a high soil temperature during storage season.

Different time periods of the storage season were simulated. There are several factors that influence the time length of the storage season; the end temperature of the soil, the storage efficiency and the electricity consumption. The end temperature should be as high as possible so the storage could be

used in direct heating. It was found that the best time period for the storage season is from May to October, because the storage had reached a high temperature and the amount of stored heat is high. The disadvantage of longer storage season was the increased electricity consumption of the circulation pumps.

Simulations of the solar direct heating mode showed that this mode can cover 37% of the load. January had the lowest solar fraction because of low solar radiation and high heating demand in this month. The direct heat exchange mode could cover 25% of the heating demand. The results of the simulations of this mode showed that when the soil temperature dropped below 30°C, it was not possible to maintain the set temperature of the reference building. For the simulation of the geothermal heat pump mode, the focus was on the inlet and outlet temperature of the heat pump. For the base case 2 it was clearly that the borehole depth of 10 meters was too short to work together with a heat pump. It led to low and unstable inlet temperatures of the heat pump. Calculations showed that the temperature decrease of the soil in the heating season was 4 times higher than the temperature increase in the storage season. This effect could be dampened by increasing the borehole depth by 4 times. The simulations of the geothermal heat pump showed the importance of balancing the heat extraction and heat injection. The heat pump has to cover the remaining heat load, which is 38% of the heating load. It seems like the volume of the base case 2 was most suitable for direct heat exchange with the ground.

After simulation and comparison of a system with and without solar collector it is shown that there are two major reasons for combining solar collectors and geothermal heat pumps; to decrease the use of electricity in the system and to raise the temperature in the boreholes. For this system, the raised soil temperature had most effects on the operation mode 3. Since we had to increase the volume in operation mode 4, the ground temperature was reduced and thereby the positive effect of increased temperature was also reduced. The COP of the system with heated storage was just a little bit higher than the system with unheated storage. For the system with and without solar collector the COP was found to be 4.5 and 4.2 respectively. Compared to the traditional system, 26.1% of the electricity use can be saved by combining the solar collector with the heat pump. The reduction of electricity use was mostly due to the reduced operation time of the heat pump.

It is very hard to give general recommendations for systems with geothermal heat pumps, ground storage and solar collectors because these systems are very complex. With a well planned operation and system solution it is possible to achieve reduced electricity use. If the system is well designed regarding borehole depth, heating demand and all subsystems work well, the best use of solar heat in Shanghai is to use it for the borehole during storage season (May-October) and space heating during heating season (November-March). The optimized dates of changing the use of the solar collector depend on the heat demand, storage losses and electricity use. A careful design of the system is important in order to make use of the system in a most efficient way.

12 Further work

Different control strategies of the system in the heating season should be evaluated in further work. The control strategies of the system can be studied though various operating limits of the circulation pumps. A pump could be turned on and operated between the operating limits. The operating limits could be temperature levels or temperature differences. The pumps will decide which of the heating modes should operate according to temperature levels. The challenge is to achieve optimum operation, so that the optimal operation mode is used at the right time. Flexible control strategies should be tested and evaluated to minimize energy use and to ensure a stable system.

The simulations have been performed for a time period of 1 year. Since the operation models were not connected together in the simulation models, it was difficult to see the influence of the ground temperature over several years. In the continuation of the work it should be done further studies on the ground temperature over a longer period since the performance of the geothermal heat pump is dependent on this temperature. It is important to check if the balance of the thermal load is kept and if the ground temperature keeps a decreasing, neutral or increasing tendency.

It is only performed simulations for the climate in Shanghai. Since the system is relatively dependent on the climate conditions it would be interesting to perform simulations for different climate conditions, especially for colder climates where the heating demand is even bigger and the solar radiations are lower.

As the heating system involves high investment expenses it should be performed economic evaluations. Economic calculations should be performed on similar realized projects, if figures are available, in terms of energy savings, investment costs, monitoring- and life cycle costs. In addition, it should be carried out analysis of life cycle costs associated with the different equipment in the system. The different system components have different lifespan and needs of replacement, it can be performed a life cycle analysis in relation to this.

The solar collector could also be used for other purposes during the heating season. When the temperatures from the solar collector are too low to be used for direct heating, the solar heat may be used raise the temperature to the evaporator. This could give the heat pump better operational conditions.

Bibliography

Andresen, I. (2008). *Planlegging av solvarmeanlegg for lavenergiboliger og passivhus. En introduksjon.* Oslo: Sintef Byggforsk.

Ataer, O. E. (2006). *Storage of thermal energy.* Oxford: Eolss Publishers.

Bauer, D. (2009). *German central solar heating plants with seasonal heat storage.* Elsevier B.V.

Bauer, D., Heidemann, W., & Steinhagen-Müller, H. (2009). *Modelling and simulation of groundwater influence on borehole thermal energy stores.* Stuttgart: Insitute of Thermodynamics and Thermal Engineering, University of Stuttgart.

Chapuis, S., & Bernier, M. (2009). *Seasonal storage of solar energy in borehole heat exchangers .* Montréal: Département de génie mécanique, École Polytechnique de Montréal .

Engineering Toolbox. (2011). Hentet May 2012 fra Engineering Toolbox: http://www.engineeringtoolbox.com/heat-pump-efficiency-ratings-d_1117.html

Favero & Milan Engineering. (2008). *Green Energy Laboratory - GEL, Conceptdesign_Final issue.* Favero & Milan Engineering.

Franke, R. (1998). *Modeling and optimal design of a central solar heating plant with heat storage in the ground using Modelica.* Ilmenau: Technical University of Ilmenau.

Gao, Q. et al (2008). *Review of development from GSHP to UTES in China and other countries.* Elsevier B.V.

Gentry, J. E. et al (2006). *Simulation of Hybrid Ground Source Heat Pump Systems and Experimental Validation.* Oklahoma: School of Mechanical Engineering - Oklahoma State University.

Han, Y. M. et al (2008). *Thermal stratification within the water tank.* Elsevier B.V.

Hellström, G. (1989). *Duct Ground Heat Storage Model - Manual for Computer Code.* Lund: Departement of Mathematical Physics, University of Lund.

Hoffman, O. (2012, April 5). Hentet June 2012 fra Patentdocs: http://www.faqs.org/patents/app/20120080163#b#ixzz1zWNBIMr1

Holmberg, H. (2009). *Analysis of Geo-Energy Systems with Focus on Borehole Thermal Energy Storage.* Lund: Faculty of Engineering - Lund University.

IEA Heat Pump Centre. (2012). Hentet April 2012 fra IEA Heat Pump Centre: http://www.heatpumpcentre.org/en/aboutheatpumps/heatpumpperformance/Sidor/default.aspx

Kalogirou, S. A. (2004). *Solar thermal collectors and applications.* Elsevier B.V.

Kjellsson, E. (2009). *Solar Collectors Combined with Ground-Source Heat Pumps in Dwellings.* Lund: Lund University.

Klein, S. A. et al (2006). *TRNSYS 16 - Manual.* Madison: Solar Energy Laboratory, University of Wisconsin-Madison.

Kovács, P., & Pettersen, U. (2002). *Solvärmda kombisystem - En jämförelse mellom vakuumrör och plan solfångare genom mätning och simulering.* Borås: SP Rapport .

Kroll, J. A., & Ziegler, F. (2011). *The use of ground heat storages and evacuated tube solar collectors for meeting the annual heating demand of family-sized houses.* Elsevier.

Martínez, P. J., Velázquez, A., & Viedma, A. (2004). *Performance analysis of a solar energy driven heating system.* Energy and Buildings - Vol. 37.

Meteotest. (2009). *Meteonorm - Version 6.1 .* Bern: Meteotest.

Moran, M. J., & Shapiro, H. N. (2006). *Fundamentals of Engineering Thermodynamics.* West Sussex: John Wiley & Sons Ltd.

Mumma, S. A. (2003). *Meeting Air Change Criteria .* ASHRAE.

Pahud, D. (2002). *Ground heat storage .* Labarotorio di Energia, Ecologia ed Economia.

Pardo, N. et al (2010). *Efficiency improvement of a ground coupled heat pump system from energy management.* Valencia: Instituto de Ingenieria, Universidad Politécnica de Valencia.

Pavlov, G. K., & Olesen, B. W. (2009). *Seasonal solar thermal energy storage through ground heat exchangers - Review of system and applications.* Lyngby: Department of Civil Engineering, Technical University of Denmark.

Persson, H., Perers, B., & Carlsson, B. (2011). *Type12 and type56: a load structure comparison in TRNSYS.* Linköping: Worl Renewable Energy Congress.

Rawlings, R. et al (2004). *Domestic Ground Source Heat Pumps: Design and installation of closed-loop systems.* Energy Saving Trust.

RETScreen International . (2005). *Ground-Source Heat Pump Project Analysis.* Natural Sources Canada.

Reuss, M., Beck, M., & Müller, J. P. (1997). *Design of a seasonal thermal energy storage in the ground.* Munich: Institute of Agricultural Engineering, Technical University Munich.

Rindal, L. B., & Salvesen, F. (2008). *Solenergi for varmeformål - snart lønnsomt?* Oslo: NVE.

Rönnelid, M., & Tepe, R. (2004). *Solvärme och värmepump. Utvärdering av ett värmesystem i Uppsala.* Borlänge: Högskolan Dalarna.

Sanner, B. et al (2003). *Current status of ground source heat pumps and underground thermal energy storage in Europe.* Elsevier B.V.

Sanner, B. (2003). Current status of ground source heat pumps in Europe. *Futurestock 2003.* Warsaw: Insitute of Applied Geosciences - Justus-Liebig-University.

Schmidt, T., & Miedaner, O. (2012). *Solar district heating guidelines.* www.solar-district-heating.eu.

Schmidt, T., Mangold, D., & Müller-Steinhagen, H. (2003). *Central solar heating plants with seasonal storage in Germany.* Elsevier B.V.

Self, S. J. (2012). *Geothermal Heat Pump Systems: Staus Reviwe and Comparison with other Heating Options.* Elsevier B.V.

Shah, L. J. (2005). *TRNSYS models of Evacuated Tubular Collectors.* Lyngby: Danmarks Tekniske Universitet.

Spitler, J. et al (2009). *Preliminary intermodel comparison of ground heat exchanger simulation models.* Oklahoma: Oklahoma State University.

Struckmann, F. (2008). *Analysis of a Flat-plate Solar Collector.* Lund: Faculty of Engineering - Lund University.

Trillat-Berdal, V., Souyri, B., & Fraisse, G. (2006). *Experimental study of a ground-coupled heat pump combined with solar collectors.* Hentet fra http://www.sciencedirect.com/science/article/pii/S0378778806001022

Värmebaronen. (2011). Hentet May 2012 fra Värmebaronen: www.varmebaronen.com

Wang, E. et al (2011). *Performance predition of a hybrid solar ground-source heat pumps system.* Elsevier B.V.

Xi, C. et al (2011). *Experimental studies on a ground coupled heat pump with solar thermal collectors for space heating.* Elsevier B.V.

Xi, C., Lin, L., & Hongxing, Y. (2011). *Long term operation of a solar assisted ground coupled heat pump system for space heating and domestic hot water.* Hong Kong: Elsevier B.V.

Yang, W. et al (2009). *Current status of ground source heat pumps in China.* Elsevier B.V.

Yuehong, B. (2004). *Solar and ground source heat-pump system.* Elsevier B.V.

Zogou, O., & Stamatelos, A. (2007). *Optimization of thermal performance of a building with ground source heat pump system.* Energy Conversion and Management 48.

Appendix A Numerical values from simulations in TRNSYS

In this appendix some of the numerical values from the simulations in TRNSYS is presented.

Influence of the mass flow rate

Figure 56 shows the numerical values of the simulations in chapter 10.4.2.

	0.5 m/s	1 m/s	1.5 m/s Base	2 m/s	2.5 m/s
Eu [MJ]	127297	121907	113988	102533	92567
Eload [MJ]	103012	98094	91477	82123	73884
Estore [MJ]	63378	60699	57059	51900	46972
Etl [MJ]	21484	20578	19168	17102	15298
Esl [MJ]	39634	37395	34418	30223	26912

Figure 56: Numerical values for simulations of mass flow rate

Influence of borehole depth

Figure 57 shows the numerical values of the simulations in chapter 10.4.3.1.

Borehole depth [m]	Area surface losses [MJ]		
	Top	Side	Bottom
10 m/Base case	6763	19744	7911
20 m	3500	28460	5698
30 m	1822	32715	4556
40 m	826	35209	3878
50 m	183	37055	3448

Figure 57: Numerical values for storage losses

Influence of the borehole spacing

Figure 58 shows the numerical values of the simulations in chapter 10.4.3.2.

Energy [MJ]	Spacing [m]				
	2	3	4	5/Base case	6
Eu	101800	108872	112445	113988	114856
Eload	75080	84453	89244	91473	92654
Estore	22154	36220	48049	57055	65011
Qtl	22511	20609	19695	19168	18950
Esl	52926	48229	41191	34418	27638

Figure 58: Numerical values for energy amounts

Optimization of number of boreholes and spacing

Figure 59 shows the numerical values of the simulations in chapter 10.4.3.4.

Spacing	0.5	1	1.5	2	2.5	3	3.5	4	4.5	5	5.5	6	6.5
Boreholes	900	225	100	56	36	25	18	14	11	9	7	6	5
T_storage	37.95	37.03	37.05	36.91	36.49	35.76	35.27	34.3	33.49	32.57	32.02	31.09	30.4
E_tl	7253	7074.511	7851	9040	10482	12126	14060	15707	17544	19168	21349	22604	24812
Eu	159955	160682	157682	152508	147099	140538	133429	126733	120012	113988	106117	100956	95676
E_load	152264	153167	149179	142527	135320	126728	117199	108579	99555	91473	80837	74086	66574
E_top_loss	19968	15750	14522	13568	12628	11647	10385	9158	7922	6763	5496	4495	3565
E_side_loss	53961	46975	43185	39408	35776	32425	29014	25611	22586	19744	17102	14657	12567
E_bottom_loss	25559	21792	19373	17128	15238	13541	11785	10389	9053	7911	6570	5677	4789
E_sl	99487	84517	77081	70103	63642	57614	51185	45158	39561	34418	29168	24829	20920
E_store	52776	68650	72098	72424	71677	69114	66014	63421	59995	57055	51669	49257	45653

Figure 59: Numerical values for energy amounts

The influence of storage insulation

Figure 60 shows the numerical values of the simulations in chapter 10.4.4.

Insulation thickness [m]	Surface area losses [MJ]		
	top	side	bottom
0 m	6763	19744	7911
0.2 m	4974	20151	7917
0.4 m	3925	20376	7921
0.6 m	3239	20519	7923
0.8 m	2755	20619	7924

Figure 60: Numerical values for energy losses.

The influence of tank volume

Figure 61 shows the numerical values of the simulations in chapter 10.4.5.

Figure 61

Tank volume	5	10	15	20	25	30
T_storage	31.13	32.25	32.55	32.57	32.44	32.26
E_tl [MJ]	8796	11713	15092	19168	22843	26207
Eu [MJ]	88521	100376	107769	113988	118484	122070
E_load [MJ]	82196	89295	91070	91473	90678	89357
E_top_loss [MJ]	5902	6552	6688	6763	6690	6539
E_side_loss [MJ]	17780	19243	19563	19744	19589	19266
E_bottom_loss [MJ]	7129	7711	7839	7911	7850	7722
E_sl [MJ]	30811	33506	34090	34418	34130	33527
E_store [MJ]	51385	55789	56980	57055	56548	55830

Figure 61: Numerical values for energy amounts.

Simulations of operation conditions

Figure 62 and Figure 63 show the numerical values of the simulations in chapter 10.6.

	Apr	May	Jun	Jul	Aug	Sep	Oct
T_storage							
Apr. 30 [°C]	22.52						
May. 31 [°C]	25.84	22.49					
Jun. 30 [°C]	28.43	25.92	22.58				
Jul. 31 [°C]	31.86	30.10	27.66	24.27			
Aug. 31 [°C]	34.13	32.78	30.87	28.38	23.80		
Sep. 30 [°C]	37.33	36.06	34.58	32.81	29.38	25.07	
Oct. 31 [°C]	37.95	36.91	35.71	34.34	31.74	28.56	23.52
E_tl [MJ]	10769	9040	7445	5919	3932.00	2333	694
Eu [MJ]	171521	152508	133602	114116	86405.00	60054	26929
E_inj [MJ]	160216	142527	124939	106691	80643	55593	23885
E_top_loss [MJ]	16989	13568	10486	7582	4214	1896	34
E_side_loss [MJ]	46753	39408	32346	25182	16242	8916	1740
E_bottom_loss [MJ]	20049	17128	14277	11333	7569	4343	969
E_storage_losses [MJ]	83791	70104	57109	44097	28025	15155	2743
E_store [MJ]	76424	72424	67829	62594	52618	40438	21142

Figure 62: Numerical values for storage temperatures and energy amounts.

	Apr	May	Jun	Jul	Aug	Sep	Oct
Electricity solar collector [MJ]	3562	3170	2692	2193	1589	1012	499
Electricity BTES [MJ]	154	132	110	89	66	44	22

Figure 63: Numerical values for electricity use

Simulations of operation mode 2 – Solar direct heating

Figure 64 and Figure 65 shows the numerical values of the simulations in chapter 10.8.3.

Month	Heating load	Energy supplied via fan coil
November	17472	11279
December	31397	19549
January	36949	12028
February	29495	20029
March	24433	16100

Figure 64: Numerical values for heating load and energy supplied via fan coil.

Heating season	SF
Nov	0.39
Dec	0.37
Jan	0.31
Feb	0.42
Mar	0.41

Figure 65: Numerical values for the solar fraction for every month in the heating season.

Appendix B Steady state calculations of ΔT during storage season and heating season

Equation for heat that is stored or extracted into the ground:

$$Q = \rho c_p V \Delta T$$

ρc_p=2016kJ/m^3*K

Volume in case A=1948m^3

Calculation for one typical day in June in storage season:

Q = Heat that can be stored during one typical day in June = 347534kJ

ΔT = 347534/ (2016*1948) = 0.088 K

Calculation for one typical day in January in heating season:

Q = Heat load for one typical day in January = 1455647kJ

ΔT = 1455647/ (2016*1948) = 0.371 K

So the deltaT in heating season with case A is almost four times higher than the delta T in storage season.

Appendix C Calculation of the average soil temperature

This appendix presents the calculatin for the soil temperature after the storage volume is increased in chapter 10.8.7.

Equation for average temperature between the initial temperature of the base case in operation mode 4 and the average mean temperature in Shanghai:

$$\rho c V_1 (T_{30} - T_a) = \rho c V_2 (T_a - T_{18})$$

V_1= 1948 m^3

T_{30}=30°C

V_2 = 7758 m^3

Based on the equation above, T_a can be expressed and calculated in following way:

$$T_a = \frac{V_1 T_{30} + V_2 T_{18}}{V_1 + V_2}$$

$$T_a = \frac{(1948 \times 30) + (7758 \times 18)}{1948 + 7758}$$

$$T_a = 20.4°\text{C}$$

The estimate of the average ground temperature was found to be $20.4°\text{C}$.

Appendix D Draft report

Modeling the heating of the Green Energy Lab in Shanghai by the geothermal heat pump combined with the solar thermal energy and ground energy storage

Candice Yu[a], Yong Li[b1], Ruzhu Wang[b], Trygve M. Eikevik[a]

[a] *Department of Energy and Process Engineering, Norwegian University of Science and Technology, Trondheim, Norway*

[b] *Institute of Cryogenics & Refrigeration, Shanghai Jiao Tong University, Shanghai, China*

Abstract

This paper introduces a heating system that combines solar collector, geothermal heat pump and ground storage used in an office building for space heating. The simulation results of the system's detailed operating performance are presented. A simulation tool with several models has been developed in the simulation software TRNSYS based on the proposed heating system at the Green Energy Laboratory (GEL) under the meteorological conditions of Shanghai. Four operation modes worked in two different seasons, storage season and heating season. The operational characteristic of each operation modes were studied. The ground storage mode was studied thoroughly by varying design parameters of interest. The simulation results showed that a compact borehole pattern with a big number of boreholes and small borehole spacing is favorable for borehole thermal energy storages. The performance of a ground storage is directly linked to the storage size. The solar collector efficiency is highly dependent on the return temperature of the ground storage. The simulation of the heating modes showed that the solar direct heating, direct heat exchange with the ground and geothermal heat pump could cover 37%, 25% and 38% of the heating demand, respectively. The simulation results showed that the proposed heating system could save 26.1% of the electricity use. The savings was mostly due to the reduced operation time of the heat pump, since other heating modes could be used. The studies showed that due to the complexity of such systems it is very important to perform simulations to optimize the performance. There are many factors that play an important role since there are so many components involved. The simulations showed that sizing of the system is critical for the system performance.

1 Introduction

In China the buildings are expected to account for more than 35% of the national energy use by the year 2020, where heating, ventilation and air-conditioning systems will account for more than 65% of the energy use in buildings (Xi et al, 2011). Most space heating plants are still predominantly fueled by coal and domestic hot water is widely provided by electric resistance heaters in China (Xi, Lin, & Hongxing, 2011). Coal accounted for 69.5% of the national energy consumption in 2007 (Yang et al, 2009). Considering that the coal emits more CO_2 and other pollutants than other energy resources, it

[1] Corresponding author. E-mail address: liyo@sjtu.edu.cn

can be concluded that it is very important to promote use of renewable energy sources and energy conservation in China. Ever since China's participation in the Kyoto Protocol, reducing CO_2-emission as well as energy saving have been propelling researchers to explore substitutes of traditional space heating and water heating systems in China. The Renewable Energy Law (RE Law) took into effect in 2006 in China; by 2020, 15% of all energy should come from renewable energy, including wind energy, solar energy, water energy, geothermal energy, etc (Gao et al, 2008). Therefore, renewable resources have a great potential for application in environmental friendly buildings.

Solar energy is an important alternative energy source for heating applications. It is not the amount of solar heat that is a barrier for its use but the fact that the availability and demand are often out of phase (Kroll & Ziegler, 2011). In order to make use of abundant renewable energy resources, such as solar energy, it is necessary to combine the heating systems with thermal energy storages. Seasonal thermal energy storages enable greater and more efficient use of fluctuating energy resources by matching the energy demand with the supply. Geothermal heat pump with vertical/horizontal ground heat exchangers, known as ground coupled heat pump systems, are considered relatively efficient for heating, air-conditioning or hot water supply. Because the underground soil temperature is kept higher than the ambient air in winter, the ground coupled heat pump system has made the operation of heat pump systems more reliable and practical under cold weather conditions. Heat pumps also reduce the amount of bought energy. Recent years there have been a growing interest in solar assisted ground source heat pump systems. The solar thermal energy is stored in the ground and extracted by geothermal heat pump, because a high initial temperature in the ground is beneficial for the heat pump during heating. Without the heat injection the ground temperature would tend to decreasing annually. There are many different ways to couple the solar collector and the heat pump. If efficient seasonal use of solar energy can be combined with the underground thermal energy storage for the use of GSHP then it could be a great substitute of traditional space heating and water heating systems in China.

The SAGHCP was first introduced by Penrod in 1956 (Xi et al, 2011). However, the interest in combining solar collectors with heat pumps started to increase in the end of 1970s due to the oil (Trillat-Berdal, Souyri, & Fraisse, 2006). At that time the focus was on the positive effect of the increased temperature in the ground, but there was not made any economic evaluations on these systems (Kjellsson, 2009). During the 1980s, the International Energy Agency (IEA) established three research programs; "Solar Heating and Cooling Programme", "Energy Storage Programme" and "Advanced Heat Pump Programme". Some of the research focus was on the design and economics. The interest was great in this period, but it started to decline when it became apparent that many of the SAGSHP systems were marked by technical and economical problems (Rönnelid & Tepe, 2004).

2 Description of the system and operation principles

2.1 Overview of the system

The proposed heating system at the GEL combines a solar collecting system with borehole thermal energy storage and a ground-coupled heat pump. The solar collector and the ground storage are connected through a water tank. The simulated system also includes the indoor air-conditioning system. Valves are used to switch between the two heat sources; solar thermal energy and ground storage thermal energy. The working fluid throughout the whole system is water, because then the working fluid can flow though the solar collector, the fan coils, the borehole thermal energy storage, the hot water tank and the heat distribution system. The whole system can be divided into four different operation modes. One of the operation modes is used in the storage season. The remaining three operation modes are used in the heating season. The hot water production is not included in this system. Working places and offices often have a negligible hot water demand.

The four operation modes:

- Operation mode 1: Solar thermal ground storage → Storage season
- Operation mode 2: Solar direct heating
- Operation mode 3: Direct heat exchange with the ground storage } Heating season
- Operation mode 4: Geothermal heat pump

The heating is provided by the fan coils with the hot water coming from the solar storage water tank if the water is hot enough. If the tank water is not hot enough then the hot water is provided directly from the ground storage. If the water circulating through the ground storage is not hot enough for direct heating, then the hot water heated by the heat pump (using the remaining stored solar energy in the ground) is used.

The solar collector subsystem includes evacuated tube collectors with an area of 216 m^2. The tank is connected to the ground storage and the space heating distribution system with the help of flow diverters, mixers and controllers. The switching between the different heating modes is based on tank temperature, storage temperature and solar radiation. The tank has a volume of 20 m^3. The ground storage volume consists of 9 boreholes. Each borehole has a length of 10 meters and a spacing of 5 meters. The geothermal heat pump is a water-to-water heat pump. Later on, some of the parameters presented in this section will be varied.

2.2 Working principles of the main operation modes

The working principles of each mode will be presented. The sketches shown are only used as an illustration and do not show the exact setup with all components in the system. The valves and the controllers that connect and control the whole system are omitted from the drawings to give an easier view of the operation modes. The sizes of the components are not exact relative to each other.

Operation mode 1: Solar ground thermal storage

Solar thermal energy collected by the solar collectors is transferred to the water tank. Then the water in the tank exchanges heat to the heat carrier fluid. The heat carrier fluid circulates through the boreholes. The thermal energy is injected to the ground through the interaction between the boreholes and the ground. The whole ground temperature keeps an increasing tendency. This mode takes effect through the whole storage season. The solar collector is controlled by an ON/OFF differential controller.

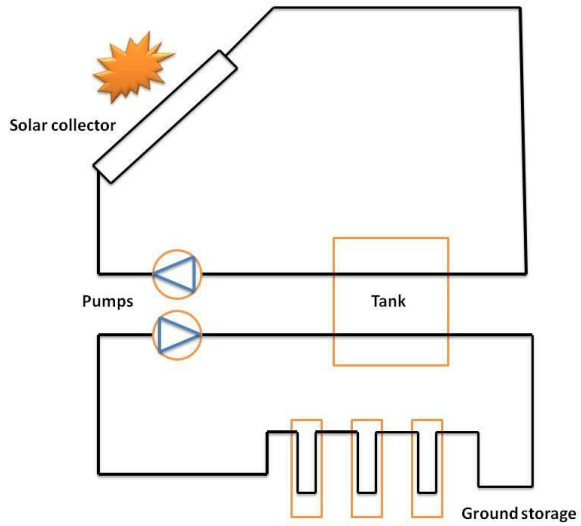

Figure 1: Sketch of operation mode 1: Solar ground thermal storage

Operation mode 2: Solar direct heating mode

Solar collector is used to produce heat for the heating system during the heating season. When the water temperature in the tank is high enough for space heating (around 30-35°C for a fan coil heating terminal), the system can deliver hot water directly to the fan coil heating terminal. The hot water circulates through the tank. The hot water in the tank then exchanges heat with the air passing though the fan coil unit.

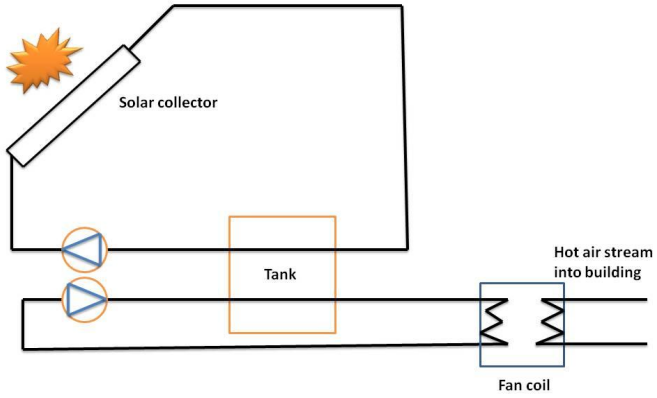

Figure 2: Sketch of operation mode 2: Solar direct heating

Operation mode 3: Direct heat exchange with the ground storage

The boreholes are utilized to provide heating by direct heat exchange. After the storage season the ground has reached a certain temperature. The heat injected in the storage season is extracted from the ground by the ground heat exchangers to satisfy the space heating requirements. The ground temperature should be higher than 30°C to operate in this mode. This mode takes effect when the solar collectors cannot produce sufficiently high enough temperatures to be used for the heating system. The whole ground temperature keeps a decreasing tendency. Since high temperatures is not desired at the inlet of the evaporator of the heat pump, it is favorable to use this mode first, so the ground temperature will be decreased. The proposed heating system combines both use of direct heating and heat pump.

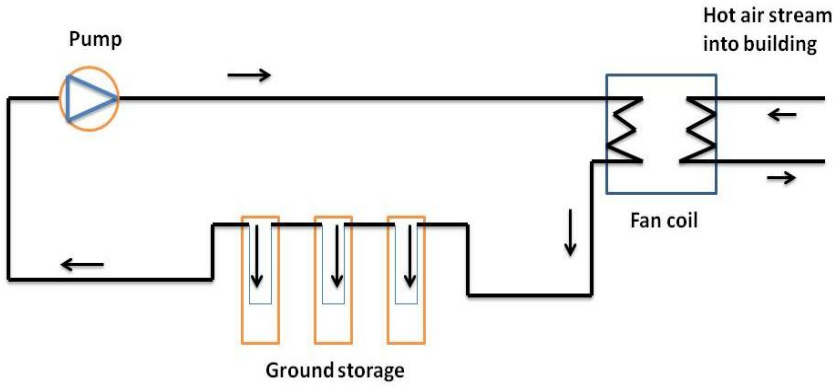

Figure 3: Sketch of operation mode 3: Direct heat exchange with the ground

Operation mode 4: Geothermal heat pump

This mode takes effect when the ground temperature has dropped to a certain level and the temperature is not high enough to be utilized in direct heat exchange. The remaining heat in the ground storage is extracted by a heat pump. The ground storage acts as a heat source for the heat pump. The whole ground temperature keeps a decreasing tendency. The ground temperature has been heated to a higher level, so the COP of this heat pump will be higher than a normal geothermal heat pump with unheated ground. The compressor needs less work input. For a system without solar collector the source temperature may be only 10-18 °C in Shanghai, but for a system with solar collector, the source temperature may be around 20-30 °C.

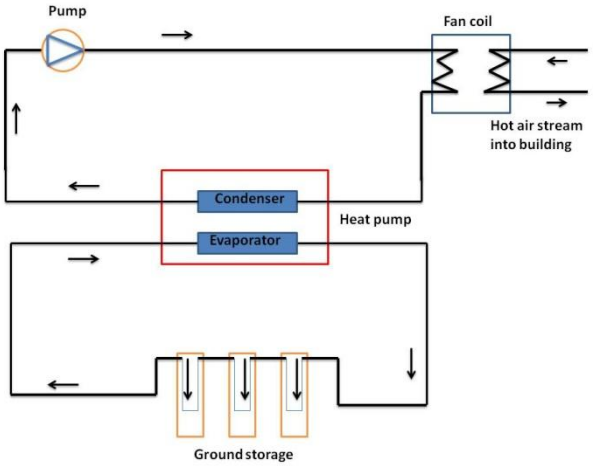

Figure 4: Operation mode 4: Geothermal heat pump

3 Mathematical model of the system

The mathematical models used in this paper are the ones that are implemented in TRNSYS.

3.1 Solar Collector

Type 538 is the evacuated tube collector model adopted to model the performance of solar collectors. The model of the evacuated tube solar collector assumes that the efficiency (η) versus a ratio of inlet temperature of the fluid minus the ambient temperature to radiation ($\Delta T/I$) curve can be modeled as a quadratic function (Klein et al, 2006).

$$\eta = a_0 - a_1 \frac{\Delta T}{I} - a_2 \frac{\Delta T^2}{I}$$

Equation 1: Thermal efficiency

3.2 Geothermal heat pump

Type 668 models a single-stage water to water heat pump. The model is based on user-supplied catalogue data for the heating capacity and power demand, based on the entering load and source temperatures. The model is able to interpolate data, within the range of input values specified in the data files. The COP of the heat pump and the outlet conditions can be calculated by:

$$COP = \frac{Q_{load}}{W_{cycle}}$$

Equation 2: COP for heat pump

$$Q_{source} = Q_{load} - W_{input}$$

Equation 3: Energy absorbed from the source fluid stream

$$T_{source,out} = T_{source,in} - \frac{Q_{source}}{\dot{m}_{source} cp_{source}}$$

Equation 4: Source outlet temperature

$$T_{load\ ,out} = T_{load,in} - \frac{Q_{load}}{\dot{m}_{load} cp_{laod}}$$

Equation 5: Load outlet temperature

3.3 Borehole Thermal Energy Storage

This model, type 557, is the most commonly in ground heat exchange applications and was developed by the Department of Physics in Lund University (Hellström, 1989). The model assumes that the boreholes are uniformly placed within a cylindrical ground storage volume. The volume is calculated by:

$$V = \pi \times Number\ of\ boreholes\ \times Borehole\ depth \times (0.525 \times Borehole\ spacing)^2$$

Equation 6: Volume of the ground storage

The rate of injection to the storage volume is given by:

$$Q_{injection} = c_f Q_f (T_{fin} - T_{fout})$$

Equation 7: Rate of injection of energy to the storage volume

3.4 Fan coil

The heating system uses fan coils to distribute heating to different parts of the building. Type 753 in TRNSYS models a heating coil. The fan coil model assumes that the temperature final air temperature is the same as the average temperature of the fluid in the coil (Pardo et al, 2010). The unstrained control mode was used in the simulations. The flow was chosen to be free-floating because there is a room thermostat that controls the zone temperature by switching on/off the pump that supplies water to the heat sources.

The energy transferred from the fluid to the air stream is calculated by:

$$Q_{fluid} = \dot{m}_{air}\left(1 - f_{airbypass}\right)\left(h_{air,coilout} - h_{air,in}\right)$$

Equation 8: Energy transfer from liquid to air in a fan coil

3.5 Base case

Table 1 presents the main characteristics of the components used in the simulations. The values of the characteristics were used as inputs and parameters to the base case in the simulations. Parameters and inputs were varied one at a time, while the remaining parameters and inputs were kept constant.

Table 1: Main characteristics of the base case

Characteristics	Value	Comments
Solar collector		
Collector area [m^2]	216	Inspected at the roof at the GEL
Fluid specific heat [kJ/kg*K]	4.19	Specific heat for water
a_0 [-]	0.734	Given by the producer
a_1 [kJ/hrm^2K]	5.5044	Given by the producer
a_2 [kJ/hrm^2K^2]	0.0432	Given by the producer
Mass flow [kg/hr]	9771.6	Based on available equipment at the GEL
Water tank		
Tank volume [m^3]	20	
Tank loss coefficient [kJ/hrm^2K]	2.5	
Ground storage		
Ground		
Initial temperature [C°]	18	Annual average air temperature in SH
Thermal conductivity [kJ/hrmK]	5.22	

Heat capacity [kJ/m^3/K]	2016	
Boreholes		
Borehole radius [m]	0.15	
Number [-]	9	
Depth [m]	10	
Borehole spacing [m]	5	
Storage volume [m^3]	1948.3	
Ground heat exchangers		
Inner radius of U-tube pipes [m]	0.013	
Outer radius of U-tube pipes [m]	0.016	
Pipe thermal conductivity [kJ/hrmK]	1.656	Pipe material is polyethylene
Pumps		
Rated power [kJ/hr]	2684	
Total pump efficiency	0.6	

4 Simulations results and discussion

4.1 Weather conditions and load characteristics

By using the weather model in TRNSYS it was possible to obtain the solar radiation in Shanghai. Figure 5 shows the monthly global solar radiation on a horizontal plate in Shanghai. The figure shows the solar radiation is highest in July and is lowest in January. Figure 6 shows the monthly average temperature in Shanghai. It can be observed that the lowest outdoor temperature occurs when the solar radiation is weak, which challenge some parts of the proposed heating system in winter operation. Due to its huge area, China is divided into five climatic zones from north to south within the thermal design and engineering field Shanghai belongs to the hot summer and cold winter zone (Gao et al, 2008). This means there is abundant solar energy in the summer and a large heat load in the winter, so the use of seasonal storages is very convenient. Shanghai is located in Yangtze River Delta in the eastern part of China at 31°12''N 121°30''E. Shanghai is located in the subtropical monsoonal climate. Winters are chilly and damp, and winds from Siberia causes temperatures to drop below 0°C. Summers are hot and humid with occasional and thunderstorms.

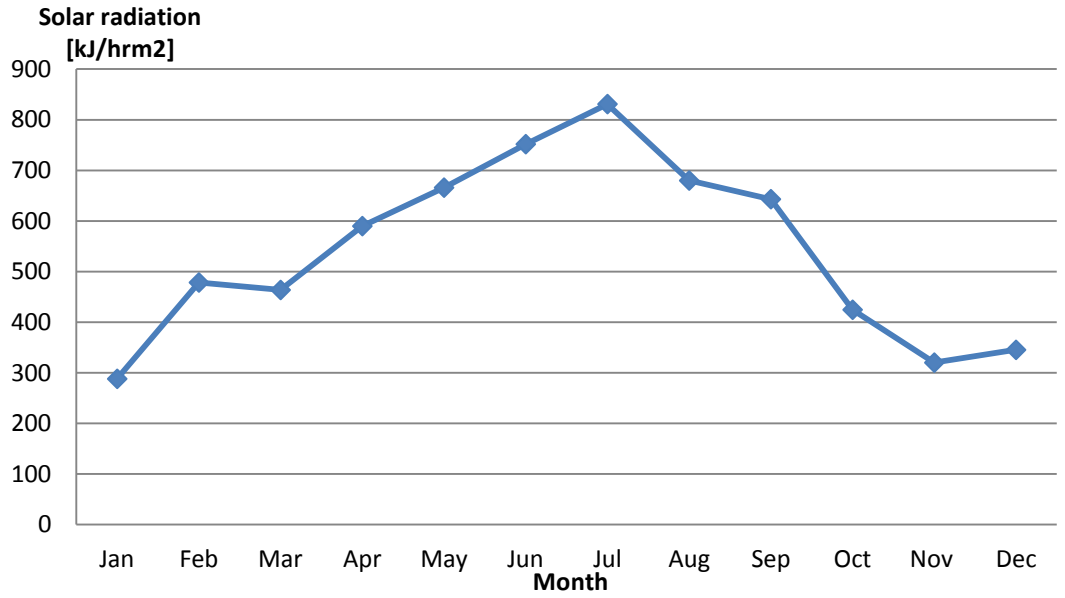

Figure 5: Monthly solar radiation on a horizontal plate in Shanghai. Weather data obtained from TRNSYS.

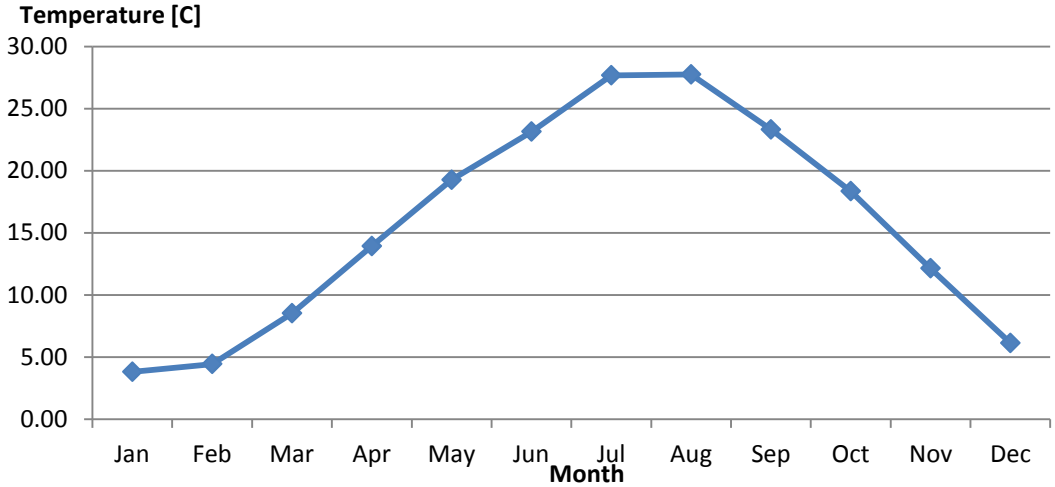

Figure 6: Monthly average temperature in Shanghai. Weather data obtained from TRNSYS.

The heat demand of the ground floor in the Green Energy Building was simulated in TRNSYS. The simulations were later used as the heating load in the simulations of the heating modes. Normally, the first floor is used by students as work place. The simulated work place area comprises 816.5 m^2 and work place volume comprises 3429.2 m^3. The work place is planned to be used by around 30 students.

Energy demand

Table 2Table 14 provides an overview of the energy demand for space heating of the reference building in different units.

Table 2: Simulation results of the energy demand of the reference building.

	Specific energy demand [kWh/m^2]	**Total energy demand [kWh/year]**	**Specific energy demand [MJ/m^2]**	**Total energy demand [MJ/year]**
Energy demand	33.4	27233.0	120.1	98038.8

Power demand

Table 3 provides an overview of the power demand for space heating of the reference building.

Table 3: Simulation results of the power demand of the reference building.

	Average power demand [W/m^2]	**Peak power demand [W/m^2]**	**Average power demand [kJ/hrm^2]**	**Peak power demand [kJ/hr m^2]**
Power demand	11.3	31.0	40.7	111.6

Figure 7 shows the heat power demand for every month. The figure shows that the peak power demand occurs, in January, at the same time with the adverse environmental conditions. This is because the largest temperature difference between outdoors and indoors temperature occurs at these conditions. The heating season will last from the beginning of November to the end of March, since there are only heating demand in these months.

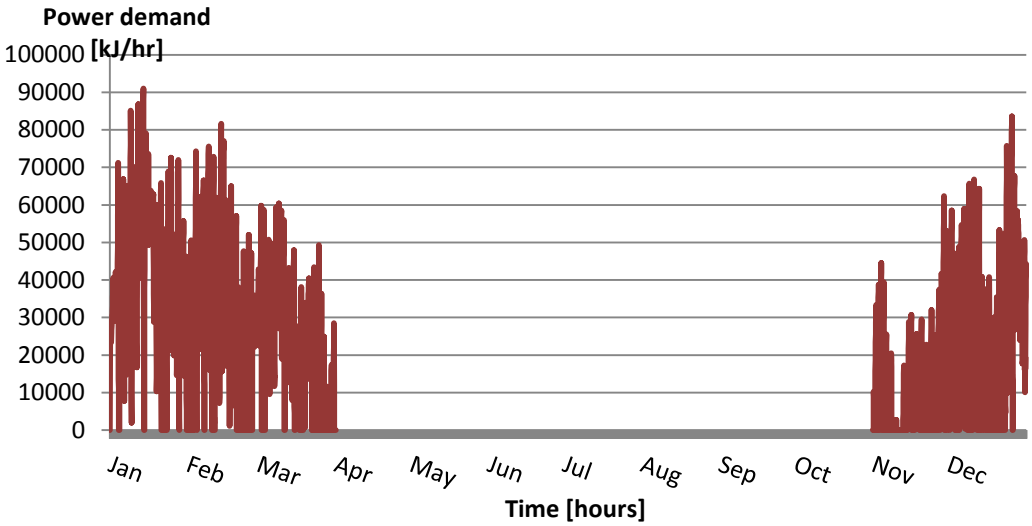

Figure 7: Annual heat power demand profile for the first floor (816.5 m2) at GEL. Results obtained from TRNSYS.

4.2 Simulations of the ground storage – Operation mode 1

In this section the design parameters with influence on the system performance and behavior will be studied by varying the different parameters. Each parameter will be taken into consideration separately so as to examine the influence on system efficiency. In order to do such an analysis the base case of GEL became the reference of the possible comparisons.

The influence of the solar collector area

The solar collector area is the area of the solar system that is exposed to the sun. Four collector areas were used to study the influence of this parameter. In addition to the collector of 216 m^2, there were also made simulations for areas of 250, 300 and 350 m^2. Figure 8 shows the storage temperature in the end of every month in the storage season. It is seen that when the collector area is larger, the ground temperature is higher. The ground temperature increases with the solar collector area, because the outlet temperature of the solar collector is increased. This is because when the area increases the amount of solar radiation hitting the collector surface also increases.

When the storage temperature is higher, the heat loss from the storage surfaces to the surrounding ground is larger. Also, the heat loss from the collector to the surrounding is larger because the return temperature is higher, which leads to decrease of the efficiency of the solar collector.

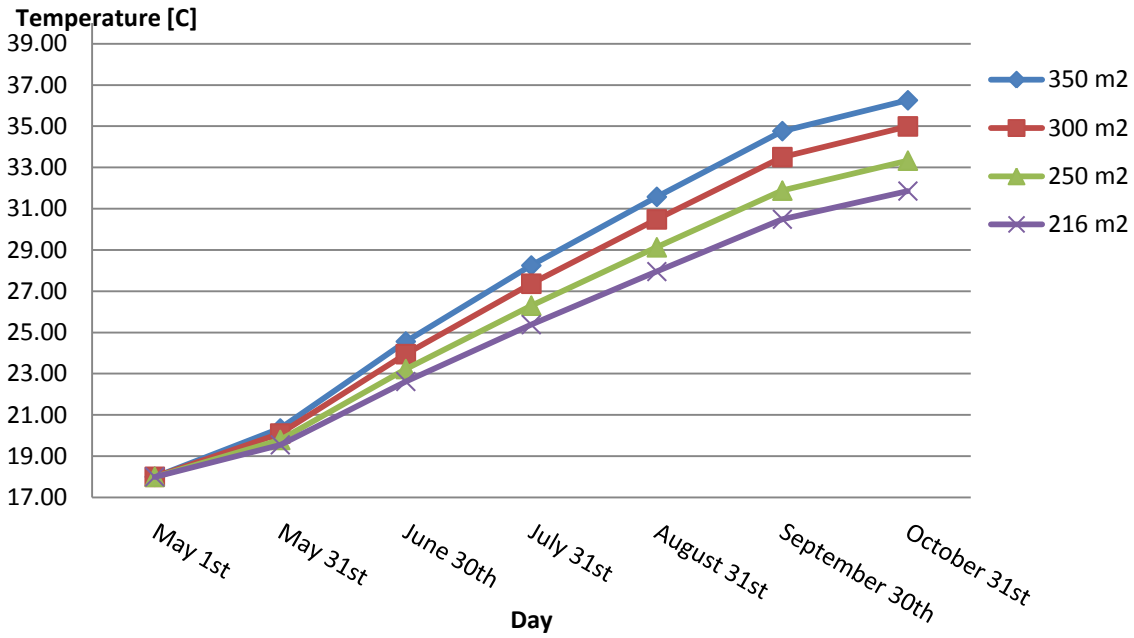

Figure 8: Storage temperature for varied collector area

The influence of the number of boreholes

We wanted to test the effects of the heat transfer by changing the number of boreholes without changing the volume. By increasing the number of boreholes the heat transfer will also increase. In this simulation the volume was kept constant by increasing or reducing the number of boreholes and spacing. By keeping the volume constant, we could see the effects isolated. The constant volume is the same as in the base case, 1948 m^3. By varying the spacing between 2-6 meters, the number of boreholes is found by Equation 6.

Table 4: Varied parameters

Spacing	Number of boreholes
0.5	900
1	225
1.5	100
2	56
2.5	36
3	25
3.5	18
4	14
4.5	11
5	9
5.5	7
6	6
6.4	5

By keeping a constant volume and only change the number of boreholes and spacing, it is observed that having more boreholes the heat transfer to the ground will increase. The cases with smallest spacing are very favorable for heat storage, because the boreholes will thermally influence each other and thereby raise the heat transfer. The heat transfer area increases with number of boreholes and reduced spacing. The storages with more boreholes reach higher storage temperatures, shown in Figure because more heat is transferred into the ground.

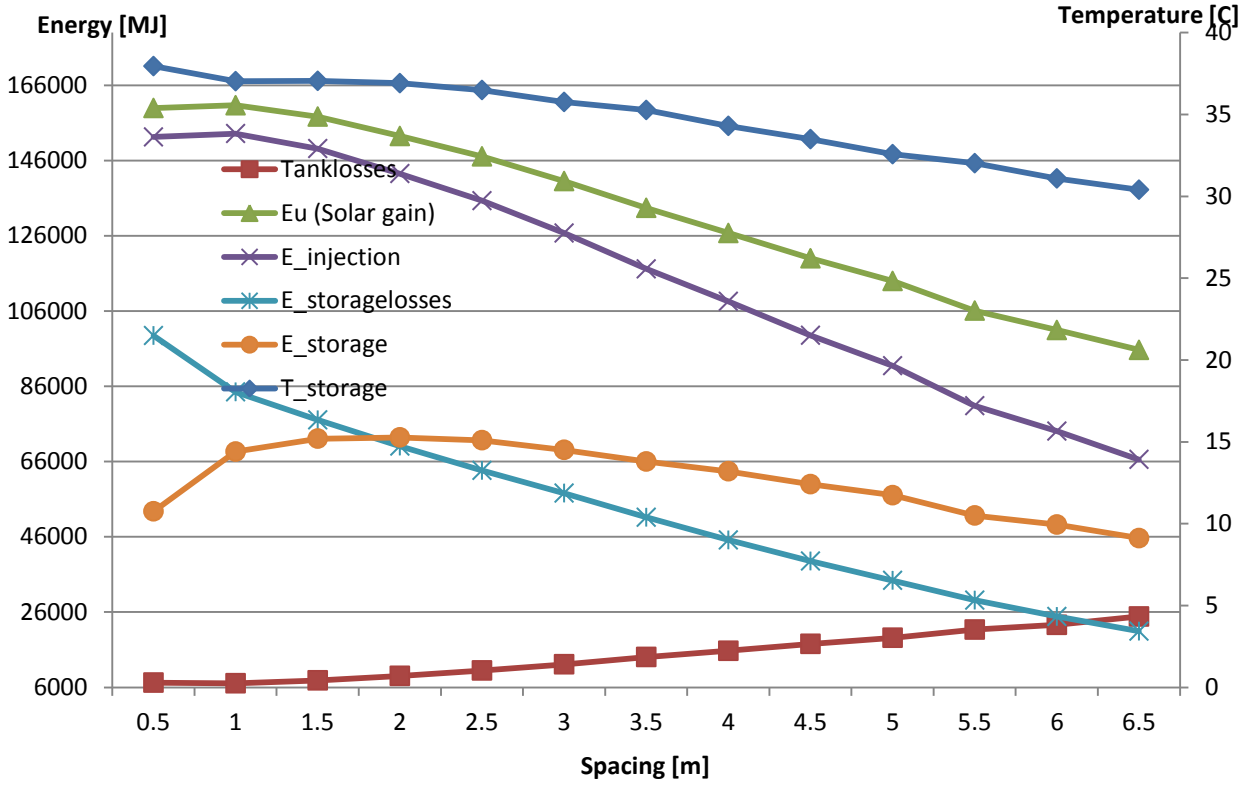

Figure 9: Storage temperature, energy gains and losses with varied spacing and number of boreholes.

The amount of stored heat in the storage is at its highest when the spacing is 2 m, as seen in figure 9. The amount of stored heat is 72424 MJ. This is because for smaller spacing the temperature is too high so the storage losses are higher than the stored heat. For bigger spacing and reduced boreholes the heat transfer area is smaller, so the heat transfer will be smaller. The configuration with spacing of 2 meter and 56 boreholes appeared to be the most efficient configuration for the storage volume of 1948 m^3 with borehole depth of 10 meters. This configuration can store the biggest amount of heat. The reduction of tank losses is very limited for spacing smaller than 2 m. The increase in solar gain is also very limited for spacing smaller than 2 m. The storage temperature graph starts to flat out for spacing of 1-2 m.

It was decided to continue to work on the case with 56 boreholes and 2 m spacing. It is because this storage showed most promising efficiencies for the use of storing thermal energy and reaches a high soil temperature during storage season. We wanted to test further how this borehole configuration works during heating season, especially with a heat pump.

4.3 Simulation of solar direct heating model – Operation mode 2

The objective of this simulation was to find out how much of the heat load can be covered by the solar direct heating mode.

January has the highest heat load and also the lowest energy supplied, which leads to a low solar fraction. The heat load is dependent on the ambient temperature. January has the lowest average ambient temperature, refer to Figure 6, which will cause the largest difference between the indoor and outdoor temperature. This month is normally the coldest, which gives the highest heating demand. The solar fraction is low because of the low solar radiation in January. The graph of the solar fraction is closely related to the curve of solar radiation, see Figure 10. The solar fraction has almost the same changing tendency as the solar radiation curve, except in November. The solar fraction is higher in November than December even though November has lower solar radiation than December. This is because November has a relatively small heat load. There are many cloudy and rainy days in November which gives low solar radiation, but the average ambient temperature is high in this month which gives a smaller heat load.

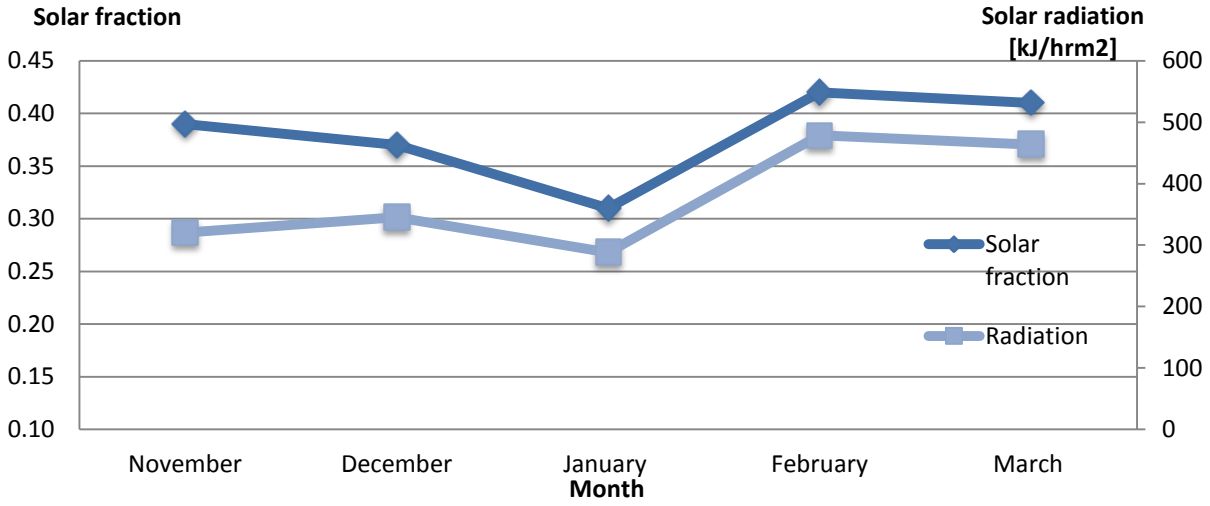

Figure 10: The solar fraction (Energy supplied by the coil/Heating load) in the different months of the heating season

4.4 Simulation of direct heat exchange with the boreholes model – Operation mode 3

The objective of this simulation was to find out how much of the heating load can be covered by the direct heat exchange of the boreholes and how long time the heating can keep the room at set temperature.

Figure 11 shows the room temperature after operation mode 3 has been turned on. Figure 11 shows that when the soil temperature drops below 30° C, the direct heat exchange with the ground is not able to maintain the set temperature of 20° C. This is due to the fact that the storage temperature is lower than the minimum temperature required for space heating, 30°C. The black line in the figure shows the difference in room temperature when the soil temperature is higher or lower than 30°C. To the right of the black line the room temperature is stable. For a short period in the beginning of the heating season the ambient temperature is high, so heating is not required. The ground provide some heat after the ground temperature drops below required temperature, so that the room temperature is a little bit higher than the ambient temperature, but it is not enough to maintain a stable temperature of 20 °C. So the room temperature varies a lot with the ambient temperature. Heat transferred from the storage to the room is 24934MJ. This will cover around 25% of the heat demand.

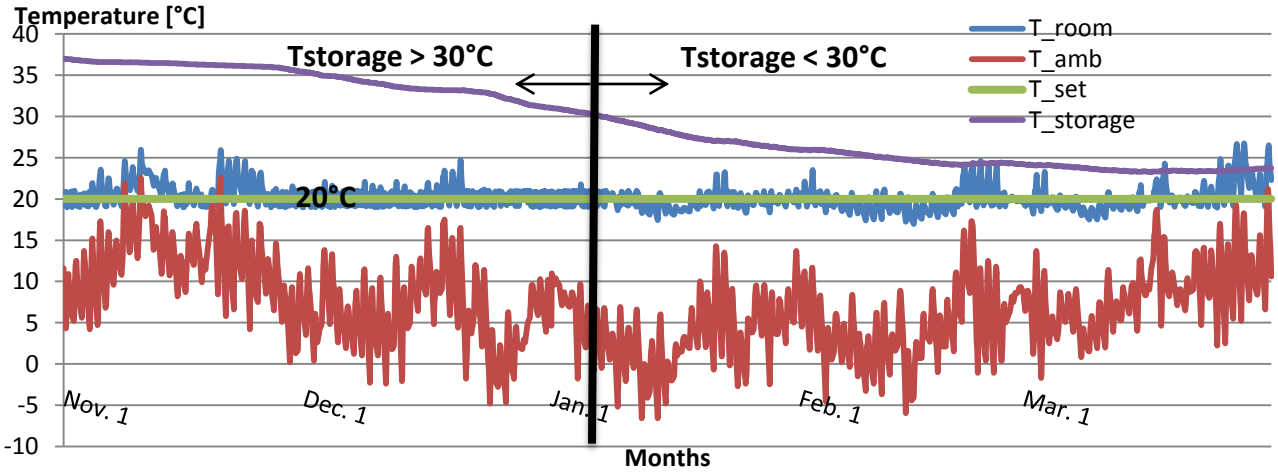

Figure 11: Simulations of direct heat exchange with the ground for the whole heating season.

4.5 Simulations of geothermal heat pump model – Operation mode 4

The objective of this simulation was to find the compatibility of the ground storage with the heat pump. The temperature in the boreholes is an indicator of performance of the heat pump system and one interesting objective is to analyze this temperature. Another model of a traditional geothermal heat pump system without solar collectors was used under the same environmental conditions and load characteristics as references for comparison of COP and electricity use.

The estimation by the steady-state calculations shows that the temperature increase in the soil during summer and the temperature decrease in the soil during winter are not balanced. The big temperature decrease during winter is due too short boreholes and too small volume. The heat transfer rate is bigger in the heating season due to short depths. Since the temperature difference is 4 times higher in heating season than in storage season, we tried to balance the heat extraction and injection by increasing the volume by 4 times in heating season. This can be done by increasing the

depth to 40 meter. Figure 12 shows the inlet and outlet temperature of the storage after increasing the borehole depth to 40 meters. It shows that for a bigger volume, the temperatures are more stable and higher. Deeper depth has more stable temperatures, because it is not very influenced by the surface temperature. The heat pump has big enough capacity to provide heating for the whole heating season, but the heat pump is only needed when the other operation modes cannot provide sufficient heating. As shown in Figure 12 the ground temperature keeps decreasing at the beginning of December. The descending tendency of the temperature does not cease until the beginning of March, when higher ambient temperature alleviates the heating load and solar radiation is higher. Space heating was activated at the beginning of November. The heat load is very small and high ground temperature is observed for the same reason at the end of the heating period.

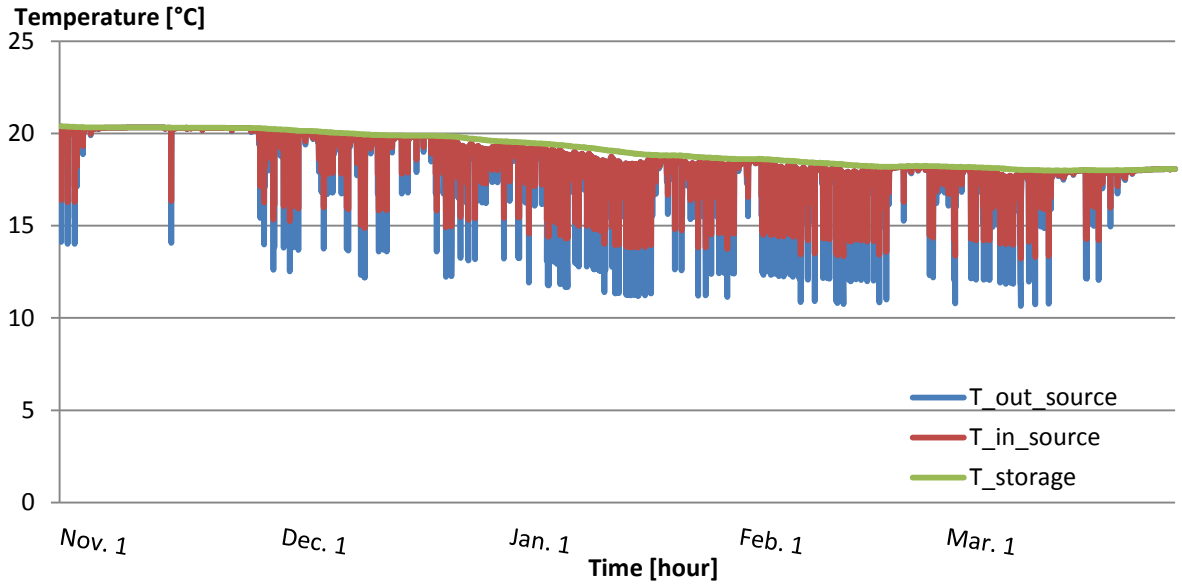

Figure 12: Inlet and outlet temperature of the ground storage with borehole depth of 40 meters.

The COP for the heat pump with heated storage for the whole heating period was found to be 4.5. The COP for the heat pump with unheated storage for the whole heating period was 4.2. Since the temperature inlet of the evaporator is raised, the COP is also raised. In this case the COP is calculated for the whole heating season performance. As we can see the COP is dependent on the temperatures in the system and the borehole depth.

4.6 Summarization of the results of the heating modes

There are totally three operation modes during heating season and the results for each operation mode are listed in Table 5.

Table 5: Simulation results for each mode in heating season

Operation mode	Supplied heat [MJ]	Percentage of the load
Mode 2	36203	37%
Mode 3	24934	25%
Mode 4	36901	38%

From the results it can be concluded that the solar direct heating mode and geothermal heat pump supplies almost the same amount of the heat demand. Operation time of the heat pump is significantly reduced because of the use of other heating modes. Operation mode 2 and operation mode 3 can cover 37% and 25% of the load respectively, so operation mode 4 must cover the remaining heat load, which accounts for 38% of the load.

We also wanted to evaluate the electricity use of the proposed system. The total electricity use was found to be 11083 MJ. The total electricity use for the system without solar collectors was found to be 15000 MJ. The results show that 26.1% of the electricity use can be saved by combining the solar collector with the ground storage. The majority of the energy savings is due to the reduced operation time of the heat pump, because there are other heating opportunities.

5 Conclusion

The goal of this work was to evaluate a proposed heating system at the Green Energy Laboratory (GEL) in Shanghai. Emphasis was placed on studying the behavior of the ground storage with regard to parameters of influence.

After several simulations of parameters that have influence on the size of the storage it was shown that the sizing of the storage is critical. The system performance is directly linked to the size. Smaller volumes operate at higher storage temperatures, but they also have higher relative heat losses. This is due to heat losses are increasing with the storage envelope surface, while stored energy is increasing with the storage volume.

Simulations showed that if the purpose of the boreholes is to store heat, then the boreholes should be placed in a compact pattern with low spacing. A high number of boreholes with low spacing is most suitable for storage of heat. This is due to high number of boreholes increases the heat transfer area and the heat transfer to the ground is increased. Small spacing will increase the thermal interaction between the boreholes, which is favorable for storage of thermal energy.

Simulations of the solar direct heating mode showed that this mode can cover 37% of the load. January had the lowest solar fraction because of low solar radiation and high heating demand in this month. The direct heat exchange mode could cover 25% of the heating demand. The results of the simulations of this mode showed that when the soil temperature dropped below 30°C, it was not possible to maintain the set temperature of the reference building. For the simulation of the geothermal heat pump mode, the focus was on the inlet and outlet temperature of the heat pump. For the base case 2 it was clearly that the borehole depth of 10 meters was too short to work

together with a heat pump. It led to low and unstable inlet temperatures of the heat pump. Calculations showed that the temperature decrease of the soil in the heating season was 4 times higher than the temperature increase in the storage season. This effect could be dampened by increasing the borehole depth by 4 times.

The simulations of the geothermal heat pump showed the importance of balancing the heat extraction and heat injection. The heat pump has to cover the remaining heat load, which is 38% of the heating load. After simulation and comparison of a system with and without solar collector it is shown that there are two major reasons for combining solar collectors and geothermal heat pumps; to decrease the use of electricity in the system and to raise the temperature in the boreholes. For this system, the raised soil temperature had most effects on the operation mode 3. Since we had to increase the volume in operation mode 4, the ground temperature was reduced and thereby the positive effect of increased temperature was also reduced. The COP of the system with heated storage was just a little bit higher than the system with unheated storage. For the system with and without solar collector the COP was found to be 4.5 and 4.2 respectively. Compared to the traditional system 26.1% of the electricity use can be saved by combining the solar collector with the heat pump. The reduction of electricity use was mostly due to the reduced operation time of the heat pump.